ISSN 2738-0971
eISSN 2738-1013

Bulletin of Natural Sciences Research

Vol. 10, N° 2, 2020.

BULLETIN OF NATURAL SCIENCES RESEARCH

Published by
Faculty of Sciences, University in Priština – Kosovska Mitrovica
Republic of Serbia

Focus and Scope

Bulletin of Natural Sciences Research is an international, peer-reviewed, open access journal, published semiannually, both online and in print, by the Faculty of Sciences – Kosovska Mitrovica, Republic of Serbia. The Journal publishes articles on all aspects of research in biology, chemistry, geography, geoscience, astronomy, mathematics, computer science, mechanics and physics.

Editorial Office

Ive Lole Ribara 29; 38220, Kosovska Mitrovica, Serbia, e-mail: editor@bulletinnsr.com, office@bulletinnsr.com; fax: +381 28 425 397

Printed by

Sigraf, Ćrila i Metodija bb, 37000 Kruševac, tel: +38137427704, e-mail: stamparijasigraf@gmail.com

Available Online

This journal is available online. Please visit http://www.bulletinnsr.com to search and download published articles.

ISSN 2738-0971
eISSN 2738-1013

Bulletin of Natural Sciences Research

Vol. 10, No. 2
2020.

University in Priština – Kosovska Mitrovica
Faculty of Sciences
Republic of Serbia

BULLETIN OF NATURAL SCIENCES RESEARCH

Vol. 10, N^{o} 2, 2020.

CONTENTS

BIOLOGY

CHEMISTRY

GEOGRAPHY, GEOSCIENCE AND ASTRONOMY

MATHEMATICS, COMPUTER SCIENCE AND MECHANICS

PHYSICS

Bulletin of Natural Sciences Research
Vol. 10, No. 2, 2020, pp. 1-6.

DOI: https://doi.org/10.5937/bnsr10-23916
Original Scientific Paper

IMPACT OF PB, NI AND CD ON THE GERMINATION OF BARLEY SEEDS, VARIETY JADRAN

PREDRAG VASIĆ[1], TATJANA JAKŠIĆ[1], GORICA ĐELIĆ[2]

[1]Faculty of Sciences, University in Priština - Kosovska Mitrovica, Kosovska Mitrovica, Serbia
[2]Department of Biology and Ecology, Faculty of Science, University of Kragujevac, Kragujevac, Serbia

ABSTRACT

The aim of this study was to determine the effect of lead, nickel and cadmium on the germination of barley seeds (*Hordeum vulgare* L.) of Jadran variety. Based on the percentage of germination, germination energy, and root and hypocotyl length, authors done an analysis of the effects of $PbCl_2$, $NiCl_2$, $CdCl_2$ solutions, in concentrations of 10^3 mol/m^3, 10^2 mol/m^3, 10 mol/m^3, 1 mol/m^3, 10^{-1} mol/m^3, 10^{-2} mol/m^3. The results showed that germination and germgrowthin stress conditions which are caused by heavy metals depend on the type of metal and its concentrations. The most toxic effect of alltested solutions had $CdCl_2$, and the weakest toxic effect had $PbCl_2$.

Keywords: *Hordeum vulgare* L., Lead, Nickel, Cadmium, Germination.

INTRODUCTION

The harmful effects of heavy metals in soil are reflected in the entire ecosystem (Kabata-Pendias, 2011). By accumulation in soil, heavy metals are involved in biochemical processes of element circulation, and in food chains. As a consequence of an inadequate application of chemicals, artificial fertilizers, etc. in agriculture, an increased amount of heavy metals occurs in agricultural land, which leads to the manifestation of their phytotoxic and negative impact on the quality of plant products (Rajkovic et al., 2012., Djelic et al., 2012., Pesko et al., 2011). Plants that grow or which are cultivated on contaminated land present health hazard for animals and human population.

Maximum permitted levels (MPL) of hazardous and noxious substances in soil and irrigation water, which can damage or alter the agricultural production capacity and the quality of irrigation water, coming from discharges from factories, dumping, improper use of mineral fertilizers and preservatives plants, are regulated in the Republic of Serbia by the Rulebook on the allowed quantities of dangerous and harmful substances in soil and water for irrigation and methods of their testing. If land contains more than the maximum allowed levels (Tab.1), than it is not recommended for agricultural production. Barley is considered to be one of the oldest, most widespread cereal in Europe. It has been cultivated for over 10,000 years (Salamini et al., 2002).

The species of the genus Hordeum have a basic number of chromosomes 7. Grown barley *Hordeum vulgare* L. *ssp. vulgare* and its wild ancestor H. vulgare L. ssp. *spontaneum* (C. Koch.) Thell. are diploid species with 2n = 14 chromosomes.

All cultivated forms of barley belong to species *Hordeum vulgare* L., which is divided into three subspecies based on the number of developed classics (Kricka et al., 2012): double row barley (*H. vulgare ssp. distichum*), transitional barley (*H. vulgare ssp. intermedium*), row barley (*H. vulgare ssp. polystichum*).

It has short vegetation, and it istolerantto low temperatures, drought, salts, and basic soil reaction (Poehlman et al., 1985).

In order to obtain higher yields and better grain quality, numerous tests are being carried out to create new varieties resistant to biotic and abiotic stress (Zhang et al., 2001). So far, 124 varieties of barley have been created in the Republic of Serbia (Madic et al., 2011).

Barley (*H. vulgare*) is the most widespread of all cereal. It has a very rich nutritional value because it contains a large amount of vitamin B complex, and vitamins A, E, K, D. It is an excellent source of vegetable fibers, proteins, phosphorus, magnesium, zinc, iron, etc. Only 200g of barley contain 55 % of the recommended daily amount of vegetable fiber. It is gluten free and easy to digest, and due to its medicinal properties it is recommended that people consume this valuable food frequently (Tanner et al., 2016).

Table 1. Maximum permitted levels.

Chemical elements	Maximum permitted levels in soil mg/kg soil	Maximum permitted levels in water mg/lwater
Cadmium	to 3	to 0.01
Lead	to 100	to 0.1
Nickel	to 50	to 0.1

The Jadran variety is spring barley which is cultivated during summer time. It is characterized by a low stalk and good resistance to lodging. The quality of the grain and malt is excellent. The aim of this study was to determine the effect of different concentrations of heavy metals Pb, Ni, Cd on the germination, germination energy, root length and hypocotyl of barley (*H.vulgare*) seeds of the Jadran cultivar.

* Corresponding author: gorica.djelic@pmf.kg.ac.rs

EXPERIMENTAL

Materials and methods

The toxic effect of heavy metals on barley seeds of Jadran cultivar was investigated using a solutions of $PbCl_2$, $NiCl_2$, $CdCl_2$, prepared in distilled water,in 7 different concentrations as follows: 10^3 mol/m^3, 10^2 mol/m^3, 10 mol/m^3, 1 mol/m^3, 10^{-1} mol/m^3, 10^{-2} mol/m^3 and 0 mol/m^3 (control)

100 seeds were planted for each concentration. 7 petri boxes were used on the bottom of which the filter paper was loaded with: 7 different concentrations of each heavy metal. Petri boxes with seeds were placed in a thermostat at a temperature of + 22º C. The experiment was done in three repetitions.

The length of the root, hypocotyl, was determined on the fifth day after placement of the experiment.

Germination energy was calculated by the form:

$$\frac{\sum(n \, x \, p)}{\sum m} \qquad (1)$$

where: n - germination time (first day, second day…); p - number of germinated seeds; m- total number of germinating seeds (Komljenović & Todorović, 1998).

The analyzed parameters are shown in the mean values and were statistically processed by the method of analysis of variance using two-factor trial, and the significance of differences was tested by LSD test for P 0.05 and 0.01.For statistically process the results it was used SPSS Statistics program (SPSS 16 for Windows).

RESULTS AND DISCUSSIONS

The percentage of germination of spring barley (*H. vulgare*) seeds of the Jadran variety in distilled water (control) is 85% (Fig. 1). Increase of heavy metal concentrations significantly decreased the germination percentage of barley.

Lead content in soil is very variable. This variability is mainly caused by the parent substrate on which the soil was formed. It is even more absorbed than Cu, Zn, Cd, which behave similarly in soil as lead (Steiger, 1996). The pH reaction of the soil significantly affects the bioavailability of Pb, because increased acidity of soilincreases Pb solubitily. However, this process is relatively slow (Kabata-Pendias, 2011). Usually Pb in soil is highly adsorbed to soil particles and it creates precipitates in high degree. Only about 0.005–0.13% Pb in soil solution is available to plants (Kabata-Pendias, 2011).

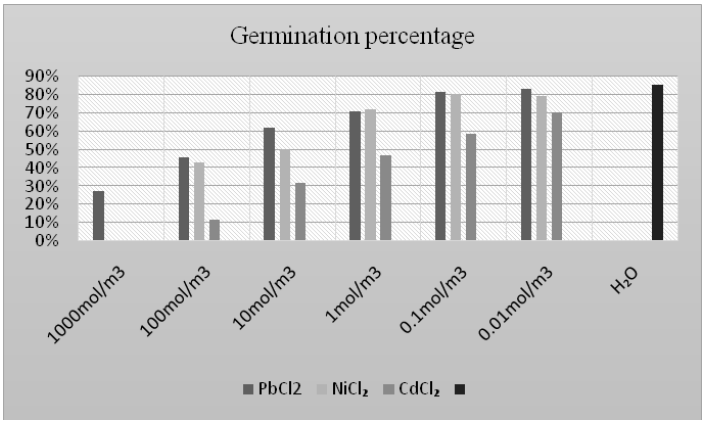

Figure 1. The germination percentage of barley seeds (*Hordeum vulgare* L. varieties Jadran) in solutions of different concentrations of $PbCl_2$, $NiCl_2$, $CdCl_2$

Research results from Azmat et al. (2006) show that lead inhibits germination of seeds, decreases germination percentage, germination index, and root/hypocotyl length in *Phaseolus mungo* and *Lens culinaris* species.

Our research (Tab. 2) shows that the $PbCl_2$ solution has the highest toxicity to germination of the seeds of spring barley (*H. vulgare*) of the Jadran variety at a concentration of 10^3 mol/m^3 where germination is reduced by 58% in relation to control. At the lowest concentration of 10^{-2} mol/m^3 seed germination was reduced by 2% compared to the control.

Table 2. The percentage of germination of barley seeds (*Hordeum vulgare* L. varieties Jadran) in solutions of different concentrations of $PbCl_2$, $NiCl_2$, $CdCl_2$.

	10^3mol/m^3	**10^2mol/m^3**	**10mol/m^3**	**1mol/m^3**	**10^{-1}mol/m^3**	**10^{-2}mol/m^3**
$PbCl_2$	27%	45.5%	61.5%	70.5%	81%	83%
$NiCl_2$	0%	42.5%	50%	71.6%	80%	79%
$CdCl_2$	0%	11.5%	31.5%	46.6%	58.3%	70%
H_2O	85%					

Nickel is an essential element required for plant growth and iron resorption (Chen et al., 2009). It is part of the urease enzyme that hydrolyzes urea in plant tissues (Polacco et al., 2013). The main mechanisms by which plants take up Ni are passive diffusion and active transport (Ahmad & Ashraf 2011). Excess Ni affects the absorption of nutrients at the root, decreases plant metabolism, inhibits photosynthesis and transpiration, causes ultrastructural modifications and oxidative stress (Chen et al., 2009). Nickel disrupts the Krebs cycle and electron transport in the process of oxidative phosphorylation.

Nickel, unlike lead, has good motility in both xylem and phloem and in large quantities is accumulated in fruits and seeds. Leaves usually have the highest nickel content, the younger parts have a higher content than the older ones, and the seeds have a

higher content than the straw..Nickel adversely affects not only the mobility or translocation of iron, but also its uptake.

Leone et al. (2005) indicate that the strongest toxic effect on seed germination has Ni in the form of $NiCl_2$, and weaker as Ni sulfate and Ni acetate.

The results of this studyshow that seeds of *H. vulgare*,Jadran varieties did not germinate in $NiCl_2$ solution, with concentrations of 10^3 mol/m^3 (Fig.1), so this concentration is lethal to seeds of this species. The sublethal concentration is 10^2 mol/m^3 because it is the concentration in which 11.5% seeds germinate, which is 74% less than the control. $NiCl_2$ solution in concentrations from 10 mol/m^3 to 10^{-2} mol/m^3 reduces the germination rate by up to 7% compared to the control (Tab. 1).

Cd is not an essential element for plants, but they adopt it (Porębska & Ostrowska, 1999). Cadmium absorbed from the nutrient medium is generally retained in the root. High concentrations of cadmium in plants inhibit respiration and electron transport in the process of oxidative phosphorylation, inhibit metabolism due to interactions with zinc, induce chlorosis and thus reduce the intensity of photosynthesis. The toxic effect of cadmium on plants has been the subject of numerous studies (Djelic et al., 2016, 2018; Ahmad et al., 2015; Shafi et al., 2010; Stankovic et al., 2010; Khan et al., 2006; Peralta-Videa et al., 2002; Jiang et al., 2001). The obtained results show that the germination of seeds of barley, Jadran variety, in the weakest Cd concentration is 15% less in comparison with the control, 13% less in comparison with the solution of the same Ni concentration and 9% less in comparison with the Pb solution. With increasing concentration of $CdCl_2$ solution, the germination percentage decreases drastically (Tab. 2). The lethal concentration is 10^3 mol/m^3.

Based on the toxic effect on the % germinated seeds of barley (*H. vulgare.*), Jadran variety, we can compare the following: Cd > Ni > Pb.

The average root length on tested seeds of barley (*H. vulgare*) Jadran variety, in water (control) is 76.3 mm (Xmin - 18 mm, Xmax - 132 mm), and the mean hypocotyl length is 71.2 mm (Xmin - 19 mm, Xmax - 135 mm).

The lead solution exhibited the least toxic effect (Tab. 3) of all tested metals, on root and hypocotyl growth. The toxicity of $PbCl_2$ solution was more pronounced on root and hypocotyl length than of% germinated seeds. At a concentration of 10^3 mol/m^3, the root length is 3.1 mm, which is 73.2 mm, is 95,8% shorter than the control and the germination rate at this concentration is reduced by 58%. At a concentration of 10^2 mol/m^3 the root length was 70.7 mm shorter than the control (Tab. 2), and the hypocotyl length 61 mm shorter than the control. Root length in solution of 10 mol/m^3 is 33.1 mm (43.4%), concentration of 1 mol/m^3 is 31 mm (40.6%), concentrations are 10^{-1} mol/m^3 by 23.1 mm (30.3%), concentrations are 10^{-2} mol/m^3 is 22.3 mm (29.26%) smaller than in control. In all $PbCl_2$ tested solutions, there was a significant shortening of hypocotyl length (Tab. 4) relative to the control.

$NiCl_2$ has a stronger toxic effect on root growth and hypocotyl of barley germ than $PbCl_2$. A high level of toxicity can also be observed at a concentration of 10^2 mol/m^3 since the measured root length at this concentration is only 2.3 mm, which is 74 mm (97%) less than the control. The length of the hypocotyl at this concentration is also small (1,6 mm). The solution in concentration of 10 mol/m^3 has slightly weaker toxic effect where the root length is 7.9 mm which is 68.4 mm shorter than the control (Tab. 1) and the length of the hypocotyl is 38.6 mm which is 37.7 mm shorter than the control. If we compare with the values in the solution of $PbCl_2$in concentration of 10 mol/m^3, we will notice that the root length in the nickel solution is shorter by 35.3 mm and the hypocotyls by 33.2 mm shorter than the values measured in the lead solution.

This result indicates a stronger toxic effect of nickel than lead. The root and hypocotyl lengths at a concentration of 1mol/m_3 are 38.6 mm and 52.7 mm, which is 38 mm and 23.9 mm less than the control. and at this concentration $NiCl_2$ has a stronger toxic effect than $PbCl_2$. Concentrations of 10^{-1} mol/m^3 and 10^{-2} mol/m^3have the least toxic effect, but they also significantly reduce root length and hypocotyl.

The root length of the germ of barley (*H. vulgare.*), Jadran variety, at all concentrations of $CdCl_2$ solution is shorter than that in control. In the solution of concentration 10^2 mol/m^3, the root was shorter by 98.8% compared to the control, compared to $PbCl_2$ by 4.6 mm and 82.1%, respectively, and by 1.3 mm and 56.2% shorter than $NiCl_2$. A significant decrease in root growth was also observed in the solution of concentration of 10 mol/m^3, where the root length is 3.4 mm, which is 42.9 mm shorter than the control and 39,8 mm shorter than rootsin $PbCl_2$solution. A significant decrease in the root length of the germ of barley, Jadran variety, was also observed in solutions of 1 mol/m^3, 10^{-1} mol/m^3, 10^{-2} mol/m^3 (Tab.3). The results shown in Tab.4. show that the development of hypocotyl at all tested $CdCl_2$ concentrations have a strong toxic effect.

Based on the toxic effect on the root length and hypocotyl of the germ of barley (*H.vulgare*), Jadran variety, all tested metals can be compared in the series: Cd> Ni> Pb.

Analyzing the variance of the two-factor trial and testing the significance of differences by LSD test for the P 0.05 and 0.01 risk level, we found that there were statistically significant to highly significant differences in root growth (Tab.3) and hypocotyl (Tab.4). The obtained results relate to all tested heavy metals and most of their concentrations compared with the control as well as for the interactions of heavy metals and concentrations.

Germination energy indicates seed quality. If the seeds germinate quickly and at a steady pace, better results are obtained in sowing, and the development of plant is more lush. It is actually a computerized method of utilizing data from the

germination log in which are entered the type and variety of seeds, the date of placement of the sample, the number of germinated seeds per day and the number of germinated seeds at the end of the test (Komljenović & Todorović, 1998).The smaller obtained number, the higher the seed germination energy, since more seeds germinated in shorter period of time.

Data on germination energy is important for practice because it indicates faster growth and independence of some cultivated plant species, which means that crops with higher germination energy will better resist the negative effects of initial growth.

Table 3. Root length (mm) of barley, Jadran variety, treated with heavy metal compounds $PbCl_2$, $NiCl_2$, $CdCl_2$.

solution/ concentration	*$PbCl_2$ (min.-max. mm)*	*$NiCl_2$ (min.-max.mm)*	*$CdCl_2$ (min.-max.mm)*
10^3 mol/m^3	3.1 (1-14)	0 (0-0)	0 (0-0)
10^2 mol/m^3	5.6 (1-26)	2.3 (1-5)	1 (0-1)
10 mol/m^3	43.2 (2-77)	7.9 (1-30)	3.4 (1-69)
1 mol/m^3	45.3 (1-67)	38.6 (3-110)	21.2 (2-132)
10^{-1} mol/m^3	53.2 (11-85)	54.9 (2-112)	35 (1-108)
10^{-2} mol/m^3	54.2 (25-100)	66 (4-107)	47.9 (1-115)
Control	*76.3 (19-135)*	*76.3 (19-135)*	*76.3 (19-135)*
LSD	*A*-Concentratio of heavy metals	*B*- type of heavy Metal	*AB*
0,05	2.111	1.515	7.017
0,01	3.140	2.233	10.510

Table 4. Length of hypocotyl (mm) in barley of Jadran variety treated with heavy metal compounds $PbCl_2$, $NiCl_2$, $CdCl_2$

solution/ concentration	*$PbCl_2$ (min.-max. mm)*	*$NiCl_2$ (min.-max. mm)*	*$CdCl_2$ (min.-max. mm)*
10^3 mol/m^3	2,3 (1-15)	0 (0-0)	0 (0-0)
10^2 mol/m^3**,**	10.2 (1-28)	1.6 (1-5)	1 (0-1)
10 mol/m^3	41.8 (2-79)	8.6 (1-30)	31.6 (1-65)
1 mol/m^3	56.5 (1-105)	52.7 (3-110)	51.2 (2-105)
10^{-1} mol/m^3	57.2 (11-105)	62.1 (2-112)	52.8 (1-106)
10^{-2} mol/m^3	62 (25-100)	63.5 (4-107)	60.6 (1-110)
Control	*71.2 (18-132)*	*71.2 (18-132)*	*71.2 (18-132)*
LSD	*A* Concentration of heavy metals	*B* type of heavy metal	*AB*
0,05	1.277	1.459	4.812
0,01	2.462	2.690	5.440

The results obtained for the germination energies of barley seeds in solutions of different concentrations of $PbCl_2$, $NiCl_2$, $CdCl_2$ (Tab. 5) indicate that the tested solutions at all concentrations significantly reduce the energy of germination of barley seeds (*H. vulgare*), Jadran variety. It is observed that germination energy decreases with increasing solution concentration.

Table 4. Comparative energy overview of the seed seeds in the solubility of various concentrations of $PbCl_2$, $NiCl_2$, $CdCl_2$.

	10^3 mol/m^3	10^2 mol/m^3	10 mol/m^3	1 mol/m^3	10^{-1} mol/m^3	10^{-2} mol/m^3
$PbCl_2$	4.5	3.5	2.9	2.7	2.1	1.8
$NiCl_2$	0	3.9	3.1	3	2.3	1.9
$CdCl_2$	0	5	4.3	3.9	3	2
H_20	1.5					

The germination energy in the control is 1.5. In a solution of $NiCl_2$, and $CdCl_2$ at a concentration of 10^{-2} mol/m^3 is the smallest decrease in germination energy. $PbCl_2$ solution has the weakest toxic effect compared to all tested metal. Seed germination occurred at all concentrations of this metal. However, the development of the germ shows that the lead has a toxic effect. A particularly good indicator of its toxicity is germination energy. In the solution of concentration 10^{-2} mol/m^3 germination energy is 1.8. and this indicates that it takes longer for seeds to germinate than in control. The tested heavy metals at all concentrations showed a stronger toxic effect on germination energy than ongermination percentage.

Based on the toxic effect on the germination energy of barley seeds (*H. vulgare*), Jadran variety, the tested metals can be compared in the following order: Cd> Ni> Pb.

In plants, these metals directly or indirectly cause a wide range of physiological and biochemical dysfunctions that lead to reduced yield (Amari et al., 2017). Cd, Pb, and Ni show phytotoxic effects on germination and germ development in *Lactuca sativa*, *Brassica oleraceae*, *Lycopersicon esculeatum*, *Raphanus sativus* (Johnson et al., 2011), *Helianthus annus* (Jadia & Fulekar, 2008).

CONCLUSION

Based on the results obtained by testing different concentrations of $PbCl_2$, $NiCl_2$, $CdCl_2$ solutions, on the percentage of germination, germination energy, root length and hypocotyl of the species (*Hordeum vulgare* L.), Jadran variety, it can be concluded that: barley seeds have significantly reduced germination in the presence of all tested heavy metals and germination length, root length and hypocotyl, as well as germination energy depend on the type of heavy metal and solution concentrations. The most toxic effect has Cd and the weakest toxic effect has Pb.

REFERENCES

Ahmad, M. S., & Ashraf, M. 2011. Essential roles and hazardous effects of nickel in plants. Rev Environ Contam Toxicol. 214, pp. 125-67. doi: 10.1007/978-1-4614-0668-6_6

Ahmadi, I., Javed Akthar, M., Zahir A. Z., & Jamil, A. 2012. Effect of cadmium on seed germination and seedling growth of four wheat (*Triticum aestivum*L.) cultivars. Pak. J. Bot., 44(5), pp. 1569-1574.

Amari, T., Ghnaya, T., & Abdelly, C. 2017. Nickel, cadmium and lead phytotoxicity and potential of halophyticplants in heavy metal extraction, South African Journal of Botany, 111, pp. 99-110. doi.org/10.1016/j.sajb.2017.03.011

Azmat, R., Haiderand, S., & Askari S. 2006. Phytotoxicity of Pb: I Effect of Pb on Germination, Growth, Morphology and Histomorphology of *Phaseolus mungo* and *Lens culinaris*, Pakistan Journal of Biological Sciences, 9(5), pp. 979-984. doi: 10.3923/pjbs.2006.979.984

Chen, C., Huang, D., & Liu, J. 2009. Functions and Toxicity of Nickel in Plants: Recent Advances and Future Prospects, Clean 37(4-5), pp. 304-313. doi.org/10.1002/clen.200800199

Djelic, G., Staletic, M., & Milovanovic, M. 2012. Germination of oat (*Avena sativa*) seeds under heavy metal stress, Ecological movemetn of Novi Sad, Eco-conference 2012, pp. 251-259.

Djelic, G., Markovic, M., Brankovic, S., Brkovic, D., Vicentijevic-Markovic, G., & Markovic, G. 2016. Efekat teških metala (Cd, Fe, Ni, Zn) na klijanje sem*ena Robinia pseudoacacia* L. Zbornik radova XXI Savetovanja obiotehnologiji sa međunarodnim učešćem, Čačak, 21(23), pp. 373-378.

Djelic, G., Novakovic, M., Brankovic, S., Timotijevic, S., & Simic, Z. 2018. Comparative analysis of metal bioaccumulation et species *Petroselinum crispum* Mill, *Seselirigidum*W et K, *Daucus carota*L., *Conium maculatum* L. Third Scientific Conference on Ecology, November 2th -3th 2018, Plovdiv, Program & Abstracts, pp 57.http://web.uni-plovdiv.bg/ecology/TACE2018/TASCE_2018_program_&_book_of_abstracts.pdf.

Jadia, D. C., & Fulekar, H. M. 2008. Phytoremediation: the application of vermicompost to remove zinc, cadmium, copper, nickel and lead by sunflower plant, Environmental Engineering and Management Journal, 7(5), pp. 547-558. doi: 10.30638/eemj.2008.078

Jiang, W., Liu, D., & Hou, W. 2001. Hyperaccumulation of cadmium by roots, bulbs and shoots of garlic. Biores. Technol., 76, pp. 9-13. doi: 10.1016/s0960-8524(00)00086-9

Johnson, A., Singhal, N., & Hashmatt M. 2011. Metal-plant Interactions: Toxicity and Tolerance in: Khan, SM, Zaidi, A., Goel, R., Musarrat J., (eds): Biomanagement of Metal-Contaminated Soils, Springer Dordrecht Heidelberg London New York, pp. 29-67.

Kabata-Pendias, A. 2011.Trace elements in soils and plants, 4th ed. CRC Press, Taylor&Francis Group, Boca Raton London New York Washington, D.C.

Kenedy, S. P., Bingham, I. J., & Spink, J. H. 2017. Determinants of spring barley yield in a high-yieldpotential environment, The Journal of Agricultural Science, 155(1), pp. 60-80. doi.org/10.1017/S0021859616000289

Khan, N. A., Ahmad, I., Singh, S., & Nazar, R.. 2006. Variation in growth, photosynthesis and yield of five wheat cultivars exposed to cadmium stress. World J. Agri. Sci., 2, pp. 223-226.

Komljenovic, I., & Todorovic, V. 1998. Opsteratarstvo-udzbenik Poljoprivredni fakultet. Banja Luka.

Kricka, T., Kis, D., Matin, A., Brlek, T., & Bilandžija, N. 2012. Tehnologija mlinarstva, Poljoprivredni fakultet u Osijeku, Agronomski fakultet u Zagrebu.

Leone,V., Rabier, J., Notonier, R., Barthelemy, R., Moreau, X., Bouraima-Madjebi, S., Viano, J., & Pineau, R. 2005. Effects of Three Nickel Salts on Germinating Seeds of *Grevilleaexul* var. *rubiginosa*, an Endemic Serpentine Proteaceae, Ann Bot. 95(4), pp. 609–618. doi:10.1093/aob/mci066

Madic, M., Knezevic, D., & Paunovic, A. 2011. Osnovni parametri u oplemenjivanju jecma (*Hordeum vulgare* L.) naprinos I kvalitet. u: Medjunarodni naučni simpozijum agronoma AGROSYM Jahorina, 2011, Republika Srpska, Zbornik radova, pp. 276-286.

Peralta-Videa, J. R,. Gardea-Torresdey, J. L, Gomez, E., Tiermann, K. J., Parsons, J. G., & Carrillo, G.. 2002. Effect of mixed cadmium, copper, nickel and zinc at different pHs upon alfalfa growth and heavy metal uptake. Environ. Pollut., 119, pp. 291-301. doi: 10.1016/s0269-7491(02)00105-7

Pesko, M., KráÍová, K.,, & Masarovicová, E. 2011. Phytotoxic effect of same metal ions on selected raspeseed cultivars registered in Slovakia. Proceedings of ECOpole, 5(1), pp. 83-86.

Poehlman, J. M. 1985. Adaptation and distribution. In: Rasmusson DC, editor. Barley. Madison, Wisconsin: American Society of Agronomy, Inc., Crop Science Society of America, Inc., Soil Science Society of America, Inc. pp. 1-17. doi.org/10.5772/intechopen.68359

Polacco J. C., Mazzafera P., & Tezotto T. 2013. Opinion: nickel and urease in plants: still many knowledge gaps. Plant Sci. 199-200, pp. 79-90. doi: 10.1016/j.plantsci.2012.10.010

Porebska, G., & Ostrowska. A. 1999. Heavy Metal Accumulation in Wild Plants: Implications for Phytoremediation, Polish Journal of Environmental Studies, 8(6), pp. 433-442.

Rajkovic, M., Stojanovic, M., Glamoclija, Dj., Toskovic, D., Miletic, V., Stefanovic, V., & Lacnjevac, C. 2012. Pšenica i teškimetali, Journal of Engineering & Processing Management, 4(1), pp. 85-125 doi:10.7251/JEPM1204085R

Salamini, F., Özkan, H., Brandolini, A., Schäfer-Pregl, R., & Martin, W. 2002. Genetics and geography of wild cereal domestication in the near east. Nature Reviews Genetics. 3(6), pp. 429-441. doi: 10.1038/nrg817

Shafi, M., Zhang, G.. P.,Bakht, J., Khan, M. A. ,Islam, E., Dawood, M. K., & Raziuddin, I. 2010. Effect of cadmium and salinity stresses on root morphology of wheat. Pak. J. Bot., 42(4), pp. 2747-2754.

SPSS Inc. Systat 10.0 Statistics I software. Chicago; 2000. p. 663.

Stankovic, M., Markovic, A., Pavlovic, D., Topuzovic, M., Djelic, G., Bojovic, B., & Brankovic, S. 2010. Toksicni efekat kadmijuma (Cd) na klijanje semena psenice *(Triticum aestivum L.)*. Zbornik radova sa XV Savetovanja o biotehnologiji. 15(17), pp. 975-980.

Steiger B. V., Webster, R., Schulin, R., & Lehmann, R. 1996. Mapping heavy metals in polluted soil by disjunctive kriging. Environ. Pollut., 94, pp. 205–215. doi:10.1016/s0269-7491(96)00060-7

Zhang J, Zheng H. G., Aarti, A., Pantuwan,G,, Nguyen, T. T., Tripathy, J. N., Sarial, A. K., Robin, S., Babu, R. C., Nguyen, B. D., Sarkarung, S., Blum, A., & Nguyen, H. T. 2001. Location genomic regions Barley (*Hordeum vulgare* L.) Improvement Past, Present and Future associated with components of drought resistance in rice: Comparative mapping within and across species. Theoretical and Applied Genetics, 103, pp. 19-29. doi.org/10.5772/intechopen.68359 63

Tanner, G. J, Blundell, M. J, Colgrave, M. L., & Howitt, C. A. 2016. Creation of the first ultra-low gluten barley (*Hordeum vulgare* L.) for coeliac and gluten-intolerant populations, Plant Biotechnol J. 14(4), pp. 1139-1150. doi: 10.1111/pbi.12482

Bulletin of Natural Sciences Research
Vol. 10, No. 2, 2020, pp. 7-11.
DOI: https://doi.org/10.5937/bnsr10-23098
Original Scientific Paper

MORPHOLOGICAL VARIABILITY AND SEXUAL DIMORPHISM OF NOBLE CRAYFISH *Astacus astacus* FROM THE BALKANA LAKE

RAJKO ROLJIĆ[1], VERA NIKOLIĆ[2], NEBOJŠA SAVIĆ[3]

[1]Genetic Resources Institute University City, University of Banja Luka, Banja Luka, Bosnia and Herzegovina
[2]Faculty of Biology, University of Belgrade, Beograd, Serbia
[3]Faculty of Agriculture University City, University of Banja Luka, Banja Luka, Bosnia and Herzegovina

ABSTRACT

This paper presents the information about morphological variability and sex dimorphism of the Noble crayfish (*Astacus astacus*) in the area of the Balkana Lake in Mrkonjic Grad. The crayfish were caught by hand made baited traps from October 9nd 2018. until May 31th 2019. A total of 58 crayfish were caught, of which 38 males and 20 females. The eight morphometric characteristics: body weight (W), body length (TBL), claw length (CLL), cephalothorax length (CFL), carapace width (CPW), abdomen length (ABL), rostrum length (ROL) and rostrum width (ROW) were measured, both in males and females. Also, the body condition was determined for all specimens. The results of morphometric characteristics partially matched into the already known range of variations. These data represent first ones for the observed area. The t-test showed that there were significant differences between the sexes in W, TBL, CLL, CFL and CPW which are explained by the emphasized sex dimorphism of the noble crayfish.

Keywords: Noble crayfish, Morphometric features, Sex dimorphism, The Balkana Lake.

INTRODUCTION

The morphometric features of crayfish are the basic criteria for specifying the taxonomic status of the species. Precise crayfish taxonomy involves the application of these methods combined with anatomical, morphological, cytogenetic, biochemical, physiological, ecological, evolutionary, and other methods (Vukovic et al., 1978). A study of morphometric features of certain crayfish species from various water ecosystems to determine their systematic position and status was conducted by numerous authors such as Trozic-Borovac et al. (2007), Trozic-Borovac (2012a, 2012b) and Rajkovic (2012). Maguire (2010) emphasizes the importance of research of morphometric feature variability in species from the genus *Astacus* and *Austropotamobius* in order to produce an efficient key for determination, given the present difficulties in determination thereof.

There is a lack of information available of morphometric features of for species *Astacus astacus* from numerous places within their distribution area. The Noble crayfish lives in rivers and lakes with muddy or gravel bed, and seeks for the shelter by the coast covered with aquatic vegetation, or digs the holes (Maguire, 2010). This species is present and dominate in Bosnia and Herzegovina (Trozic-Borovac, 2011) and neighboring countries such as Serbia (Simic et al., 2008), Croatia (Maguire & Gottstein-Matocec, 2004), Montenegro (Rajkovic, 2012) and Kosovo and Metochia (Zivic et al., 2014).

A significance of morphometric study of crayfish from the *A. astacus* species is justified by the fact that it is autochthonous European species being on the IUCN list of endangered species. According to IUCN criteria the said species was assigned to the VU (Vulnerable) category for the European region (Edsman et al., 2010) and is listed on the national Red List of Bosnia and Herzegovina as vulnerable species.

This study aims to determine variability of selected morphometric features of male and female specimens of the Noble crayfish from the Balkana Lake in Mrkonjic Grad.

MATERIALS AND METHODS

The Tourist and Recreational Center "Balkana" is located in the northwest of the Municipality of Mrkonjic Grad, 4-5 km away from the city and next to the motorway Jajce- Mrkonjic Grad-Bihac (formerly known as the "AVNOJ road"). It is situated at 750 m above sea level, in the foothill of the Lisina Mountain (1.650 m altitude).

What makes this complex very special are the Balkana Lakes at the altitude of 750 m. Surface of the small lake (downstream) is 10.800 m^2 and surface of the big lake (upstream) is 42.300 m^2 (Figure 1, 2). The lakes were formed by natural depression which volume increased when a dam was constructed. The lake is separated in two parts by a lateral embankment. Principal filling of the lake is made by two smaller watercourses (Cijepalo from the right side composed of two springs - the Kovacko and Lazino spings from the left side of the thermal spring) that flows into the Big Lake and airfoil spring at

* Corresponding author: rajkoroljic@gmail.com

the bottom of the Big Lake. The Crna Rijeka river flows out from the Lake (Crnogorac et al., 2013).

Figure 1. The Small Lake of Balkana.

Figure 2. The Big Lake of Balkana.

Field studies were conducted in the period from October 9, 2018 until May 31, 2019. Sampling period included three seasons of crayfish activity: autumn, winter and spring. Sampling was carried out in two locations – one location was in the Malo jezero lake and the other location was the Veliko jezero lake. Crayfish were sampled with baited LiNi traps (Westman et al., 1978). We left traps overnights and collected crayfish the next morning. Then, 58 crayfish specimens were collected. Time of collection, apparent physical defects, signs of illness and parasites were recorded for each specimen. Afterwards, sex was determined for each collected specimen and morphometric features were measured.

Morphometric features such as: total body length (TBL), claw length (CLL), carapace length (CPL), carapace width (CPW), abdomen length (ABL), rostrum length (ROL), rostrum width (ROW) and values of body weight (W) were analyzed.

The fit/fitness coefficient was also calculated: Fulton´s Conditions Factor (Ricker, 1975) and Crayfish Constant (Adegboye, 1981).

Fulton's Conditions Factor (FCF):

$$FCF = \frac{W}{TBL^3}$$

Where: W – total weight, TBL – total length

Crayfish Constant (CC):

$$CC = \frac{W}{TBL \times CPL \times CPW}$$

Where: W – total weight, TBL – total length, CPL – carapace length, CPW– carapace width (Streissl & Höld, 2002).

Each specimen was measured with caliper to the nearest 0.02 mm and weight to the nearst 0.01 g with technical balance (type ''Kern'' PFB Version 2.2). Obtained values of morphometric features were processed statistically (minimum, maximum, mean value, standard deviation and variation coefficient) by applying statistical program Microsoft Office Excel 2007, interpreted and compared to available data from related literature.

Database with photos was created and each specimen was captured from dorsal and ventral side. Such photos can serve to analyze body color and to identify re-collected specimen.

RESULTS

There were 58 analyzed specimens of which 38 (in particular 65.52%) were male and 20 (in particular 34.48%) were female (sex ration close to 1.9 : 1) (Figure 3).

Figure 3. *Astacus astacus* – noble crayfish (male left, female right).

Measurement results of morphometric parameters of the Noble crayfish specimen from the Balkana Lake are given in tables as mean value, minimum (min), maximum (max), standard deviation (SD) and coefficient of variation (CV) (Table 1, 2).

The values obtained for male specimens show that the average body weight was 27.99 g, an average body length was 85.57 mm, the claw length was 36.25 mm, the cephalothorax length was 41.57 mm, the carapace width was 23.94 mm, the abdomen length was 36.78 mm, the rostrum length was 11.19 mm and the rostrum width was 5.5 mm. Based on these values,

the standard deviation (SD) was obtained and had the highest value for body length (17.46), slightly smaller value for the total body length (17.2), the claw length (9.63), the abdomen length (9.03), the cephalothorax length (7.82), the carapace width was (5.82), and the least value was for the rostrum length (2.75) and width (0.38). The only steady feature at male specimens (CV < 10%) showed a morphometric feature (ROW) (CV = 6.87%). CFL (CV = 18.8%) falls into a low variable (10% - 20%). Most of the analyzed morphometric features were moderately variable (CV 20% - 30%, Table 1). Morphometric feature W (CV = 62.37%) at male specimens is the only feature that shows high variability (CV > 30%) (Table 1).

Table 1. Descriptive statistics - mean value, standard deviation, ranges of measured morphometric characteristics for males of species *Astacus astacus* from the Balkana lake.

Statistical parameters	Mean	Min	Max	SD	CV
W	27.99	5.8	72	17.46	62.37
TBL	85.77	56.35	114.14	17.2	20.1
CLL	36.25	18.8	56.71	9.36	26.56
CFL	41.57	28.16	51.79	7.82	18.8
CPW	23.94	13.7	39.1	5.82	24.3
ABL	36.78	18.9	43.37	9.03	24.55
ROL	11.19	7.39	15.81	2.75	24.54
ROW	5.5	5.08	6	0.38	6.87

The values obtained for female specimens show that the average body weight was 17.09 g, an average body length was 74.34 mm, the claw length was 24.81 mm, the cephalothorax length was 31.34 mm, the carapace width was 18.56 mm, the abdomen length 32.15 mm, the rostrum length was 11.54 mm and the rostrum width was 5.46 mm.

Based on these values, the standard deviation (SD) had the highest value for the total body length (16.38) and the body weight (11.54), slightly smaller for the abdomen length (8.78), the cephalothorax length (8.0), the claw width (6.64) and the carapace width (4.64) while the least value was for the rostrum length (1.99) and the width (0.58). The observed morphometric features are moderately variable (CV 20% - 30%), while a morphometric feature W (CV = 63.17%) was the only highly variable (CV > 30%). None of analyzed features (Table 2) was a steady morphometric feature in female samples (CV < 10%).

Males and females differ significantly ($p < 0.05$) in five morphometric features W ($p = 0.009$), TBL ($p = 0.013$), CLL ($p = 0.000$), CFL ($p = 0.025$) and CPW ($p = 0.001$) (Table 3). There is no statistically significant difference ($p > 0.05$) for ABL ($p = 0.195$, ROL ($p = 0.403$) and ROW ($p = 0.441$) (Table 3). By comparing the mean values of the abdomen length and rostrum width and length among the sexes, the Noble crayfish males have a higher mean value for the previously mentioned morphometric features compared to females, but that difference is not significant in statistical terms.

Table 2. Descriptive statistics - mean value, standard deviation, ranges of measured morphometric characteristics for females of species *Astacus astacus* from the Balkana lake.

Statistical parameters	Mean	Min	Max	SD	CV
W	17.09	6.5	48	11.54	67.5
TBL	74.34	46.1	105.6	16.38	22.03
CLL	24.81	12.24	37.44	6.64	26.75
CFL	31.34	19.19	40.8	8.0	25.52
CPW	18.56	11.6	26.4	4.64	25.02
ABL	32.15	17.92	41.47	8.78	27.3
ROL	11.54	8.55	14.0	1.99	17.25
ROW	5.46	4.4	6.0	0.58	10.66

Table 3. Significance of differences between mean values of morphometric characteristics of crayfish species *Astacus astacus* from the Balkana lake.

No.	Character	P	No.	Character	p
1.	W	0.009409	5.	CPW	0.000586
2.	TBL	0.012641	6.	ABL	0.19451
3.	CLL	0.000016	7.	ROL	0.402779
4.	CFL	0.024528	8.	ROW	0.44076

The correlation between total body length and weight of males (90.43%) and females (81.68%) was calculated (Figure 4). Which shows that body weight increases as the body length increases.

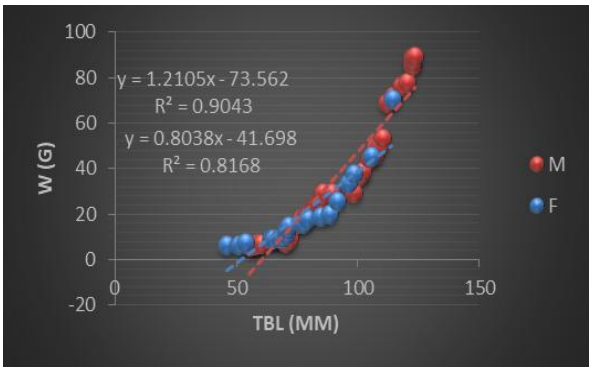

Figure 4. The ratio of body length and body weight of males and females of Noble crayfish.

The correlation between body weight and the claw length in both males, females is made and we notice a positive correlation, which means that the claw growth accompanies the body weight. The correlation coefficient is 93.42% in males and 93.14% in females (Figure 5).

Based on the correlation coefficient by applying regression analysis, it is observed that the coefficient is highly significant in statistical terms between the carapace width and the body length. The correlation coefficient is 97.76% and 92.2% in females (Figure 6).

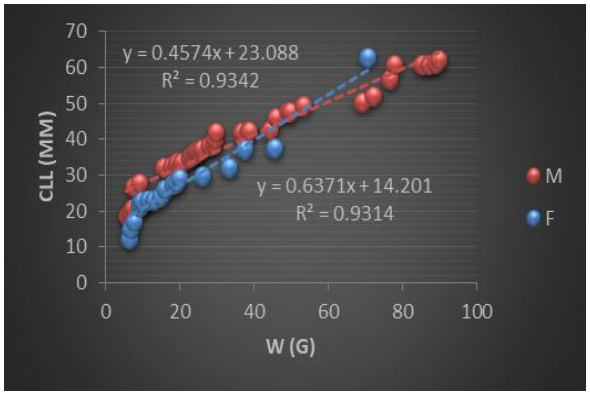

Figure 5. Relation of body weight and claw length in males and females of Noble crayfish.

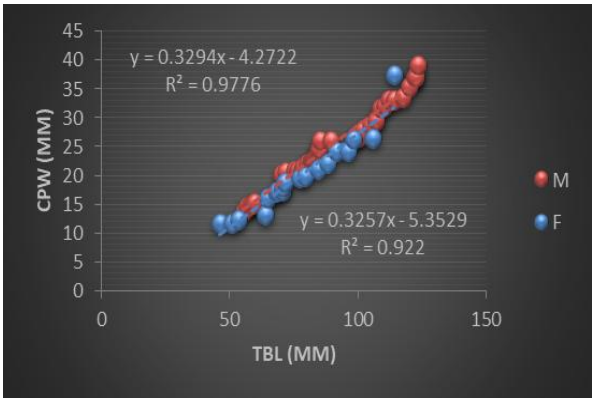

Figure 6. The ratio of body length and width of a carapace in males and females of Noble crayfish.

The least CC is 0.228 and the highest CC is 0.401 (for females). The mean value is 0.309 for females and 0.386 for males. The least FCF is 0.022 and the highest is 0.039 (for females). The mean value is 0.029 for females and 0.037 for males (Table 4).

Table 4. Values for condition factor for Noble crayfish specimen.

Statistical parameters	FCF				
Sex	Mean	Min	Max	SD	CV
M	0.037	0.026	0.055	0.011	30.91
F	0.029	0.022	0.039	0.007	22.64
Statistical parameters	CC				
Sex	Mean	Min	Max	SD	CV
M	0.386	0.272	0.488	0.09	24.41
F	0.309	0.228	0.401	0.066	21.47

DISCUSSION

Sex ration between male and female was 1.9:1 (males : females). A higher degree of male presence in the sample can be correlated with the fact that five female specimens with brooding eggs were sampled during the study period, pointing out to a season of a lower female activity (Rajkovic, 2012). Having information on the sex ratio in population is significant because it tells us about the health and stability of the population (Jurkovic, 2016)

Population of the noble crayfish at the observed location has relatively stable age structure. At the explored location on the Balkana Lake, the largest group was 101 - 120 mm long with a 60% share in population. The longest male body was 114.4 mm, and the longest female body was 105.6 mm that corresponds to the range from 80 to 120 mm applicable to the Noble crayfish mentioned in the related literature (Obradovic, 1988), and values recorded by Trozic-Borovac et al. (2012b) and Rajkovic (2012). The heaviest male was 72 g and the heaviest female was 48 g. The higher average male weight can be attributed to the fact that males has bigger claws that contributes to their higher body weight compared to females (Jurkovic, 2016).

Morphometric features of males and females from the *A. astacus* species found in the Balkana Lake considerably differ in statistical terms ($p < 0.05$), where higher mean values were noticed for most of male features (Table 3). Obtained results can be correlated with the expressed sex dimorphism of crayfish from this species, where males are bigger than females (Trozic-Borovac et al., 2012b; Rajkovic, 2012).

According to values of calculated factors we notice that males are more fit. A study of the Noble crayfish specimen fit factor in the Praca river supports the foregoing (Trozic-Borovac et al., 2012b).

CONCLUSION

Morphometric features of the Noble crayfish (*Astacus astacus*) in the Balkana Lake were monitored.

Seven morphometric features and two fit factors were analyzed on all 58 specimens (38 males and 20 females).

Obtained values for morphometric features of the Noble crayfish in the area of Mrkonjic Grad partially match the known scope of variability and represent first data for the investigated area.

Presence of statistically significant difference among adult specimens in body mass, total body length, the claw length, the cephalothorax length and the carapace width at males compared to females is justified by emphasized sex dimorphism in the Noble crayfish.

Data presented in this paper can serve as a basis for further research of *Astacus astacus* in this area.

ACKNOWLEGMENTS

The paper presents the result achieved by realization of Program for the conservation and sustainable use of genetic resources of Republic of Srpska, financed by the Ministry of

Scientific and Technological development, Higher Education and Information Society performs of the Republic of Srpska and implemented by the Institute of Genetic Resources of the University of Banja Luka.

Expert opinion on the research of biodiversity was issued by the Republic Institute for the Protection of Cultural, Historical and Natural Heritage (No. 30 / 625-723 / 18, 09.10. 2018th year; number 07/1.30/625-020/19, dated 23.1. 2019).

REFERENCES

Crnogorac, C., Trbic, G., Rajcevic, V., Dekic, R., Pesevic, D., Lolic, S., Milosevic A., & Celebic, M. 2013. Rijecna mreza opstine Mrkonjic Grad - fizickogeografska i ekoloska istrazivanja. Geografsko drustvo Republike Srpske, 147.

Edsman, L., Füreder, L., Gherardi, F., & Souty-Grosset, C. 2010. *Astacus astacus*. The IUCN Red List of Threatened Species 2010: e.T2191A9338388. Downloaded on 24 October 2019.

Jurkovic, T. 2016. Populacijske znacajke potocnog raka *Austropotamobius torrentium* (Schrank, 1803) u potoku Dolje. Diplomski rad, Prirodoslovno-matematicki fakultet Sveucilista u Zagrebu, 50.

Maguire, I. 2010.Slatkovodni rakovi, Prirucnik za inventarizaciju i pracenje stanja. Drzavni zavod za zastitu prirode, Zagreb, 44.

Maguire, I., & Gottstein-Matocec, S. 2004. The distribution pattern of freshwater crayfish in Croatia. Crustaceana, 77(1), pp. 25-47. doi: 10.1163/156854004323037874

Obradovic, J. 1988. Slatkovodni rakovi. Ribar. Jugoslavija, 43, pp. 55-59.

Rajkovic, M. 2012. Distribucija, filogenija, ekologija i konzervacija rakova iz familije *Astacidae* na podrucju Crne Gore. Doktorska disertacija. Prirodno-matematicki fakultet, Univerzitet u Kragujevcu.

Simic, V., Petrovic, A., Rajkovic, M., & Paunovic, M. 2008. Crayfish of Serbia and Montenegro – The population status and the level of endangerment. Crustaceana, 81, pp. 1153-1176. doi: 10.1163/156854008X374496

Streissl, F., & Hödl, W. 2002. Growth, morphometrics, size at maturity, sexual dimorphism and condition index of *Austropotamobius torrentium* Schrank. Hydrobiologia, 477, pp. 201-208. doi: 10.1023/A:1021046426577

Trozic-Borovac, S 2011. Freshwater crayfish in Bosnia and Herzegovina: the first report on their distribution. Knowledge and Management of Aquatic Ecosystems, 401, pp. 26. doi: 10.1051/kmae/2011048

Trozic-Borovac, S., Deljanin, L., & Dautbasic, M. 2007. Ekolosko-biosistematske karakteristike potocnog raka *Austropotamobius torrentiumm* (Shrank, 1803.) iz Nahorevskog potoka, Radovi Sumarskog fakulteta, Univerzitet u Sarajevu, pp. 39-55.

Trozic-Borovac, S., Macanovic, A., & Skrijelj, R. 2012a. The morfometrics characterics and condition index of *Austropotamobius pallipes* in the Neretva river basin. Works of the Faculty of Forestry, University of Sarajevo, 2, pp. 13 - 30.

Trozic-Borovac, S., Nuhefendic, I., Gajevic, M., & Imamovic, A. 2012b. Morphometrics characters of *Astacus astacus* L.(Astacidae) from the Praca river. Works of the Faculty of Forestry University of Sarajevo, 1, pp. 1-10.

Vukovic, T., N . Guzina, N., Vukovic, D, Seratlic, E. Durovic., & Sofradzija. A. 1978. Problemi razvoja biosistematskih istrazivanja slatkovodnih riba u Bosni i Hercegovini. Godisnjak Bioloskog Instituta Univerziteta u Sarajevu, 31, pp. 207-211.

Westman K., Pursiainen M., & Vilkman R. 1978. A new folding trap model which prevents crayfish from escaping. Freshwater Crayfish, 4, pp. 235-242.

Zivic, V. N., Atanackovic, A., Milosevic, S., & Milosavljevic, M. 2014. The distribution of Astacidae (Decapoda) fauna in Kosovo and Metohija. Water Research and Management, 4(4), pp. 35-40.

Bulletin of Natural Sciences Research
Vol. 10, No. 2, 2020, pp. 12-16.

DOI: https://doi.org/10.5937/bnsr10-26133
Original Scientific Paper

SYNTHESIS AND COMPLETE NMR SPECTRAL ASSIGNMENTS OF NEW BENZYLAMINO COUMARIN DERIVATIVE

VIDOSLAV DEKIĆ[1*], NIKO RADULOVIĆ[2], MILENKO RISTIĆ[1], BILJANA DEKIĆ[1], NOVICA RISTIĆ[1]

[1]Faculty of Sciences, University in Priština - Kosovska Mitrovica, Kosovska Mitrovica, Serbia
[2]Department of Chemistry, Faculty of Sciences and Mathematics, University of Niš, Niš, Serbia

ABSTRACT

This research involves the reaction of 4-chloro-3-nitrocoumarin and (4-methoxyphenyl)methanamine, whereby a novel coumarin derivative 4-[(4-methoxybenzyl) amino]-3-nitro-2*H*-chromen-2-one was obtained in good yield. The reaction was carried out in ethyl acetate, in the presence of triethylamine. Also, a detailed spectral analysis of a new coumarin derivative is presented. Resonance assignment was achieved using one- (^{1}H NMR and ^{13}C NMR) and two-dimensional NMR techniques (^{1}H-^{1}H-COSY, NOESY, HSQC, and HMBC). The NOESY correlations of protons from arylamino substituent and coumarin core indicate their spatial orientation.

Keywords: Coumarins, Synthesis, Spectral analysis, ^{1}H NMR, ^{13}C NMR, 2D NMR.

INTRODUCTION

Coumarins are important, naturally occurring heterocyclic compounds (Barry, 1964; Murray, 1989; O'Kennedy & Thornes, 1997). Secondary metabolites occurring in plants include a large number of different groups of compounds. Coumarins represent one of them and they are found in all plant vegetative and reproductive organs, from root to seed. Their function is far from clear, but suggestions include the role of the waste products, plant growth regulators, fungistats and bacteriostats (Murray et al., 1982). Coumarins have long been recognized to possess anti-inflammatory, anti-oxidant, anti-allergic, hepatoprotective, anti-thrombotic, anti-viral, anti-microbial and anti-carcinogenic activities (Jung et al., 2008). Many coumarin derivatives represent the compounds with an important role in the dyes industry. Also, they have characteristic properties that allow them to be used as optical brighteners, laser dyes, nonlinear optical chromophores, solar energy collectors, fluorescent labels and probes in biology and medicine, and two-photon absorption (TPA) materials (Turki et al., 2007; Li et al., 2007; Melavanki et al., 2008; Yu et al., 2009).

The bioactivities of coumarins are based on the influence of the coumarin nucleus, but a significant role in the pharmacological and biochemical properties of coumarins also depends on the pattern of substitution (Jiménez-Orozco et al., 1999; Finn et al., 2001). Due to their medicinal and physiological properties, coumarins have been intensively studied, and a large number of synthetic organic chemists emphasized their simplest and most efficient synthesis.

The physical and chemical properties of coumarins are well-known, but little attention has been paid to their properties in nuclear magnetic resonance. As a part of our continuing investigations about coumarins (Dekić et al., 2010; Dekić et al., 2014), we report herein the synthesis of new coumarin derivative and complete assignments of his ^{1}H and ^{13}C NMR spectral data based on a combination of 1D and 2D NMR experiments.

EXPERIMENTAL

Materials and methods

Melting points were determined on a Kofler hot-plate apparatus and are uncorrected. HRMS(EI) spectra were recorded on a JEOL Mstation JMS 700 instrument (JEOL, Germany). Thermo Nicolet 6700 FTIR spectrophotometer was used for IR measurements. For TLC, silica gel plates (Kiesel 60 F254, Merck) were used. TLC plates were caused by spraying with aqueous sulfuric acid (1:1, *v*/*v*) and heating afterward. All solvents (HPLC grade) and other chemicals were purchased from Sigma-Aldrich (USA), Merck (Germany), and Fluka (Germany).

NMR measurement

All NMR spectra were recorded at 25 °C in DMSO-d_6 with TMS as an internal standard. Chemical shifts are reported in ppm (δ) and referenced to TMS (δ_H = 0 ppm) in ^{1}H NMR spectra or to residual DMSO-d_5/$^{13}CD_3SOCD_3$ (δ_H = 2.50 ppm, δ_C = 39.52 ppm) in heteronuclear 2D spectra. Scalar couplings are reported in Hertz.

The ^{1}H and ^{13}C NMR spectra of the synthesized compound were recorded on a Bruker Avance III 400 MHz NMR spectrometer (^{1}H at 400 MHz, ^{13}C at 100 MHz), equipped with a 5-mm dual ^{13}C/^{1}H probe head.

Synthesis

Synthesis of 4-chloro-3-nitrocoumarin (3)

The synthesis of 4-chloro-3-nitrocoumarin (3) was carried out according to a previously published procedure (Kaljaj et al., 1987). 4-Hydroxycoumarin (1) was nitrated with a mixture of

* Corresponding author: vidoslav.dekic@pr.ac.rs

HNO_3 (72%) and glacial acetic acid to afford 4-hydroxy-3-nitrocoumarin. The synthesis of the starting compound, 4-chloro-3-nitrocoumarin (3) was carried out in the second reaction step by the following manner: *N*, *N*-dimethylformamide (DMF, 4 ml, 52 mmol) was cooled to 10 ºC in an ice bath. With stirring, $POCl_3$ (8.0 g, 52 mmol) was added dropwise, and the obtained mixture was stirred for an additional 15 min. After the expiration of the estimated period time, the reaction was continued at room temperature for the next 15 minutes. Afterward, the solution of 4-hydroxy-3-nitrocoumarin (10.8 g; 52 mmol) in DMF (25 ml) was added dropwise and the obtained mixture was stirring for another 15 minutes. Finally, to stop the reaction, 30 ml of ice-cold water was added. The precipitated solid was collected by filtration and washed with saturated sodium bicarbonate solution and water. Recrystallization from the mixture of benzene-hexane (1:1, *v*/*v*) yielded yellow crystals of 4-chloro-3-nitrocoumarin (10.2 g) in 87% yield, m.p 162-163 ºC.

Synthesis of 4-[(4-methoxybenzyl)amino]-3-nitro-2H-chromen-2-one (5)

The solution of 4-chloro-3-nitrocoumarin (3) (1 g, 4.4 mmol) and (4-methoxyphenyl)methanamine (4) (0.55 g, 4.4 mmol) in ethyl acetate (10 ml) was refluxed in the presence of triethylamine (1 ml, 7.2 mmol) for 3 h. After cooling, the precipitated solid was filtered off and washed with ethyl acetate and water. The flow of reaction was monitored by TLC. The target product, 4-[(4-methoxybenzyl)amino]-3-nitro-2*H*-chromen-2-one (5), was obtained as a pale yellow powder, m.p. 194-196 °C, in very good yield - 78%. HRMS(EI): M^+ ($C_{17}H_{14}N_2O_5$) 326.0915, requires 326.0903 (Δ = +1.2 mmu). IR (neat): 3344 (N-H), 3083 (Ar-H), 2940 and 2845 (C-H), 1681 (C=O), 1607 (C=C), 1515 and 1335 (NO_2), 1176, 1026, 914, 815, 738 cm^{-1}.

RESULTS AND DISCUSSION

Chemistry

The target compound, 4-[(4-methoxybenzyl)amino]-3-nitro-2*H*-chromen-2-one (5), were prepared in the reaction of 4-chloro-3-nitrocoumarin (3) and (4-methoxyphenyl)methanamine (4) in ethyl acetate in the presence of two equivalents of triethylamine. The product was obtained in a good yield of 78% (Scheme 1). The structure of the synthesized compound was confirmed by spectral means (HRMS(EI), IR, ^1H and ^{13}C NMR).

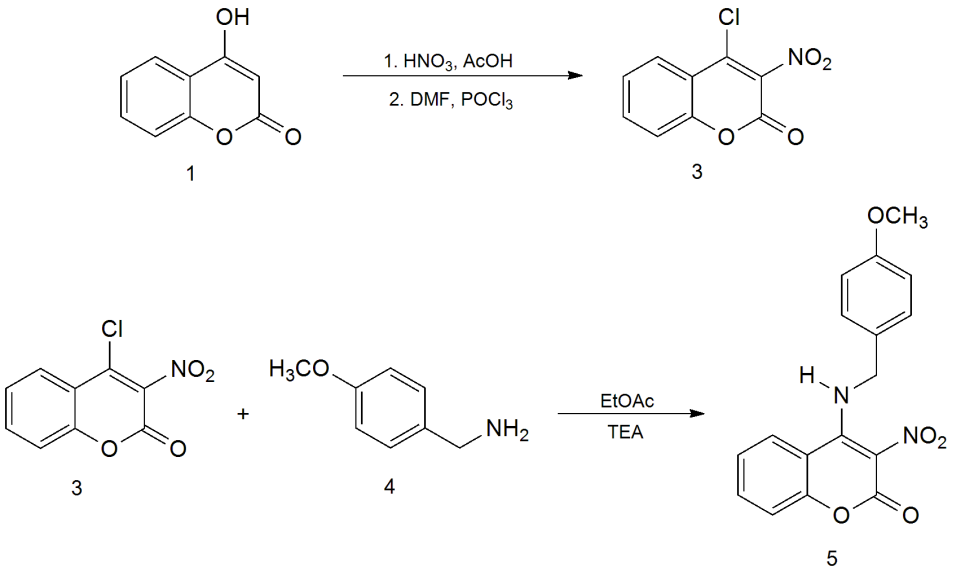

Scheme 1. Synthesis of 4-[(4-methoxybenzyl)amino]-3-nitro-2*H*-chromen-2-one.

High-resolution electron impact mass spectrometry (HR-EIMS) of synthesized compound indicated a molecular formula of $C_{17}H_{14}N_2O_5$ ($[M]^+$ at *m*/*z* 326.0915, Δ = +1.2 mmu). The IR spectra contained characteristic vibrations of the Ar-H and N-H bonds at 3083 and 3344 cm^{-1}, respectively. The strong band at 1681 cm^{-1} corresponding to absorptions of the C=O bond. The IR absorptions due to the presence of the NO_2 group appeared at 1335 and 1515 cm^{-1}.

The ^1H NMR spectrum of synthesized compound exhibited six aromatic methine signals, four sets of doublet of doublets at 8.36, 7.41, 7.23 and 6.91 ppm and two sets of doublet of doublet of doublets at 7.74 and 7.45 ppm. The NOESY correlations differentiated two separate proton spin systems (Figure 1). The first spin system comprised four signals, two sets of doublet of doublets at 8.36 and 7.41 ppm, and two sets of doublet of doublets of doublets at 7.74 and 7.45 ppm, while the second spin system contains two sets of doublet of doublets at 7.23 and 6.91 ppm.

The number of resonances suggests that a group of four signals belongs to the protons of coumarin moiety. Additionally,

integration of the ^{1}H NMR spectra shows the double intensity of signals at 7.23 and 6.91 ppm and assigns them to chemically equivalent protons in the positions of H-3'/7', and H-4'/6'. The assignment of these two groups of signals is provided due to NOESY correlation of broad range singlet at 9.01 ppm, assigned to the proton of the secondary amino group. This signal showed the cross peak with the signal at 8.36 ppm, which assigns H-5. The rest protons bounded to the coumarin core were easily assigned based on their mutual NOESY interactions (Figure 1, Table 1). The mentioned proton of the secondary amino group in the same spectrum showed two more interaction, with the signals at 4.42 and 7.23 ppm. According to chemical shift and integral (corresponding to two protons) from ^{1}H NMR, the signal at 4.42 ppm is attributed to two methylene protons. The simultaneous interaction of the doublet of doublets at 7.23 ppm with the signals of N-H and methylene protons assigned the two equivalent protons which occupy positions 3' and 7' on the substituent ring. The remaining aromatic protons (H-4' and H-6') was assigned to the signal at 6.91 ppm, which was confirmed by its interaction with the last signal in the ^{1}H NMR at 3.75 ppm attributed to methoxy protons.

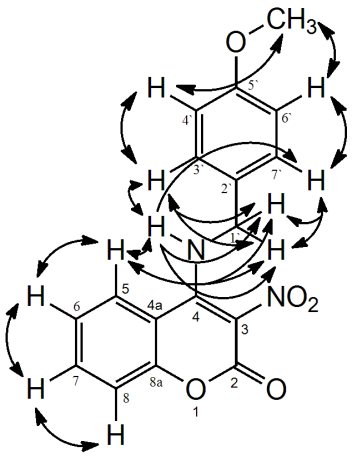

Figure 1. The NOESY correlations of 4-[(4-methoxybenzyl) amino]-3-nitro-2*H*-chromen-2-one.

The chemical shift of carbon atoms to which these protons were bonded was subsequently determined from the HSQC spectrum (Table 1). The assignment of these protons and carbons was additionally supported through the corresponding HMBC correlations (Figure 2).

The quaternary carbons C-4a and C-8a were assigned according to HMBC spectrum data. Existence of simultaneous interactions of protons H-6 and H-8 with the carbon signal at 114.7 ppm, as well as H-5 and H-7 with the signal at 151.4 ppm, assigns C-4a and C-8a, respectively.

Also, in HMBC spectrum is observed a characteristic interaction through two bonds between H-8 and the quaternary C-8a, similar to the previously studied compounds (Dekić et al. 2010, 2014). Additionally, H-5 showed through three bonds interactions with the signal at 147.7 ppm, attributed to quaternary carbon C-4. On the other hand, C-4 showed a cross peak with the methylene protons signal at 4.42 ppm, which confirms the existence of the amino bridge and position of substituent on the coumarin core. The HMBC correlations between proto resonance of the secondary amino group (9.01 ppm) and carbon atom at 116.6 ppm, assigned C-3.

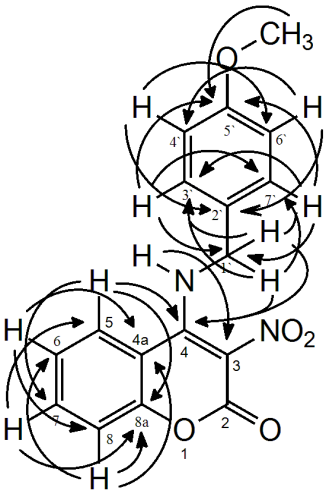

Figure 2. The HMBC correlations of 4-[(4-methoxybenzyl) amino]-3-nitro-2*H*-chromen-2-one.

Table 1. NMR data of compound (5) in DMSO-d_6.

Position	δ_H, m (*J*, Hz)	δ_C	NOESY[a]	HMBC[b]
2		155.6		
3		116.6		
4		147.7		
4a		114.7		
5	8.36 dd (8.4, 1.2)	124.8	6, 1', N-H	7, 4, 8a
6	7.45 ddd (8.4, 7.2, 0.8)	125.1	5, 7	4a, 8
7	7.74 ddd (8.4, 7.2, 1.2)	134.5	6, 8	5, 8a
8	7.41 dd (8.4, 0.8)	117.9	7	4a, 6, 8a
8a		151.4		
N-H	9.01 brs		5, 1', 3'/7'	3
1'	4.42 d (5.2)	48.1	5, 3'/7', N-H	3'/7', 4
2'		128.7		
3'/7'	7.23 dd (6.8, 2.0)	129.3	1', 4'/6', N-H	3'/7', 5', 1'
4'/6'	6.91 dd (6.8, 2.0)	114.5	3'/7', 8'	2', 4'/6'
5'		159.4		C-2'
8'	3.75 s	55.6	4'/6'	5'

[a] NOESY interactions of the hydrogen from the column "Position" with the corresponding hydrogen from the column "NOESY".

[b] HMBC interactions of the hydrogen from the column "Position" with the corresponding carbons from the column "HMBC".

The remaining carbon of the substituent side group was assigned at 159.4 ppm, trough cross-peaks of this signal and signals at 7.23 ppm (H-3' and H-7') and 3.75 ppm (methoxy protons) observed in the HMBC spectrum. Finally, the last carbon signal at 155.6 ppm was attributed to the lactone carbonyl (C-2) based on their chemical shifts, since no H interactions were observed in any 2D spectra and by comparison with the analogous signals in related compounds (Dekić et al., 2010; Dekić et al., 2014).

The mutual spatial relation between the coumarin core and arylamino substituent (Figure 3) can be ascertained from proton NOESY interactions. The correlations of H-5 with methylene hydrogens and N-H proton in the NOESY spectrum suggest that the coumarin core and secondary amino group are not in the same plane but rather are at an angle to one another. On the other side, the proton of the secondary amino group showed through space interactions with H-3` and/or H-7`. The abovementioned cross-peaks suggest that the substituent ring is oriented away from the coumarin framework. Simultaneous correlations of H-5 with methylene hydrogens and N-H proton, as well as a mentioned proton of the amino group with H-3' and H-7' cannot appear in a single conformation of the molecule, but may result from single-bond rotation around the C4 –N in the first, and N-C1 and C1-C2 in the second proton interaction giving rise to different conformations that are close in energy (this was confirmed by energy minimization calculations using MM2 force field from the ChemDraw 11.0 software package).

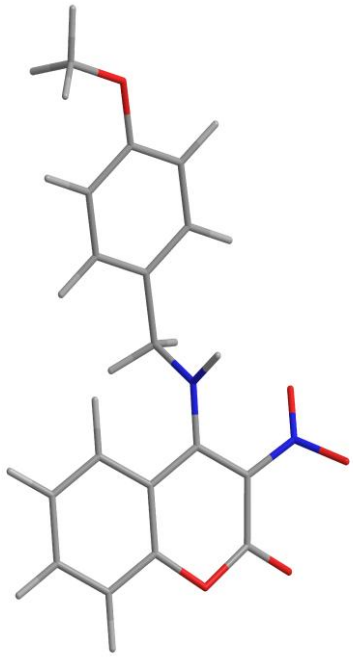

Figure 3. Spatial orientation of coumarin core and arylamino substituent in the molecule of 4-[(4-methoxybenzyl)amino]-3-nitro-2*H*-chromen-2-one.

CONCLUSION

In a nutshell, this research is presented synthesis and detailed spectral characterization of a new coumarin derivative 4-[(4-methoxybenzyl)amino]-3-nitro-2*H*-chromen-2-one. The spectral assignment was performed by combining 1D- (^{1}H NMR and ^{13}C NMR) and 2D-NMR techniques (^{1}H-^{1}H-COSY, NOESY, HSQC, and HMBC). NOESY correlations of protons of the arylamino substituent and the coumarin moiety indicate their mutual spatial orientation.

ACKNOWLEDGMENTS

Financial support for this study was granted by the Ministry of Education, Science and Technological Development of Serbia [Project No. 172061 and 45022].

REFERENCES

Barry, R. D. 1964. Isocoumarins. Developments science 1950. Chemical Reviews, 64(3), pp. 229-260. doi: 10.1021/cr60229a002

Dekić, V., Dekić, B., & Radulović, N. 2013. ^{1}H and ^{13}C NMR spectral assignments of an amino acid-coumarin hybrid. Facta Universitatis Series: Physics, Chemistry and Technology, 11(3), pp. 101-107. doi: 10.2298/fupct1301101d

Dekić, V., Radulović, N., Vukićević, R., Dekić, B., Skropeta, D., & Palić, R. 2010. Complete assignment of the ^{1}H and ^{13}C NMR spectra of antimicrobial 4-arylamino-3-nitrocoumarin derivatives. Magnetic Resonance in Chemistry, 48(11), pp. 896-902. doi: 10.1002/mrc.2681

Finn, G. J., Creaven, B., & Egan, D. A. 2001. Study of the *in vitro* cytotoxic potential of natural and synthetic coumarin derivatives using human normal and neoplastic skin cell lines. Melanoma Research, 11(5), pp. 461-467. doi: 10.1097/00008390-200110000-00004

Jiménez-Orozco, F. A., Molina-Guarneros, J. A., Mendoza-Patiño N., León-Cedeño, F., Flores-Pérez, B., Santos-Santos, E., & Mandoki, J. J. 1999. Cytostatic activity of coumarin metabolites and derivatives in the B16-F10 murine melanoma cell line. Melanoma Research, 9(3), pp. 243-247. doi: 10.1097/00008390-199906000-00005

Jung, K., Park, Y. J., & Ryu, J. S. 2008. Scandium(III) Triflate–Catalyzed Coumarin Synthesis. Synthetic Communications, 38(24), pp. 4395-4406. doi: 10.1080/00397910802369513

Kaljaj, V., Trkovnik M., & Stefanović-Kaljaj, L. 1987. Syntheses of new heterocyclocoumarins starting with 3-cyano-4-chlorocoumarin. Journal of the Serbian Chemical Society, 52(4), pp. 183-185.

Li, X., Zhao, Y. X., Wang, T., Shi, M. Q., & Wu, F. P. 2007. Coumarin derivatives with enhanced two-photon absorption cross-sections. Dyes Pigments, 74(1), pp. 108-112. doi: 10.1016/j.dyepig.2006.01.020

Melavanki, R. M., Kusanur, R. A., Kulakarni, M. V., & Kadadevarmath, J. S. 2008. Role of solvent polarity on the fluorescence quenching of newly synthesized 7,8-benzo-4-azidomethyl coumarin by aniline in benzene-acetonitrile mixtures. Journal of Luminescence, 128(4), pp. 573-577. doi: 10.1016/j.jlumin.2007.08.013

Murray, R. D. H. 1989. Coumarins. Natural Product Reports, 6, pp. 591-624.

Murray, R. D. H., Mendez, J., & Brown, S. A. (1982) The Natural Coumarins: Occurrence, Chemistry and Biochemistry. New York: Wiley & Sons.

O'Kennedy, R., & Thornes, R. D. (1997) Coumarins - Biology, Applications and Mode of Action. Chichester: John Wiley & Sons.

Turki, H., Abid, S., Fery-Forgues, S., & El Gharbi, R. 2007. Optical properties of new fluorescent iminocoumarins: Part 1. Dyes Pigments, 73(3), pp. 311-316. doi: 10.1016/j.dyepig.2006.01.001

Yu, T., Zhang, P., Zhao, Y., Zhang, H., Meng, J., & Fan, D. 2009. Synthesis and photoluminescent properties of two novel tripodal compounds containing coumarin moieties. Spectrochimica Acta Part A: Molecular and Biomolecular Spectroscopy, 73(1), 168-173. doi: 10.1016/j.saa.2009.02.013

Bulletin of Natural Sciences Research
Vol. 10, No. 2, 2020, pp. 17-22.
DOI: https://doi.org/10.5937/bnsr10-27576
Original Scientific Paper

SPECTROPHOTOMETRIC DETERMINATION OF ASCORBIC ACID BY HORSERADISH PEROXIDASE

VLADAN R. ĐURIĆ[1*], NEBOJŠA R. DELETIĆ[1]

[1]Faculty of Agriculture, University in Priština – Kosovska Mitrovica, Lešak, Serbia

ABSTRACT

L-ascorbic acid is one of the essential nutrients and most common food supplements, fortificants, and preservatives. It is commercially available as solutions, drops, tablets, capsules, crystal powder, beverage mixtures, multivitamin formulations, and multi antioxidant formulations. The usual daily dose is from 25 mg to 1.5 g. Ascorbic acid is a distinctly reducing agent with low redox potential (0.18 and 0.08 V at pH 4.5 and 6.4, respectively). Based on ascorbate property, numerous methods for its quantitative determination are developed, from titrimetric, electrochemical, and chromatographic methods, to fluorometric and kinetic ones. Enzyme peroxidase is interfered with by ascorbic acid, which decreases the oxidation speed of its co-substrates during hydrogen peroxide decomposition by peroxidase. Absorbance changes at the wavelength of corresponding reagents are in correlation with ascorbate concentration. During this study, benzidine and o-tolidine have been used as chromogenic reagents. Reaction conditions were optimized for various buffer systems, calibration curves were constructed, and limits of detection (0.04 µmol/L) and quantification (0.12 µmol/L) were calculated. Using calibration charts, it was possible to detect ascorbic acid within limits from 0.4 to 10 µmol/L. The optimized method was applied for the determination of ascorbic acid in pharmaceutical products. The method was characterized by exceptional sensitivity and accuracy, but only for preparations not containing substances that affect enzyme peroxidase.

Keywords: L-ascorbic acid, Peroxidase, Spectrophotometry.

INTRODUCTION

Enzyme peroxidase (E.C.1.11.1.7) plays an essential role in various physiological processes of microorganisms, plants, and animals (Wen et al., 2011). Peroxidase of some biological species mostly represents a mixture of different isoenzymes. Thus from horseradish (*Armoracia rusticana* G.Gaertn., B.Mey & Scherb.), more than 40 peroxidase isoenzymes have been isolated by now, with isoenzyme C as the most abundant one (Krieg et al., 2010).

Primary substrates and the only molecules reacting directly with the enzyme are peroxides, namely both forms of them, hydrogen peroxide free form, and its organic complexes or salts.

The role of peroxidase in the cell is primarily discussed regarding the regulation of intracellular H_2O_2 level (Mittler, 2002). Peroxidase transforms peroxide into water and oxygen radicals. In the presence of co-substrate – hydrogen donor (AH_2), it further transforms oxygen radical to another water molecule while co-substrate is transformed into corresponding free radical ($AH^{\bullet}$), as presented in the following chemical equation:

$$2AH_2 + ROOH \rightarrow 2AH^{\bullet} + ROH + H_2O$$

That way, electrons from activated oxygen are being transferred to molecules of co-substrates that stabilize them by inherent resonant structures (Bagirova et al., 2001).

The co-substrate role can be played by many phenols, aminophenols, aromatic amines and acids, indophenols, leuco dyes, ascorbic acid, some amino acids nitrites, as well as a series of other compounds.

The general mechanism of peroxidase (PER) catalytic activity is presented in scheme 1.

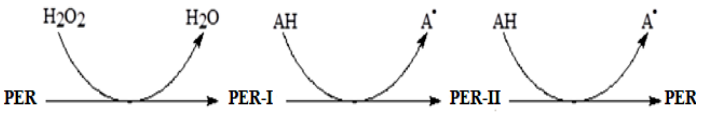

Scheme 1. AH and $A^{\bullet}$ represent a reduced and oxidized form of co-substrate (hydrogen donor).

The first step of the catalytic cycle is the reaction between H_2O_2 and Fe(III)-center of a relaxed enzyme (PER) and the formation of the so-called compound I (PER I). It is an intermediary with a higher oxidation state, which involves oxyferril center and porphyrin cation radical. The formation of so-called compound II (PER II) demands the presence of co-substrate – the donor of hydrogen. Both Fe(IV) oxyferril species, as well as compound I and compound II, are powerful oxidants with redox potential close to +1V. The next reduction step with co-substrate turns compound II back to the enzyme's original state (PER).

"Transfer" of electrons from peroxide to co-substrate can involve ascorbic acid (vitamin C), which itself can become a co-substrate of peroxidase. However, its affinity for forming a

*Corresponding author: vladan.djuric@pr ac.rs

ternary complex with the enzyme and substrate is markedly lower concerning competitive co-substrates (aryl phenols and arylamines). By coupled non-enzymatic reaction, ascorbic acid instantly reduces oxidized co-substrate molecules, while itself being oxidized to dehydroascorbic acid and immobilizing peroxide electrons (White-Stevens, 1982):

$$AsA + 2A^{\bullet}\,(\text{colored}) \rightarrow DHAsA + 2AH\,(\text{colorless})$$

This reaction is quantitative, so in *vitro* trials, with a right choice of co-substrates (chromogens – indicators), it can be used for determination of ascorbic acid (Thompson, 1987; Shekhovtsova et al., 2006; Martinello et al., 2006; Arnao et al., 1996), but also for determination of the other components involved in the reaction – hydrogen peroxide, co-substrate and the peroxidase enzyme itself.

In order to measure ascorbic acid content in various samples, numerous spectrophotometric methods have been developed. Some of them, with their essential characteristics, are given in table 1.

Table 1. Review of spectrophotometric methods for the determination of ascorbic acid.

Spectrophotometric method		LOD (μmol/L)	LOQ (μmol/L)	Determination range (μmol/L)	Sample	Ref.
Peanut peroxidases	o-dianisidine			0.8–10	Fruit juices, milk, and sour-milk products	Shekhovtsova et al., 2006
	3,3',5,5'-tetramethylbenzidine			0.1-10		
Horseradish peroxidases	o-dianisidine			2–10		
	3,3',5,5'-tetramethylbenzidine			0.1-10		
Horseradish peroxidases with a quinoid dye produced				2.3-68.1	Pharmaceutical formulations	Zhu et al., 1997
Withiron(III) complex (ferritin, $[Fe(phen)3]\ 3^{+}$) in the presence of 1,10-phenanthroline				4.3–74.1	In serum and urine samples	Moghadam et al., 2011
With Cu(II) phosphate		0.3		5-40	Pharmaceutical formulations	Pereira et al., 1997
Modified CUPRAC method				8-80	Fruit juices and pharmaceutical preparations	Ozyurek et al., 2007
With 2,4-dinitrophenylhydrazine		5.68	9.65	10-550	Fruits and vegetables	Kapur et al., 2012
With Fast Red AL salt				28.4-142	Pharmaceutical preparations and fresh fruit juices	Backheet et al., 1991
With 4-chloro-7-nitrobenzofurazan				28.4-113.6	Fresh fruit juices, some vegetables, and infant milk product	Abdelmageed et al., 1995

EXPERIMENTAL

The all essential solutions have been prepared using deionized water characterized by the electrical conductivity of 0.5 μS/cm2. The all used chemicals were of p.a. purity grade.

Preparation of horseradish peroxidase of purity grade 200 kU/g was supplied from Merck KGaA (Darmstadt, Germany). Solutions of the enzyme were prepared immediately before executing the trial, within concentration range from 1 to 30 U/L, by basic dilution solution obtained by dissolving 50 mg (10000 U) of peroxidase in 1000 ml of deionized water.

Solutions of hydrogen peroxide (Merck KGaA, Darmstadt, Germany), within concentration range from 0.04 to 2 mmol/L, were prepared by basic dilution solution obtained by dissolving 95 ml of 33.3% hydrogen peroxide in 1000 ml of deionized water, and their exact concentration was controlled by the standard permanganometric method (Vajgand, 1986).

Solutions of benzidine (Reanal Laborvegyszer Kft., Budapest, Hungary) and o-tolidine (Centrohem DOO, Stara Pazova, Serbia) were prepared within the concentration range from 0.1 to 5 mmol/L, by basic dilution solution with a concentration of 50 mmol/L, obtained by dissolving 0.9210 g of benzidine in 5ml of 1% CH_3COOH, i.e., 1.0615 g of o-tolidine in 5 ml of 1% HCl, and then filled up to 100 ml by deionized water.

The basic solution (0.1 mol/L) of L-ascorbic acid (Galenika AD, Belgrade, Serbia) was prepared by dissolving 17.613 g of the substance in 1000 ml of deionized water, while working solutions were within the concentration range from 0.1 μmol/L to 10 mmol/L, with or without various stabilizing components in different concentrations. Ascorbic acid concentration of these solutions was controlled by the standard method using 2,6-dichlorophenolindophenol (Official Methods, 1995).

The following buffer systems were used as media with defined pH value: acetate buffer of pH 4 (prepared in the laboratory, 180 ml of 0.2 mol/L sodium acetate solution and 820 ml of 0.2 mol/L acetic acid solution; citrate buffers pH 5 and 6 (Farmitalia Carlo Erba Ltd., Milan, Italy); phosphate buffer of pH 7 (Fisher Scientific UK Ltd., Loughborough, UK); and borate buffer of pH 8 (Farmitalia Carlo Erba Ltd., Milan, Italy). Buffer pH values were controlled by pH-meter Hanna HI-207 (Hanna Instruments Inc., Woonsocket, RI, USA).

Spectrophotometric measurements were carried out using the Beckman DU-650 spectrophotometer (Beckman Coulter, Inc., Brea, CA, USA).

Relative activity of peroxidase was observed by spectrophotometry, measuring the change of absorbance during the emergence of the oxidized form of co-substrate, benzidine, and o-tolidine, within the corresponding time interval. Depending on the applied buffer system, absorbance change for benzidine was observed at 410 nm (in acetate and citrate buffers), at 362 nm (in phosphate buffer), and 425 nm (in borate buffer), while for o-tolidine, it was observed at 630 nm (in acetate and citrate buffers), at 411 nm (in phosphate buffer) and 436 nm (in borate buffer).

Before measurements were carried out, the all used solutions had been thermostated at the temperature of 20°C.

Measurements were carried out in glass cuvettes 1ml of volume. The reaction mixture was composed of 0.5 ml of the corresponding buffer, 0.1 ml of peroxidase, 0.1 ml of co-substrate – indicator (o-tolidine or benzidine), and 0.2 ml H_2O or ascorbic acid. Cuvettes with the reaction mixture then were thermostated at 25°C for five minutes, and after that, absorbance change was observed from the moment when 0.1 ml of H_2O_2 had been injected into the mixture.

To evaluate the proposed method, test solutions were prepared by grinding tablets and dissolving powder of different preparations in 1 L of deionized water. For that purpose, depending on ascorbic acid content, 20 to 100 tablets or bags were used. Diluted preparations firstly were filtered, and then they were used to prepare working solutions for the analyses.

The following preparations were used to make samples for evaluation of the proposed method:

- Preparation 1 – Vitamin C, tablets, 500 mg (Galenika AD, Belgrade, Serbia). Excipients: microcrystalline cellulose, croscarmellose sodium, magnesium stearate, lactose anhydrous, and corn starch.
- Preparation 2 – Vitamin C, powder, 1000 mg (BG Pharm DOO, Belgrade, Serbia), no excipients.
- Preparation 3 – Easy soluble vitamin C, powder, 50 mg (Ivančić i sinovi DOO, Belgrade, Serbia). Excipients: 450 mg of glucose.

RESULTS AND DISCUSSION

The addition of hydrogen peroxide to the analytic mixture, composed by peroxidase enzyme and one of co-substrates/chromogens, leads to the rapid oxidation of co-substrate, and that can be detected by spectrophotometry where rapid development of absorption maximum can be observed at corresponding wavelength.

The rate of oxidized co-substrate form development can serve as a measure for the relative activity of peroxidase. The starting speed (v0) can be presented graphically by the slope coefficient of the initial part of the curve, which is by the tangent of slope angle – (tgα) (figure 1). This speed depends on concentrations in the reaction mixture of all components of ternary complex enzyme-substrate-cosubstrate.

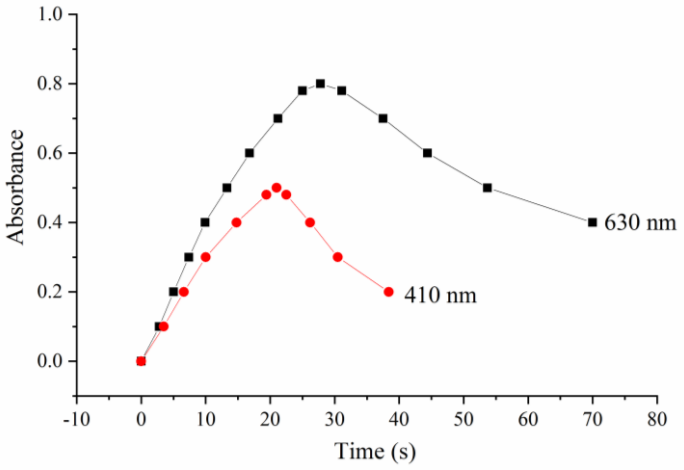

Figure 1. Formation of o-tolidine (630 nm) oxidation products and benzidine (410 nm), at equimolar concentrations, during breaking down of hydrogen peroxide by horseradish peroxidase.

During this study, two co-substrates have been used, each of them having absorption maximum within the visible part of the specter, benzidine, and its derivative o-tolidine with absorption maximums that depended on pH value.

The dependence of the initial reaction speed on the enzyme concentration was directly proportional.

Similarly, the speed of co-substrate oxidation was also directly proportional to the concentration of the substrate, i.e., hydrogen peroxide.

The introduction of ascorbic acid into the reaction mixture caused occurring a parallel non-enzymatic reaction, in which oxidized co-substrate molecules were instantly reduced to the starting point, and that resulted in delaying (lag time) appearance

of analytical signal, by the moment when ascorbic acid was quantitatively transferred to dehydroascorbic acid.

Lag time duration depended on the available amount of ascorbic acid (figure 2).

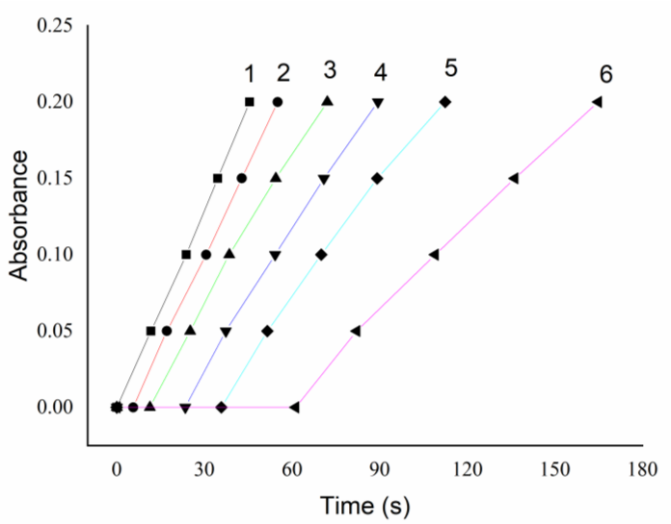

Figure 2. The effect of ascorbic acid on kinetics of peroxidase reaction. Conditions of the reaction: peroxidase 10 U/L; H_2O_2 0.1 mmol/L; o-tolidine 1 mmol/L; citrate buffer pH 6. Curve 1 represents blank, curves 2–6 $AscH_2$ concentration 5; 10; 20; 30 and 50 μmol/L, respectively. Slope coefficients of the curves were the following: 0.0041 (1); 0.0040 (2); 0.0037 (3); 0.0032 (4); 0.0029 (5) and 0.0021 (6).

Lag time at a defined concentration of ascorbic acid represented the period during which the corresponding amount of the enzyme broke down a certain quantity of hydrogen peroxide equivalent to ascorbic acid's quantity in the reaction mixture. Having in mind that co-substrate oxidation speed depends on peroxide concentration, in the moment of measurement, it was lowered proportionally to the applied amount of ascorbic acid, which was visible from the values of the slope coefficient.

This lag time proved itself a useful and accurate kinetic parameter for observing the mechanism of the studied reaction, and its values reflected reciprocal of initial reaction speed, 1/v0 i.e., 1/tgα.

During the lag time, the absorbance value change at the chosen wavelength was equal to zero (Δ[Abs] = 0). The second part of the curve after lag time, described as Δ[Abs]/Δt, represented co-substrate oxidation speed, and it also could be exploited as a parameter of the reaction system because that parameter reflected the altered state of the system after oxidation of ascorbic acid.

Calibration curves for the determination of ascorbic acid in the presence of benzidine and o-tolidine as chromogenic co-substrates are presented in figure 3.

The calibration line constructed by the use of benzidine as co-substrate of peroxidase had a more significant slope coefficient regarding the calibration line constructed by the use of o-tolidine, which pointed out to a higher sensitivity of benzidine as an indicator. However, water solutions of benzidine are unstable, and after a few hours, they convert to a colloid state, which negatively affects solution transparency during measurement and calls measurement reproducibility in question.

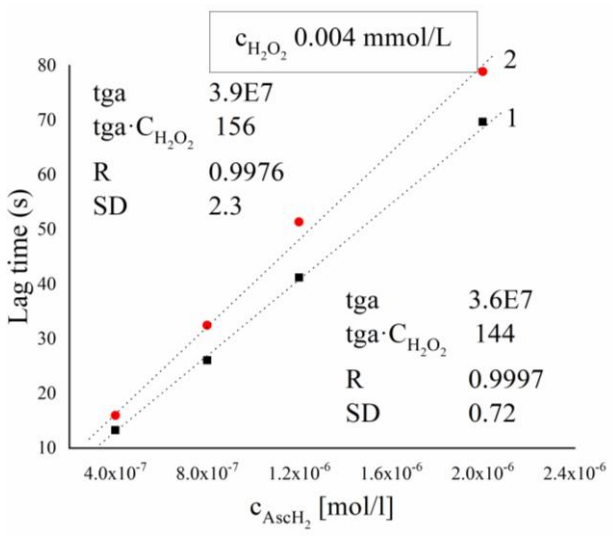

Figure 3. Calibration curves for determination of ascorbic acid, at H_2O_2 concentration of 40 μmol/L, peroxidase concentration of 10 U/L; equimolar amounts of o-tolidine (1) and benzidine (2) 0.5 mmol/L and citrate buffer pH 6.

The experiment revealed that peroxidase activity was highest in citrate buffer pH 6, and lowest in borate buffer pH 8. Previous reports pointed out the optimal pH value for peroxidase lying between 4.5 and 6.5, while enzyme activity weakened by increasing alkalinity of the environment (Shekhovtsova et al., 2006; Arnao et al., 1996).

Slope coefficients of the curves obtained using benzidine were greater than the curves obtained using o-tolidine with no exception, which suggested that transport of hydrogen from benzidine to peroxidase was slower, compared with the speed of hydrogen transport from o-tolidine to peroxidase.

The limit of detection (LOD) and limit of quantification (LOQ) amounted 0.04 and 0.12 μmol/L, respectively. Linear dependence between lag time and ascorbic acid concentration was within the determination range of 0.4 –10 μmol/L.

This study included testing the effect of numerous substances that might be present in samples containing ascorbic acid, such as solution stabilizers and extraction aids, and various components of pharmaceutical preparations (excipients) found in combination with vitamin C the accuracy of its determination. We established that the kinetic method results were comparable with results obtained by the standard DCPIP method only when ascorbic acid was determined in preparations containing no other active components.

The described method has been applied to determine ascorbic acid in several samples different from each other. The results of the measurements are presented in table 2.

Table 2. Content of ascorbic acid (mg) in various preparations, determined using the enzymatic method, with co-substrates o-tolidine and benzidine at pH 6.

Sample	c($AscH_2$) mg/one dosage	Found c($AscH_2$) with o-tolidine	RSD (%)	Recovery (%)	Found c($AscH_2$) with benzidine	RSD (%)	Recovery (%)
Preparation 1	500	511.8±18.4	3.60	102.36	510.3±12.7	2.49	102.06
Preparation 2	1000	1014.4±19.1	1.88	101.44	1009.8±11.0	1.09	100.98
Preparation 3	50	54.2±6.8	12.56	108.40	55.3±6.9	12.48	110.60

Based on the presented results, one can say that the proposed method has its advantages and disadvantages. The advantage of the method is its exceptional sensitivity, clearly visible by comparing the obtained results with the ones from table 1 and accuracy, which can be concluded based on the results from table 2. Furthermore, this method uses a simple apparatus and does not demand expensive reagents.

The disadvantage of the method, above all, is an excellent susceptibility of peroxidase enzyme because numerous foreign substances affect its relative activity (Hernandez-Ruiz, 2001; Pandey et al., 2011; Rodriguez-Lopez et al., 1997; Wen et al. 2011; Krieg et al., 2010; Bagirova et al., 2001), which shows an effect on reproducibility and accuracy of the method. To avoid this, preliminary elimination of such substances would be necessary or their transformation to an inactive state, creating a problem having in mind complete application of the method. On the other hand, a deviation from the expected values during a routine control of samples by this method could point out possible impurities present in the sample with such deviation.

CONCLUSION

Ascorbic acid is a potent antioxidant thanks to very low redox potential, preventing oxidizing other organic molecules in the environment or turning them instantaneously back to their reduced form. Thus, there are numerous co-substrates of peroxidase enzyme that facilitate, as proton donors, its transforming hydrogen peroxide to water, but being reduced themselves in ascorbic acid's presence to the moment when it is quantitatively transferred to dehydroascorbic acid. Proper choice of co-substrate, as chromogen, whose one of the redox forms absorbs in the visible part of the specter, has enabled developing a kinetic spectrophotometric method for successful determination of ascorbic acid.

The procedure, which included the presence of co-substrates benzidine and o-tolidine at various pH values, has been exploited for the determination of ascorbic acid in farmaceutical products. The presented results point to the method as one of the most sensitive and most accurate spectrophotometric kinetic methods, demanding standard laboratory equipment, and acceptable price reagents. Flaws of the method are caused by the over susceptibility of peroxidase molecule to the presence of impurities and foreign substances that interfere with measurement accuracy.

REFERENCES

Abdelmageed O. H., Khashaba P. Y., Askal H. F., Saleh G. A., & Refaat I. H. 1995. Selective spectrophotometric determination of ascorbic acid in drugs and foods. Talanta, 42(4), pp. 573-579. doi.org/10.1016/0039-9140(95)01449-L

Arnao M. B., Cano C., Hernandez-Ruiz J., Garcia-Canovas F., & Acosta M. 1996. Inhibition by l-ascorbic acid and other antioxidants of the 2,2′-azino-bis(3-ethylbenzthiazoline-6-sulfonic acid) oxidation catalyzed by peroxidase: A new approach for determining the total antioxidant status of foods. Analytical Biochemistry, 236(2), pp. 255-261. doi.org/10.1006/abio.1996.0164

Backheet E. Y., Emara K. M., Hassan F. Askal H. F., & Saleh G. A. 1991. Selective spectrophotometric method for the determination of ascorbic acid in pharmaceutical preparations and fresh fruit juices. Analyst, 116, pp. 861-865 doi:10.1039/AN9911600861

Bagirova N. A., Shekhovtsova T. N., & van Huystee R. B. 2001. Enzymatic determination of phenols using peanut peroxidase. Talanta, 55(6), pp. 1151-1164. doi.org/10.1016/S0039-9140(01)00544-6

Hernandez-Ruiz, J., Arnao M. B., A. N. P. Hiner A. N. P., Garsia-Canovas F., & Acosta M. 2001. Catalase-like activity of horseradish peroxidase: relationship to enzyme inactivation by H_2O_2. Biochem. J., 354(1), pp. 107-114. doi.org/10.1042/bj3540107

Kapur A., Hasković A., Čopra-Janićijević A., Klepo, L., Topčagić A., Tahirović, I., & Sofić, E. 2012. Spectrophotometric analysis of total ascorbic acid content in various fruits and vegetables. Bulletin of the Chemists and Technologists of Bosnia and Herzegovina 38, pp. 39-42.

Krieg, R., & Halbhuber K. J., 2010. Detection of endogenous and immuno-bound peroxidase – The status quo in histochemistry. Progress in Histochemistry and Cytochemistry, 45(2), pp. 81-139. doi.org/10.1016/j.proghi.2009.11.001

Martinello F., & Da Silva E. L. 2006. Mechanism of ascorbic acid interference in biochemical tests that use peroxide and

peroxidase to generate chromophore. Clinica Chimica Acta, 373(1-2), 108-116. doi.org/10.1016/j.cca.2006.05.012

Mittler, R., 2002. Oxidative stress, antioxidants, and stress tolerance. Trends in Plant Science, 7(9), pp. 405-410. doi.org/10.1016/S1360-1385(02)02312-9

Moghadam M. R., Dadfarnia S., Shabani A. M. H., & Shahbazikhah P. 2011. Chemometric-assisted kinetic–spectrophotometric method for simultaneous determination of ascorbic acid, uric acid, and dopamine. Analytical Biochemistry 410(2), pp. 289-295. doi.org/10.1016/j.ab.2010.11.007

Official Methods of Analysis of AOAC International. 1995. Chapter 45, Method 80, 16th ed.

Ozyurek M., Guclu K., Bektasoglu B., & Apak R. 2007 Spectrophotometric determination of ascorbic acid by the modified CUPRAC method with extractive separation of flavonoids–La(III) complexes. Analytica Chimica Acta 588(1), pp. 88-95. doi.org/10.1016/j.aca.2007.01.078

Pandey V. P., & Dwivedi U. N. 2011. Purification and characterization of peroxidase from *Leucaena leucocephala*, a tree legume. J. Mol. Catal. B: Enzym., 68(2), pp. 168-173. doi.org/10.1016/j.molcatb.2010.10.006

Pereira A. V., & Fatibello-Filho O. 1997. Flow injection spectrophotometric determination of L-ascorbic acid in pharmaceutical formulations with on-line solid-phase reactor containing copper (II) phosphate1 Analytica Chimica Acta 366(1–3), pp. 55-62. doi.org/10.1016/S0003-2670(97)00660-0

Rodriguez-Lopez J. N., Hernandez-Ruiz J., Garcia-Canovas F., Thornley R. N. F., Acosta M., & ArnaoM. B. 1997. The Inactivation and Catalytic Pathways of Horseradish Peroxidase with m-Chloroperoxybenzoic acid. Biol. Chem., 272, pp. 5469-5476. doi.org/10.1074/jbc.272.9.5469

Shekhovtsova T. N., Muginova S. V., Luchinina J. A., & Galimova A. Z. 2006. Enzymatic methods in food analysis: determination of ascorbic acid Analytica Chimica Acta, 573-574, pp. 125-132. doi.org/10.1016/j.aca.2006.05.015

Thompson R. Q. 1987. Peroxidase-based colorimetric determination of L-ascorbic acid. Anal. Chem. 59(8), pp. 1119–1121. doi.org/10.1021/ac00135a011

Vajgand V. 1986. Analitika, Rad, Beograd, 37.

Wen, B., & Moore D. J., 2011. Bioactivation of glafenine by human liver microsomes and peroxidases: identification of electrophilic iminoquinone species and GSH conjugates. drug metabolism and disposition, 39(9), pp. 1511-1521. doi.org/10.1124/dmd.111.039396

White-Stevens R. H., 1982. Interference by ascorbic acid in test systems involving peroxidase. I. Reversible indicators and the effects of copper, iron, and mercury. Clinical Chemistry, 28(4), pp 578–588. doi.org/10.1093/clinchem/28.4.578

Zhu M., Huang X., Li J., & Shen H. 1997. Peroxidase-based spectrophotometric methods for the determination of ascorbic acid, norepinephrine, epinephrine, dopamine, and levodopa. Analytica Chimica Acta 357(3), pp. 261-267. doi.org/10.1016/S0003-2670(97)00561-8

Bulletin of Natural Sciences Research
Vol. 10, No. 2, 2020, pp. 23-27.

DOI: https://doi.org/10.5937/bnsr10-25625
Original Scientific Paper

CONTEMPORARY CHANGES IN THE ETHNIC STRUCTURE OF THE POPULATION IN THE AUTONOMOUS PROVINCE OF KOSOVO AND METOHIJA

SAŠA MILOSAVLJEVIĆ[1], JOVO MEDOJEVIĆ[1]

[1]Faculty of Sciences, University in Priština – Kosovska Mtrovica, Kosovska Mtrovica, Serbia

ABSTRACT

Twenty years (1999 - 2019) after the end of the conflict in the Autonomous Province of Kosovo and Metohija, it can be stated that nowhere in Europe is there such ethnic segregation of the population as is the case with the AP of Kosovo and Metohija. Following the withdrawal of pumped security forces from the entire territory of Kosovo and Metohija and the entry of the United Nations peacekeeping force into the Serbian Autonomous Province, Kosovo Albanians carried out their persecution from Kosovo through terrorist attacks on Serbs and other non-Albanian populations (Montenegrins, Gorans, Roma, Ashkali) carried out their persecution from Kosovo and Metohija and fundamentally changed the ethnic structure of the Province. An insight into the majority of 223.081 exiles and displaced persons from Kosovo and Metohija indicates an exodus against the Serbs. The number of displaced Roma, Ashkali and Egyptians is estimated at about 100.000. The mass persecution of the Serb and other non-Albanian populations has resulted in tremendous changes in the ethnic structure of the Province, which today, with 93% of the total population, is dominated by Albanians, while other ethnic communities have a participation of 7%.

Keywords: Population, Ethnicity, Kosovo and Metohija.

INTRODUCTION

Contemporary demographic determinants indicate that today the territory of the Autonomous Province of Kosovo and Metohija is dominated by the ethnic Albanian community. Since June 1999, the violent expulsion, killings, threats, pressures of various kinds exposed to the Serb and other non-Albanian populations have resulted in a change in the ethnic structure of the population of Kosovo and Metohija. After the end of the confl ict in Kosovo and Metohija, 223,081 refugees have left this territory, with 206,879 taking refuge in Serbia and 16,202 in Montenegro. This total of refugees does not include the displaced Roma, Ashkali and Egyptians, although estimates suggest that 100,000 of them have been displaced from Kosovo and Metohija. Only from the province's capital, Priština, 23.000 Serbs, 6.000 Roma, 1.000 Muslims and 1.000 Turks fled. Nowhere in the present-day world has such severe ethnic cleansing of cities and villages been recorded as has been the case with the Serbs and Serbian settlements in Kosovo and Metohija. The large urban centers of Kosovo and Metohija such as Priština, Prizren, Peć, Đakovica, Uroševac, Gnjilane, Podujevo, Vučitrn and southern Kosovska Mitrovica are inhabited exclusively by Albanians. The Serb and other non-Albanian populations remained in rural areas where they still formed the majority, and for which the name "enclaves" became established. From June 15. 1999 to May 10. 2003 a total of 110 Orthodox churches and monasteries was burned, plundered and destroyed. The same tendencies have continued to this day, along with the desecration of cemeteries, stoning and burning of the returnees' homes (Medojević & Milosavljević, 2019a).

MATERIAL AND METHODS

The metodology in this paper is according to the subject, objectives and tasks of the research. The historical method contents the use of literature, written documents and other archive material and presents us knowledge about the demography past of the Kosovo and Metohija. Data were collected in public institutions and in the Statistical Office of the Republic of Serbia and Statistical Office of Kosovo. It should be emphasized that the 1991 census boycotted the entire Albanian, part of the Roma and part of the Muslim population, and that the 2011 census boycotted the Serb population. According to the United Nations Resolution, the census in Kosovo and Metohija can only be conducted by United Nations representatives. Despite this, the Priština authorities organized a census with the help of Eurostat (European Statistical Office), Italian Istat (Istituto Nazionale di Statistica), Swedish Sida (The Swedish International Development Cooperation Agency), UNFPA (The United Nations Population Fund) as well as the country: United Kingdom, Switzerland and Luxembourg. The census was conducted from April 1st to April 15th, 2011 in 34 municipalities, without the municipalities in the north part of Kosovo and Metohija, where the majority are Serbs: Leposavić, Zubin Potok, Zvečan, and northern Kosovska Mitrovica (Milosavljević & Punišić, 2011).

* Corresponding author: sasa.milosavljevic@pr.ac.rs

ANALYSIS OF CHANGES IN THE TOTAL POPULATION MOVEMENT OF AUTONOMUS PROVINCE KOSOVO AND METOHIJA FROM 1948 TO 2019

The population of Kosovo and Metohija has been growing steadily in the second half of the 20th century. We attribute the increase in total population to the demographic boom of the Albanian population above all. The total population of Kosovo and Metohija grew from 727.820 in 1948 to 1.954.747 in the 1991 census, an increase of 168% (Table 1). Despite all the expectations and forecasts of the last twenty years, the total population of Kosovo and Metohija has been in a slight decline and according to the last census from 2011 the population is 1.739.825, which is a decrease of 12% compared to 1991 (Medojević et al., 2011).

Not all ethnic communities have participated equally in increasing Kosovo's population. While the Albanian population had all the characteristics of a population boom, the Serb and other non-Albanian populations were in regression (Radovanović, 2004).

Table 1. Movement of total population of the Autonomous Province Kosovo and Metohija by Censuses 1948-2011.

Year	1948.	1953.	1961.	1971.	1981.	1991.	2011.
Population	727.820	808.141	963.988	1.243.693	1.584.411	1.954.747	1.739.825

Table 2. Ethnical structure of population of the Autonomous Province Kosovo and Metohija by Censuses 1948-1991 (Statistical Office of the Republic of Serbia).

	1948.	1953.	1961.	1971.	1981.	1991.
Albanians	498.242	524.559	646.805	916.168	1.226.736	1.607.690*
Serbs	171.911	189.869	227.016	228.264	209.498	195.301
Montenegrins	28.050	31.343	37.588	31.555	27.028	20.045
Muslims	9.679	6.241	8.026	26.357	58.562	57.408
Roma	11.230	11.904	3.202	14.593	34.126	42.806
Turks	1.315	34.583	25.784	12.244	12.513	10.838
Croats	5.290	6.201	7.251	8.264	8.717	8.161
Others	2.103	3.541	8.316	6.248	7.260	12.498
TOTAL	727.820	808.141	963.988	1.243.693	1.584.441	1.954.747

*estimated population

When looking at the censuses after the Second World War, we notice that the number of Serbs in the territory of Kosovo and Metohija increased from 1948 to 1971, when it reached its maximum. The Serb population increased by 56.353 during this period (Table 2). For the next twenty years there has been a continuous decline in the total number of Serbs in Kosovo and Metohija, so the 1981 census recorded 209.498 Serbs, while according to the 1991 census there were 195.301. Thus, the participation of the Serbian population in the total population from 23,6% in 1948 dropped to 9,9% in the 1991 census (Medojević & Milosavljević, 2019b).

The movement of the Montenegrin national minority over the same period has a similar tendency. The number of Montenegrins increased from 28.050 in 1948 to 37.588 in 1961, when it reached its maximum. Since 1961, the number of Montenegrins has been steadily declining, and in 1991 it was 20.045. The participation of the Montenegrin population in Kosovo and Metohija decreased for 8.005 inhabitants from 1948 to 1991, respectively their participation in the national structure decreased from 3,9% to 1% in the same period.

After Second World War, the Albanian population increased. From 1948 to 1991, their number increased threefold, from 498.242 to 1.607.690. Albanian participation in the ethnic structure of the population of Kosovo and Metohija increased from 68,4% in 1948 to 82,2% in 1991. During the 1960s and 1980s, the increase in the number of Albanians in Kosovo and Metohija had the characteristics of a population boom. The census period 1961-1971, determined the increase in the number of Albanians from 646.605 to 916.168 (a total increase of 269.563 or 42%); in the period 1971-1981. the number of Albanians increased from 916.168 to 1.226.736 (a total increase of 310.568 or 34%), and in the period 1981-1991. their number increased from 1.226.736 to 1.607.690 (a total increase of 380.954 or 31%). The causes of the population boom of the Albanian population in the second half of the twentieth century, in Kosovo and Metohija, can be found in the prolongation of life expectancy, falling mortality rates of adults and infants with stagnant birth rates.

The participation of the Muslim and Roma populations in Kosovo and Metohija in the second half of the 20th century varied from census to census. Globally, their numbers and participation in population structure have increased. The Roma population increased by 31.576 (from 11.230 in 1948 to 42.806 in 1991), respectively the participation of the Roma population in the total population increased from 1,5% to 2,2%. The growth of the Muslim population was even more pronounced. In 1948, the number of Muslims was 9.679 (participation in the total population at 1,3%), and in 1991 their number was 57.408

(participation in the total population at 2,9%) (Medojević & Milosavljević, 2015).

CONTEMPORARY ETHNIC DETERMINATES IN THE AUTONOMUS PROVINCE OF KOSOVO AND METOHIJA

After the end of the aggression against the Federal Republic of Yugoslavia in June 1999, organized terror of the Albanian population over the Serb and other non-Albanian population resulted in forced migration movements of Serbs, Montenegrins, Roma, Ashkali, Egyptians into central Serbia and Montenegro, which completely disrupted ethnic structure of the Province. Today, twenty years after the end of the aggression and the entry of international forces into the territory of Kosovo and Metohija, there is still speculation about the total number of population as well as the ethnic structure of the population. The information obtained from the 2011 census may be considered irrelevant. Their irrelevance is reflected, first and foremost, in the quantitative values that determine the ethnic composition of the population, especially the Serb community, which boycotted the census in all four municipalities in the north of the province, while Serb turnout in the areas south of the Ibar River was below 50%. During the census, the Serb population was exposed to threats, pressures and blackmail.

Table 3. Ethnical structure of population of the Autonomous Province Kosovo and Metohija by Census 2011 (Statistical Office of Kosovo).

Ethnicity	Number	%
Albanians	1.616.869	92,9
Serbs	25.532	1,5
Turks	18.738	1,1
Bosniaks	27.533	1,6
Roma	8.824	0,5
Ashkali	15.436	0,9
Egyptians	11.524	0,7
Gorans	10.265	0,6
Others	2.352	0,1
Undefined	912	0,1
It is not known	1.840	0,1
TOTAL	1.739.825	100

Based on the results of the census, the most numerous ethnic communities in Kosovo and Metohija were Albanians with 1.616.869 inhabitants, which participate with 92,9% of total population of Kosovo and Metohija (Table 3). The majority of the population was Albanian in all municipalities, except eight municipalities (four in northern Kosovo and Metohija: Leposavić, Zubin Potok, Zvečan and northern Kosovska Mitrovica and four newly formed municipalities: Mamuša, Gračanica, Ranilug and Parteš). An equal number of Albanians and Serbs were in the municipalities of Novo Brdo, Štrpce and Klokot.

The number of Serbs in this census was only 25.532 with participation of 1,5% in the total population. However, the Serbian population in the area of Kosovo and Metohija is much larger and therefore its participation in the total population is larger. The estimated number of Serbs in the four municipalities in the north of the Province is 60.000, while in the interior of Kosovo and Metohija there are more than 50 ethnically purely Serb or mixed settlements in which Serbs are represented in significant numbers.

About 40.000 Serbs live in central Kosovo. Thus, the Serbian settlements in the municipality of Vučitrn: Gojbulja, Prilužje and Grace. The Serb enclaves in Priština municipality are: Gračanica, Laplje selo, Čaglavica, Badovac, Preoce and Sušica. In the municipality of Obilić, it is Plemetina, and in the municipality of Kosovo Polje: Batuse, Ugljare, Bresje and Kuzmin. The Serb enclaves in Lipljan municipality are: Dobrotin, Livađe, Donja Gušterica, Gornja Gušterica, Suvi Do, Staro Gracko and Novo naselje. Prekovce is a Serbian enclave in Novo Brdo municipality. About 2.100 Serbs live in the Metohija settlements (the Goraždevac enclaves near Peć and Velika Hoča near Orahovac). In the municipality of Istok these are: Osojane, Crkolez, Dobruša, Banja, Ljubovo and Žač. Banja and Suvo Grlo are enclaves in Srbica municipality, and Vidanje in Klina municipality. Kosovo's pomoravlje is home to 35.000 Serbs. Thus, in the municipality of Gnjilane, the Serb population lives in the villages of: Šilovo, Pasjane, Parteš, Koretište, Donja Budriga, Stanišor, Kusce, Straža, Kmetovce and Poneš, and in Kosovska Kamenica in the villages of Ranilug, Ropotovo and Donje Korminjane. In the municipality of Vitina in the villages: Klokot, Vrbovac, Trpeza, Požaranje, Novo selo, Žitinje and Binač. In the far south of the AP Kosovo and Metohija, about 12.000 Serbs live in the Šara-mountain enclaves. They are located in the municipality of Štrpce in the following villages: Berevce, Brezovica, Viča, Vrbeštica, Gotovuša, Donja Bitinja, Drajkovce, Jažince, Sevce and Sušiće (Milosavljević, 2013). Demographic data indicate that there are currently approximately 149.100 Serbs in the entire area of Kosovo and Metohija, accounting for about 8,5% of the total population. Contemporary demographic determinants also point to the problem of the erasure of certain nationalities (Montenegrins, Muslims, Yugoslavs, Macedonians) and the formation of new ones (Bosniaks, Ashkali, Egyptians). Thus, according to the 2011 census, there are no Montenegrins at all, up to 30.000 according to earlier censuses. All this can lead us to conclude that Montenegrins have declared themselves either as Serbs, or have emigrated or are categorized as "Others", "Undefined" or "It is not known" with a total population of 5.104. This phenomenon points to the malicious tendency of the provisional Kosovo authorities to erase, all the parameters that determine the Serb ethnicity and the existence of the Serbian national being in the territory of Kosovo and Metohija.

Table 4. Population of Kosovo and Metohija by ethnicity by municipalities and cities, 2011, Census of population (Statistical Office of Kosovo).

	1	2	3	4	5	6	7	8	9	10	11	12
Dečani	39.402	3	0	60	33	42	393	1	19	2	64	40.019
Đakovica	87.672	17	16	73	738	613	5.117	13	92	71	134	94.556
Glogovac	58.445	2	5	14	0	0	2	0	22	3	38	58.331
Gnjilane	87.814	624	978	121	361	15	1	69	95	35	65	90.178
Dragaš	20.287	7	202	4.100	3	4	3	8.957	283	129	22	33.997
Istok	36.154	194	10	1.142	39	111	1.544	0	45	19	31	39.289
Kačanik	33.362	1	2	20	5	1	0	0	7	0	11	33.409
Klina	37.216	98	3	20	78	85	934	0	23	7	32	38.496
Kosovo polje	30.275	321	62	34	436	3.230	282	15	131	9	32	34.827
K.Kamenica	34.186	1.554	5	9	240	0	0	29	27	4	31	36.085
Mitrovica s.	69.497	14	518	416	528	647	6	23	47	61	152	71.909
Mitrovica n.	-	-	-	-	-	-	-	-	-	-	-	-
Leposavić	-	-	-	-	-	-	-	-	-	-	-	-
Lipljan	54.467	513	128	42	342	1.812	4	6	260	4	27	57.605
Novo brdo	3.524	3.122	7	5	63	3	0	0	2	0	3	6.729
Obilić	19.854	276	2	58	661	578	27	5	48	28	12	21.549
Orahovac	55.166	134	2	10	84	404	299	0	11	15	83	56.208
Peć	87.975	332	59	3.786	993	143	2.700	189	132	62	79	96.450
Podujevo	87.523	12	5	33	74	680	2	0	43	7	120	88.499
Priština	194.452	430	2.156	400	56	557	8	205	334	79	220	198.897
Prizren	145.718	237	9.091	16.896	2.899	1.350	168	655	386	222	159	177.781
Srbica	50.685	50	1	42	0	10	1	0	5	4	60	50.858
Štimlje	26.447	49	1	20	23	750	0	2	13	0	19	27.324
Štrpce	3.757	3.148	0	2	24	1	0	0	7	4	6	6.949
Suva reka	59.076	2	4	15	41	493	5	0	15	22	49	59.722
Uroševac	104.152	32	55	83	204	3.629	24	64	102	45	220	108.610
Vitina	46.669	113	4	25	12	14	0	7	83	12	48	46.987
Vučitrn	68.840	384	278	33	68	143	1	3	50	17	53	69.870
Zubin Potok	-	-	-	-	-	-	-	-	-	-	-	-
Zvečan	-	-	-	-	-	-	-	-	-	-	-	-
Mališevo	54.501	0	0	15	26	5	0	0	8	22	36	54.613
Junik	6.069	0	0	0	0	0	0	0	4	2	9	6.084
Mamuša	327	0	5.128	1	39	12	0	0	0	0	0	5.507
Đeneral Jan.	9.357	0	0	42	0	0	0	0	2	1	1	9.403
Gračanica	2.474	7.209	15	15	745	104	3	22	45	26	17	10.675
Ranilug	164	3.692	0	1	0	0	0	0	3	0	6	3.866
Parteš	0	1.785	0	0	0	0	0	0	2	0	0	1.787
Klokot	1.362	1.177	1	0	9	0	0	0	6	0	1	2.556
Total	1.616.869	25.532	18.738	27.533	8.824	15.436	11.524	10.265	2.352	912	1.840	1.739.825

Legend: 1-Albanians, 2-Serbs, 3-Turks, 4-Bosniaks, 5-Roma, 6-Ashkali,
7-Egyptians, 8-Gorans, 9-Others, 10-Undefined, 11-It is not known, 12-Total

The number of Bosniaks was 27.553 with participation from 1,6% of the population of Kosovo and Metohija. The most represented were in the Prizren municipality with 16.896 inhabitants, with participation from 9,5% of the municipal population. In addition to Prizren, a significant number also lived in the municipalities of Dragaš, Peć and Istok.

The population of Turks was 18.738 or 1,1% of the total population. Most of them, 93,1% were in the newly formed municipality of Mamuša, but a more serious number of them lived in the municipalities of Prizren, Priština and Gnjilane.

Ashkali had a population of 15.436 with participation in the total population of 0,9%. Significant number were the municipalities of Kosovo Polje (9,3%), Uroševac, Prizren and Lipljan.

The Egyptian ethnic minority numbered 11.524 with a total population participation of 0,7%. They were most concentrated in the municipalities of Đakovica, Peć and Istok.

Gorans ethnic minority population was 10.265, or 0,6% of the total population of Kosovo and Metohija. Most Gorans people lived in Dragaš municipality, 8.957 or 26,3% of the municipality population. The municipalities of Prizren, Priština and Peć also made significant numbers (Table 4).

Unlike earlier censuses conducted by the Republic of Serbia in the territory of the AP Kosovo and Metohija, in the 2011 census, there are no definitions for "Muslims", "Yugoslavs" and "Macedonians", which are ethnic communities that were represented until 1999 in considerable numbers. In this way, we remain deprived of comparative analyzes, monitoring of the number of the said ethnic communities as well as their participation in the total population of the Province.

CONCLUSION

The analysis of changes in the total population movement of the AP Kosovo and Metohija, during the second half of the 20th century, indicate a constant increase of the population. At the same time, with the increase of population, there are changes in the ethnic structure. The Albanian population is constantly increasing, while the Serb population is declining. Since June 1999, due to organized Albanian terror against Serbs and other non-Albanian populations, an exodus of about 320,000 people has occurred. The Serb population was expelled from all urban areas while a smaller number was held in rural areas, making up the so-called Serb enclaves. The results of the 2011 census conducted by (temporary Kosovo institutions) in Kosovo and Metohija cannot be considered relevant. Irrelevance is reflected in the inability to comprehensively understand the total population and their ethnic determinants. The Serb population did not respond to the census in the north of the Province, while in other parts it partially responded. The irrelevance of the census is also reflected in the fact that the census does not include citizens who are temporarily living abroad. Also, no displaced persons (Serbs and Montenegrins) were enumerated. The Roma community formally divided the pre-war divisions into Roma, Ashkali and Egyptians, and Bosniaks into Bosniaks, Muslims, and Gorans. Incorrectly conducted census and inexperience of training of census, takers determine the 2011 census data to be irrelevant, having only one purpose, namely, to the detriment of Serbs and the Serb community that has lived on the territory of AP Kosovo and Metohija for centuries.

REFERENCES

Medojević, J., & Milosavljević, S. 2019a. Demografski procesi na Kosovu i Metohiji od 1999. do 2019. godine, Kosovsko-metohijski zbornik 8, Srpska akademija nauka i umetnosti, Beograd, pp. 265-285.

Medojević, J., & Milosavljević, S. 2019b. Geo-demografski procesi na Kosovu i Metohiji od 1999. do 2019. godine, Zbornik rezimea sa Međunarodnog naučnog skupa „Nauka bez granica 3“, Filozofski fakultet Univerziteta u Prištini sa privremenim sedištem u Kosovskoj Mitrovici, Kosovska Mitrovica, pp. 126-127.

Medojević, J., & Milosavljević, S. 2018. Značaj geografskih determinanti u funkciji održivog opstanka srpske zajednice na Kosovu i Metohiji, Međunarodni tematski zbornik „Nauka bez granica“, Knjiga 4 Vreme i prostor, Filozofski fakultet Univerziteta u Prištini sa privremenim sedištem u Kosovskoj Mitrovici, Kosovska Mitrovica, pp. 251-266.

Medojević, J., & Milosavljević, S. 2015. Posledice progona stanovništva sa Kosova i Metohije od 1999. do 2015. Godine, Zbornik radova (Knjiga 1) sa Četvrtogsrpskog kongresa geografa sa međunarodnim učešćem „Dostignuća, aktuelnosti i izazovi geografske nauke i prakse“ povodom 150 godina rođenja Jovana Cvijića, Geografski fakultet Beograd, Srpsko geografsko društvo, Beograd, pp. 357-362.

Medojević, J., Pavlović, M., & Milosavlević, S. 2011. Demograhic analysis of forced migrations in Kosovo and Metohia from 1999 to 2011, Global Modern Demographic problems: migration and emigrational policy, Russian Academy of Sciences, Russian State University for the Humanities, Moscow, pp. 124-135.

Milosavljević, S. 2013. Demografsko-ekonomska analiza stanja u srpskim enklavama u funkciji unapređivanja strateškog razmišljanja i delovanja na Kosovu i Metohiji, Zbornik radova sa Međunarodnog naučnog skupa „Kulturno nasleđe Kosova i Metohije, istorijske tekovine Srbije na Kosovu i Metohiji i izazovi budućnosti“, Knjiga 2, Kancelarija za Kosovo i Metohiju Vlade Republike Srbije, Univerzitet u Prištini sa privremenim sedištem u Kosovskoj Mitrovici, Beograd, pp. 885-894.

Milosavljević, S., & Punišić, M. 2011. Popis stanovništva na Kosovu i Metohiji 2011. godine – između relevantnosti i irelevantnosti, Zbornik radova sa Trećeg kongresa srpskih geografa, Geografsko društvo Republike Srpske i PMF Uiverziteta u Banja Luci, Banja Luka, pp. 395-399.

Radovanović, M. 2004. Etnički i demografski procesi na Kosovu i Metohiji, Liber Press, Beograd

Statistical Office of Kosovo

Statistical Office of the Republic of Serbia

Bulletin of Natural Sciences Research
Vol. 10, No. 2, 2020, pp. 28-33.

DOI: https://doi.org/10.5937/bnsr10-29609
Original Scientific Paper

FUNCTIONAL TRANSFORMATION OF WEST MORAVA VALLEY DISTRICT SETTLEMENTS

IVANA PENJIŠEVIĆ[1], JOVAN DRAGOJLOVIĆ[1]

[1]Faculty of Sciences, University in Priština – Kosovska Mitrovica, Kosovska Mitrovica, Serbia

ABSTRACT

The existing territorial layout and the current demographic situation in the settlements of West Morava Valley District during the late 20th century and at the beginning of the 21st century are the result of the synchronized action of the process of industrialization, deagrarization and urbanization. They conditioned the selective transformation of urban and rural space, which led to the concentration of the population in urban and suburban settlements and the depopulation of the rural part of the West Morava Valley District. Within the studied region, the hierarchy of municipal centers, subcenters and communities of settlements was observed. Based on important theoretical and methodological assumptions and indicators, the paper analyzes the functional transformation of the settlements of West Morava Valley in the period between 1971- 2011. It was determined by certain quantitative methods that the changes went in the direction of reducing the share of purely agrarian settlements and increasing the share of industrial and service settlements.

Keywords: West Morava Valley District, Settlements Network, Business structures, Functional transformation of settlement.

INTRODUCTION

The area covered by the study represents the southernmost region of Peripannonian Serbia, while the time period of the research is 1971-2011. The reason for this is the fact that the most dynamic socio-economic transformation of the studied area occurred in the 1970's, caused by the influence of industrialization and urbanization. The West Morava River valley extends from west to east, including the valley of the West Morava River, from Požega in the west to Stalać in the east (Marković, 1970). The West Morava River valley is of composite character and consists of five depressions (Požega, Čačak - Kraljevo, Vrnjci, Trstenik, and Kruševac) and the same number of narrowings. This valley has great economic significance for Serbia (Lukić et al., 2018).

The West Morava Valley region was singled out on the basis of morphological and hydrological criteria of geographical regionalization, in which 230 dispersively distributed settlements were included in the research. The West Morava River valley is a large natural entity with an area of 2386.2 km^2 with 429,439 inhabitants, according to the 2011 census (SORS, 2014). Therefore, about 6.0% of the population lives on 2.7% of the territory of the Republic of Serbia (Penjišević, 2016). Both absolute and relative majority of the population lives on its most spacious part of the altitudinal belt up to 300 m (Table 1).

Table 1. Hypsometric distribution of population and settlements in the West Morava River valley.

Altitudinal Belt (m)	Area		Settlements		Population				Population Density (Pop/km sq)	
					1971.		2011.			
	km sq	%	Number	%	Number	%	Number	%	1971.	2011.
<300	1265.4	53.0	137	59.6	296,958	80.3	379,284	88.3	234.7	299.7
300-500	751.5	31.5	75	32.6	63,866	17.3	45,953	10.7	85.0	61.1
>500	369.0	15.5	18	7.8	8,886	2.4	4,202	1.0	24.1	11.4
Total	2386.2	100.0	230	100.0	369,730	100.0	429,439	100.0	154.9	179.9

Source: Comparative Population Overview 1948–2011. Data by settlements, vol. XX, SORS, Belgrade, 2014; Real Estate Cadastre Service of the Republic of Serbia; Topographic. Map 1:300.000, list Kragujevac, 1988; Author's processing.

In the altitude zone up to 300 m above sea level, which covers 53.0% of West Morava Valley, there are 137 settlements (Table 1). In 1971, there were 296,958 inhabitants (80.3% of the population), and in 2011 this number rose to 379,284 (88.3%). In the altitude zone up to 300 m above sea level, all regional centers of West Morava Valley (Čačak, Kraljevo, Kruševac, Požega, Vrnjačka Banja and Trstenik) are located, as well as other population-wise largest and functionally most important suburban settlements in the region. The concentration of population in this altitude zone arose as a consequence of industrialization in the mentioned city centers, but also as an intensive decline in the number of inhabitants in the higher zones of the studied region.

* Corresponding author: ivana.penjisevic@pr.ac.rs

MATERIAL AND METHODS

In this paper, the typological method and the method of the Horst-Ferre triangle are used. The application of the typological method is extremely important in the research of settlements, because it is possible to single out relatively homogeneously structured settlement systems and subsystems, with similar functional development laws. The typological method of settlement classification has a long tradition in the Serbian geographical school. As early as the beginning of the 20th century, Cvijić's anthropogeographical conception laid the foundations for a systemic-structural approach, which is reflected in various types of typological classification of settlements (Antić, 2015). Grčić (1999) made a significant contribution to the functional systematization of settlements, through the elaboration of methodological settings of the typological classification of settlements (Dragojlović et al., 2017). Spatial-demographic and socio-economic specifics of the settlement transformation of the West Morava Valley indicate the possibility of applying the typological classification method, as a starting point for considering changes in employment of the working population by activity sectors (Tošić, 2012). Within the studied region, the hierarchy of municipal centers, sub-centers and communities was observed.

Another method used in the paper is the Horst-Ferre triangle method, which is a graphical representation of the population activity structure. The Horst-Ferre triangle method implies the selection of nine types of settlements based on the participation of individual sectors of activity in the contingent of the population that performs the occupation (Tošić, 1999). It is represented by an equilateral triangle whose sides are divided into sections indicating the percentages of primary, secondary and tertiary activity. The inside of the diagram is divided into types denoted by a combination of numbers and letters. The functional type of settlements will be defined in the intersection of three lines, each of which has the value of a certain sector activity (Matijević, 2009). Due to the availability of the necessary data, the Horst-Ferre triangle method is fully applicable for the functional transformation of the West Morava Valley settlements analysis (Figure 1). The functional type of settlement is determined on the basis of the share of primary, secondary and tertiary sector activity in the total population performing occupation (Davies, 1967). The threshold for determining dominant belonging to a certain sector of activity is 60% (Table 2).

RESEARCH RESULTS

The dynamic functional transformation of urban and rural settlements in The West Morava River valley has been present since the mid-20th century up to today, when under the influence of the process of industrialization and urbanization, the key features of this region. Carriers of regional development were the city centers – Kraljevo, Čačak, Kruševac, Požega, Trstenik i Vrnjačka Spa. There along with the rapid development of industry, a concentration of population and development firstly of secondary, and then tertiary and quaternary activities.

The network of settlements in West Morava Valley belongs to the category of underdeveloped, with a pronounced disproportion between the level and speed of development of the above-mentioned urban settlements on one side and hilly-mountainous settlements on the other. Some rural settlements from territory City of Čačak (Vidova, Međuvršje, Prislonica), City of Kraljevo (Vitanovac, Ratina, Mataruge, Progorelica) and City of Kruševac (Maskare) developed certain functions at the beginning of the second decade of the 21st century, but they are still insufficient to establish an even regional redistribution of the population's economic activities of West Morava Valley. In non-agrarian as well as agrarian settlements of West Morava Valley, the structure of the active population largely corresponds to the structure of their functions. Deviations, conditionally speaking, can be in those settlements where the participation of daily migrants is higher. Accordingly, the criterion for functional transformation should include the function of employment as well as the centrality of the settlement (Đurkin, 2018).

Changes in the functional structure of settlements are easiest to monitor on the basis of indicators of changes in the activity structure of the active population that performs certain occupations (Tošić, 1999). According to this model, nine functional types of settlements have been differentiated in the territory of the West Morava Valley (Table 2).

By applying the mentioned methodology, from 1971 to 2011, it was concluded that the degree of functional transformation of the settlement of West Morava Valley was growing slowly. Until the middle of the 20th century, the functions of the settlements of the studied region completely depended on the way of using land and water resources, so the available natural potentials and low level of economic development conditioned their agrarian character. The functional transformation of the settlements of West Morava Valley, conditioned by the industrial development that began in the 1960s, greatly reduced the dependence of the rural economy on the natural potentials in the area of the settlement. The process of industrialization in them initiated the transfer of the rural agricultural population to non-agricultural activities. Thus, the structural changes are reflected in the gradual decrease of the share of the primary sector, on the one hand, and increase of the secondary and tertiary sectors, on the other.

The number of agro-industrial settlements from 1971 to 2011 increased from 19 to 34, and the structural changes in them are reflected in the gradual decrease in the share of the primary and the increase in the secondary sector of activity. In 1971, settlements near the main city centers, whose significant share of the population was employed in the industrial plants of Kraljevo (Adrani, Žiča, Vrba, Zaklopača, Konarevo, Šumarice), Požega

(Bakionica, Gorobilje, Prijanovići), Kruševac (Begovo Brdo and Čitluk) and Čačak (Međuvršje) belonged to this functional type. Forty years later, the number of agro-industrial settlements increased by 15, with the share of those which are active in the primary sector ranging from 38.8% (Čukojevac on the Gledić Mountains from territory City of Kraljevo) to 59.6% (Banjica on Jelica from territory City od Čačak).

Table 2. Methodology for distinguishing functional types of settlements in the West Morava Valley in 1971 and 2011.

Functional type of settlements	Criteria	1971.	2011.	Change
Agrarian	I>or=60%	179	73	-106
Agro-industrial	I>II>III	19	34	+15
Agro-service	I>III>II	0	7	+7
Agrarian total		198	114	-84
Industrial	II>or=60%	12	23	+11
Industrial-agrarian	II>I>III	14	22	+8
Industrian-sevice	II>III>I	4	59	+55
Industrial total		30	104	+74
Service	III>or=60%	0	0	0
Service-agrarian	III>I>II	0	1	+1
Service-industrial	III>II>I	2	12	+10
Service total		2	13	+11

Source: Tošić (1999); Federal Bureau of Statistics, Beograd, 1974, SORS, Beograd, 2014;Penjišević (2016)

In 1971, there were no settlements in the West Morava Valley, and in 2011 there were seven settlements: Vapa, Donja Gorevnica, Donja Trepča, Gornja Trepča, Baluga Ljubićska and Mrčajevci on the territory of the City of Čačak and Varvarin Village. These are well-connected settlements with the centers, which have developed a tourist-catering, educational and health function in the meantime.

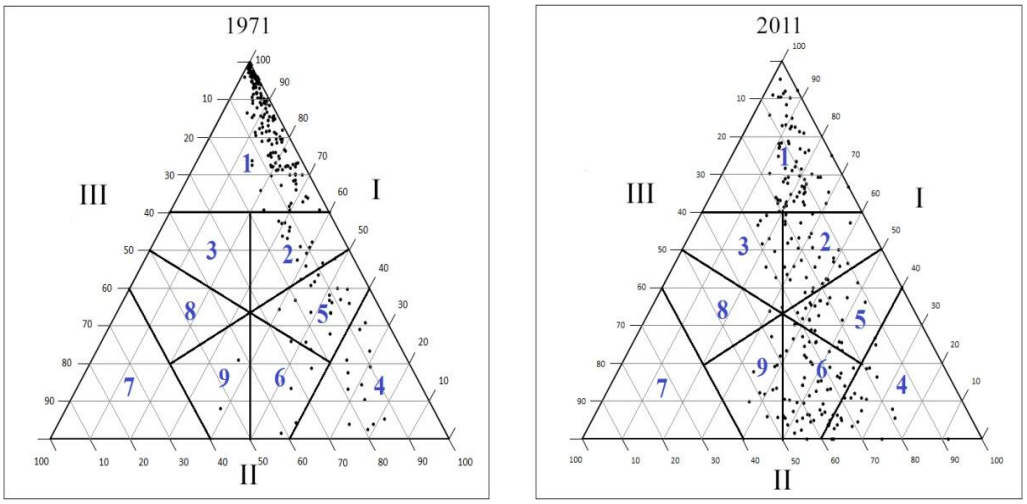

Figure 1. Changes in functional types of settlements in West Morava Valley in 1971 and 2002 by the Horst-Ferre triangle method

Legend: 1. Agrarian; 2. Agro-industrial; 3. Agro-servicing; 4. Industrial; 5. Industrial-agrarian; 6. Industrial-servicing; 7. Servicing; 8. Servicing-agrarian; 9. Servicing-industrial.

The biggest functional changes are evident in the vicinity of the gravity centers of Čačak, Kruševac and Kraljevo, as well as in settlements along important roads such as the West Moravian and Ibar highways. The expansion of the influence of urban settlements intensified the daily mobility of the population, the restructuring of activities as well as the concentration of functions, which indirectly or directly reflected on the differentiation of the settlement network into peri-urban and agrarian parts.

In 1971, 198 settlements or 86.1% of all settlements in West Morava Valley were of the agrarian type (Figure 2). Most settlements with over 60% active in the primary sector of activity were from the municipalities of Trstenik (49 out of 51 settlements), Čačak (47 out of 58) and Kruševac (31 out of 43). The studied region had an agricultural character in 1971, which is shown by the fact that 136 settlements had over 90% of the active population in the primary sector of activity. Such settlements were mostly located in the municipality of Trstenik (32), followed by Čačak (15), Kruševac (14), Kraljevo (6), while in the municipality of Vrnjačka Banja only the settlements of Vukušica and Otroci belonged to this category (Figure 2).

The intensity of the process of deagrarization of West Morava Valley can be seen based on the data on the active population by activities from the 2011 census (Figure 3). Based on the given graphic contribution, it is evident that agrarian characteristics, where more than 60% are active in the primary sector of activity, retained only 73 settlements (31.8%). This means that compared to 1971, 22 settlements in West Morava Valley have moved to a higher functional type (Table 2). The number of settlements where more than 90% were active in the primary sector in 2011 was reduced from 136 to 10 settlements, which and are the following: Brezovice and Premeća on the mountain Jelica (City of Čačak), Trgovište on Kotlenik (City of Kraljevo), Rajinac and Mala Sugubina on the Gledić Mountain (Municipality of Trstenik), as well as Lazarevac, Kamenare, Komorane, Globare and Ljubava on the northern edge of the Kruševac valley towards Temnić (Figure 3).

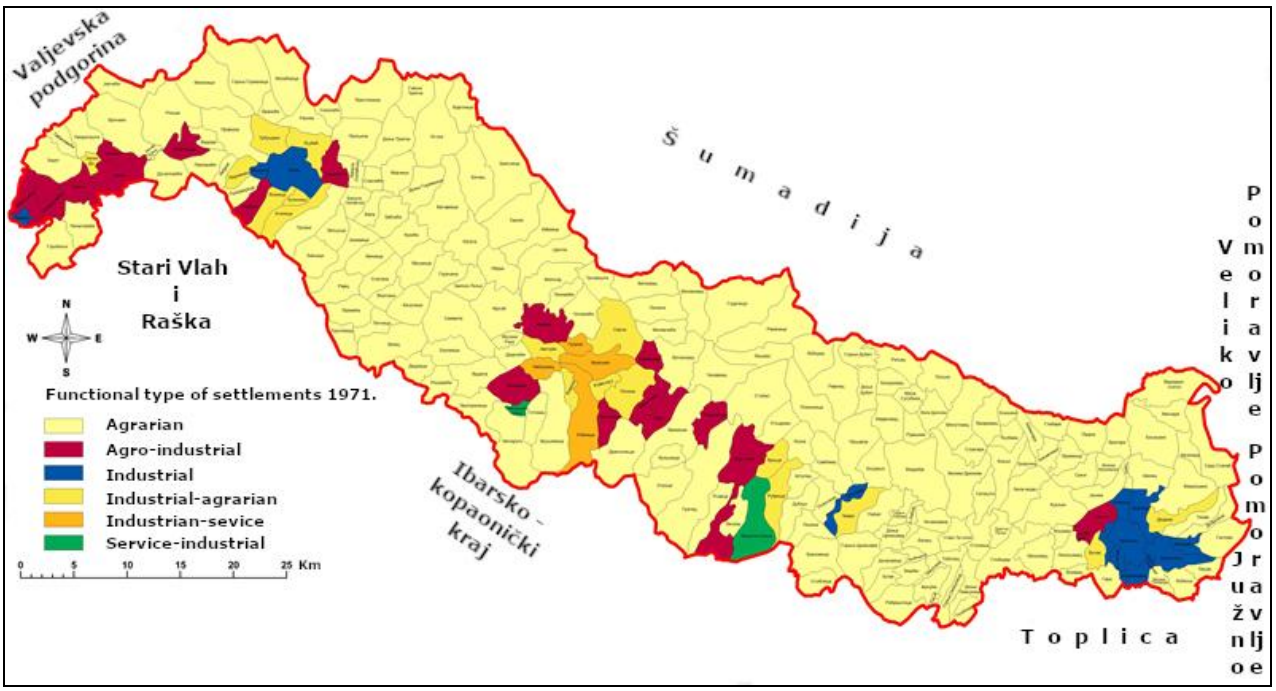

Figure 2. Functional type of settlements in West Morava Valley 1971. (Source: Federal Bureau of Statistics, Beograd, 1974; Map 1:300.000, list Kragujevac, 1988; Penjišević, 2016).

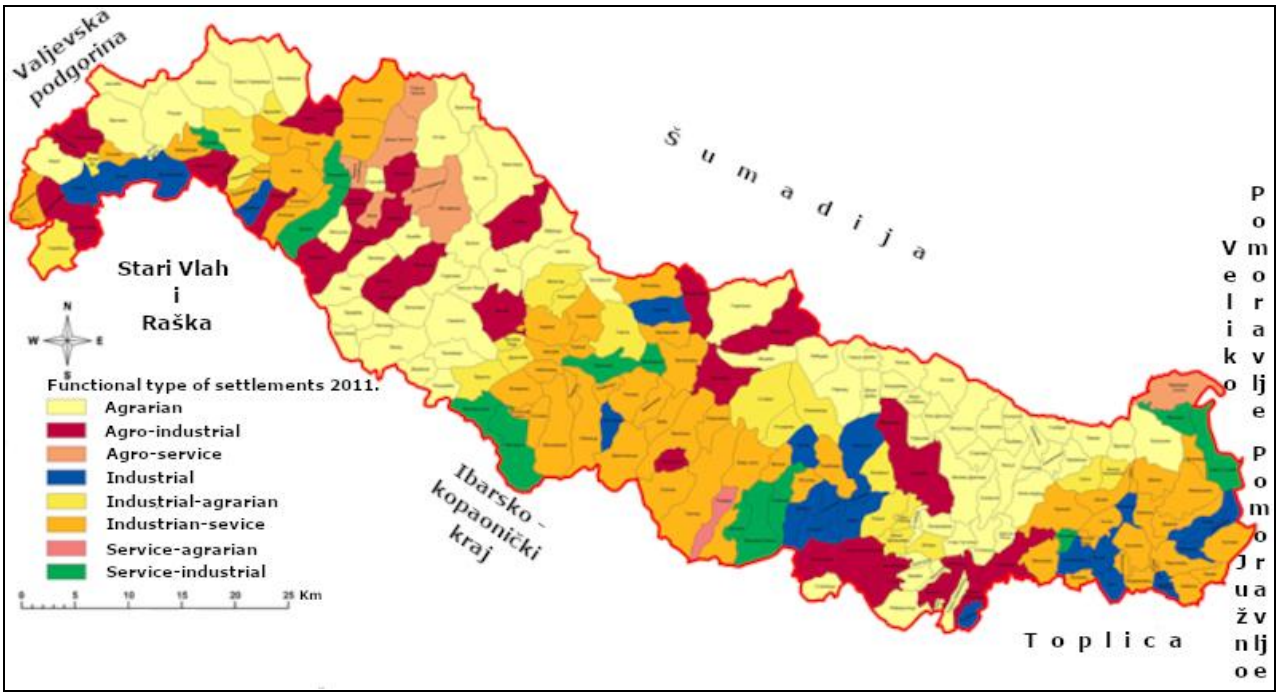

Figure 3. Functional type of settlements in West Morava Valley 2011. (Source: SORS, Beograd, 2014; Map 1:300.000, list Kragujevac, 1988; Penjišević, 2016).

DISCUSION

By analyzing the results obtained by the research, it can be concluded that in the 1970s only urban centers and a few settlements in their spatial-influential sphere had a polyfunctional character, while other settlements of West Morava Valley were monofunctional. The territorial range of the functions of Čačak, Kraljevo and Kruševac is the strongest in the neighboring cities, i.e. municipal centers - Požega, Vrnjačka Banja and Trstenik. The functional development of municipal centers proved to be insufficient for the city to actively participate in the development processes of its surroundings, which was reflected in the demographic and functional characteristics of settlements in its surroundings, especially in peripheral parts (Stamenković & Gatarić, 2007).

With the industrialization of the region, the majority of young and working-age people from the countryside are employed in urban centers and no longer live primarily from the land (Tošić & Krunić, 2005). Compared to 1971, the impact of natural potentials on the functional type of settlements in 2011 decreased significantly. However, a part of the rural population from certain settlements such as Zaklopača, Konarevo, Zablaće, Trnava, Bakionica, Stopanje and others, who work in the city, but still live in the countryside, are engaged in agriculture as an additional source of income.

Although some West Morava Valley villages are non-agrarian according to the functional typology, agriculture has remained the main function of the population in the rural areas themselves. For example, the settlement of Progorelica (City of Kraljevo), located on the border of West Morava Valley and Donjeibarsko-Kopaonik region, in 2011 was classified as a highly non-agricultural settlement of the tertiary-secondary type, with only 5.8% of the active population in the primary sector (FBS, 1974; SORS, 2014; Penjišević, 2016). Most of the population of this Kraljevo settlement is employed in industrial plants in neighboring Konarevo and the rehabilitation center "Agens" in Mataruska Banja, but in the rural area of Progorelica in the alluvial plain of the Ibar, agriculture remained the main economic function. The situation is similar with the settlements of Vrba (6.6% active in the primary sector) and Konarevo (9.4%) in the territory of the City of Kraljevo, Jezdina (7.9% in the primary sector) in the City of Čačak and Popina (11.0 %) in Municipality of Trstenik, as well as with the settlements of Gari (10.5%) and Veliko Golovode (10.9%) on the territory of the City of Kruševac. This indicates that agricultural land, as the most significant natural potential of the rural parts of West Morava Valley, remained the basis of their regional development. Modernization of agriculture, introduction of agro-technical measures, primarily mechanization, has influenced the reduction of the need for great manpower in agriculture.

Structural changes in the economy, caused by the process of industrialization and urbanization, directly affected the decrease in the participation of the active population in the primary and the increase in the participation of the active population in the secondary and tertiary sectors of activity. Indicators of the change in the structure of activities indicate that in West Morava Valley in the period from 1971 to 2011, the secondary sector developed most strongly. The number of settlements belonging to one of the three industrial types increased from 30 to 104, with the number of industrial settlements increasing from 12 to 23, industrial-agricultural from 14 to 22 and industrial-service type from 4 to 59 (Table 2).

The industry of West Morava Valley was largely based on the use of local raw materials (Stanisavljević, 1974). The economic and political situation in the country at the end of the 20th century, caused by the shutdown of a large number of factory plants, especially affected the functional development of West Morava Valley. Požega, Čačak and Kruševac have transformed from a predominantly industrial type into an industrial-service type. With the shutdown of the former giants of the metal industry, "Wagon Factory" and "Magnochrome", Kraljevo was transformed from an industrial-service to a service-industrial settlement. Thanks to the development of the functions of administration, health (Health Center "Studenica", Rehabilitation Center "Agent") and education (expansion of the network of primary and secondary schools and the opening of the Faculty of Mechanical Engineering), in 2011 the city on the Ibar River was 50.8% active in tertiary sector of activity. For forty years, Trstenik has retained the characteristics of an industrial-type settlement (62.4% active in the secondary sector), while Vrnjačka Banja was a service-industrial settlement and still is, with 53.2% of employees in the tourism and catering sector (Penjišević, 2016).

In the activity structure of West Morava Valley, in addition to the secondary sector, tertiary development was developing intensively as well, where the number of service settlements increased from 2 to 13 (Table 2). In the analyzed period, one service-agricultural settlement developed - Rsavci from Vrnjačka Banja. This is a hilly-mountainous settlement, a significant part of which is located on the slopes of Goč, according to the functional typology in 1971, it belonged to the agrarian type, with 78.2% active in the primary sector. The transformation of the Rsavci settlement into a service-agrarian type in 2011 can be explained by the proximity of Vrnjačka Banja (3 km away), with a third of the rural population employed in hotels and catering facilities of this tourist center. From 1971 to 2011, the biggest changes took place in the type of service-industrial settlements, the number of which increased from 2 to 12. In the 1970's, those were the spa settlements of Vrnjačka and Mataruška Spa. In 2011, four settlements from the territory of the city of Kraljevo, (Kraljevo, Mataruge, Progorelica and Šumarice), three settlements from the territory of the City of Čačak (Trnava, Konjevići and Vidova), three settlements from the Municipality of Vrnjačka Banja (Vrnjačka Banja, Lipova and Ruđinci), as well as the settlement of Koševi from the territory of the City of

Kruševac and Maskare from the Municipality of Varvarin belonged to this category as well (Figure 3).

CONCLUSION

Negative demographic processes and changes on the territory of The West Morava valley during the second half of the 20th century conditioned not just the processes of deagrarization, depopulation and concentration but funkctional transformation of the settlements in this region is well. These changes contributed to the development of urban settlements of The West Morava valley, but also brought the stagnation of demographic potential of rural settlements. In order for the studied region to develop more evenly, it is necessary to invest in the development of all types of modern infrastructure, which is a very important factor for more progressive development of settlements in hilly and peripheral areas. An important aspect of the regional development of rural settlements in West Morava Valley is agriculture, which due to the improvement of this industry and all the conditions for successful development, could positively affect their future transformation. Thus, in order to encourage functional decentralization, it is necessary to develop microdevelopmental nuclei in which some industrial plants would be located, preferably adapted to local raw materials. The settlements of Gornja Trepca, Prislonica, Tavnik, Ladjevci and Milutovac have predispositions to become micro-development centers of the hilly and mountainous part of West Morava Valley, and must be valorized by planned measures. In order to transform these settlements into micro development centers, it is necessary to define the minimum production and central functions, which will be developed in them. Also, since West Morava Valley is a fruit and wine region, the opening of as many processing capacities as possible would have a positive effect in the villages on the outskirts of Požeška basin (Pilatovići, Loret), Čačanska basin (Prislonica, Gornja Trnava) and Trstenička basin (Jasikovica, Bučje), which would improve their hierarchical position in the settlement network of West Morava Valley.

REFERENCES

Antić, M. 2015. Tipologija seoskih naselja kao polazište revitalizacije ruralnog prostora Srbije. Zbornik radova sa 4. Kongresa srpskih geografa. Univerzitet u Beogradu: Geografski fakultet i Srpsko geografsko društvo. pp. 453-458.

Bouldville, J. 1966. Problems of Regional Planning:Edinburgh University Press. Edinburgh.

Davies, E.K.D. 1967. Centrality and Central Place Hierarchy. Urban Studies, 4.

Dragojlović, J., Ristić, D., & Milentijević, N. 2017. Spatial functional transformation and typology of the settlement system of Toplica district. The University Thought - Publication in Natural Sciences, *7*(2), 47-51. doi:10.5937/univtho7-15574

Đurkin, D. 2018. Tipovi promena populacionog razvoja naselja Južnog Banata (Srbija). Glasnik Srpskog geografskog društva, Beograd, 91(1), pp. 107-121.

Grčić, M. 1999. Funkcionalna klasifikacija naseqa Mačve, Šabačke posavine i pocerine. Glasnik Srpskog geografskog društva, Beograd, 79(1).

Lukić, T. Dunjić, J. Đerčan, B. Penjišević, I. Milosavljević, S. Bubalo-Živković, M. & Solarević, M. 2018. Local Resilience to Natural Hazards in Serbia. Case Study: The West Morava River Valley. Sustainability 2018, 10(8), 2866, p. 1-16. https://doi.org/10.3390/su10082866

Marković, J. 1970. Geografske oblasti SFRJ. Zavod za uđžbenike i nastavna sredstva. Beograd.

Matijević, D. 2009. Spatial functional connection of the settlements Municipalities Stara Pazova with the urban sistem of Belgrade. Geographical institute Jovan Cvijić SANU. Belgrade.

Pavlović, M. & Radivojević, A. 2009. Promene u funkcionalnim tipovima naselja opštine Sokobanja. Glasnik Srpskog geografskog društva, Beograd, 89(3), pp. 81-93.

Penjišević, I. 2016. Geografski aspekti regionalnog razvoja Zapadnog Pomoravlja. Univerzitet u Novom Sadu: Prirodno-matematički fakultet. Doktorka distertacija.

Republički zavod za statistiku. 2012. Popis stanovništva, domaćinstava i stanova 2011. u Republici Srbiji. Ekonomska aktivnost, podaci po naseljima. Beograd

Republički zavod za statistiku. 2014. Uporedni pregled broja stanovnika 1948-2011. Podaci po naseljima, knj. 20. Beograd

Savezni zavod za statistiku. 1974. Popis stanovništva 1971. Aktivno stanovništvo prema delatnosti, knj. 10. Beograd.

Stamenković, S. & Gatarić, D. 2007. Čačak i njegov dnevni urbani sistem. Glasnik Srpskog geografskog društva, Beograd, 87(1).

Stanisavljević, D. 1974. Populacioni razvitak gradskih naselja u Zapadnom Pomoravlju. Univerzitet u Beogradu: Geografski fakultet. Beograd. Magistarski rad.

Topografska karta 1:300 000, list Kragujevac, 1988. Vojnogeografski institut, Beograd.

Tošić, D. 1999. Prostorno-funkcijski odnosi i veze u nodalnoj regiji Užica. Univerzitet u Beogradu: Geografski fakultet. Beograd. Doktorska disertacija.

Tošić, D. 2012. Principi regionalizacije. Univerzitet u Beogradu: Geografski fakultet. Beograd.

Tošić. D. & Krunić, N. 2005. Urbane aglomeracije u funkciji regionalne integracije Srbije i Jugoistočne Evrope. Glasnik Srpskog geografskog društva, Beograd, 85(1).

Bulletin of Natural Sciences Research
Vol.10, No.2, 2020, pp. 34-37.

DOI: https://doi.org/10.5937/bnsr10-26655
Original Scientific Paper

SOME MATHEMATICAL CONCEPTS IN GEOMETRY OF MASSES

GORDANA JELIĆ[1,⋆], DEJAN STOŠOVIĆ[1]

[1]Faculty of Technical Sciences, University in Priština, Kosovska Mitrovica, Serbia

ABSTRACT

The study of the distribution of geometrical points, loaded by some scalars plays an important role in various fields of science, of theoretical and practical character. Since such study was first applied and studied when mass had the role of played a scalar, the mass loaded point was named material point, and the discipline dealing with the arrangement of material points in space is called the geometric mass. In that discipline, in the general case under mass one should imply a scalar of arbitrary nature, which can be negative as well. For example, the discipline includes the study of distribution of magnetic or electrical masses, which can be positive and negative. This paper presents some concepts from the geometry of masses that play an important role, particularly in mechanics and physics.

Keywords: Material point, Geometry of masses, Body density, Linear density, Surface density, Homogeneous material, Non-homogeneous materials, Center of mass

INTRODUCTION

The set of material points in the final or infinite number is called the material system. The material points of system are arranged discretely or continuously. Each mass, even the smallest, needs to take up some, perhaps even a very small volume. On the other hand, for a large mass we can take a geometric point and consider that the point with the overall mass represents the mass (Awrejcewicz, 2012). If it can be prove that all the points of the entire mass move as the selected representative point, then selected geometric point represents the entire mass and exists as a discrete material point (Mirtich, 1996; Whitaker, 1992).

THE CONCEPT OF DENSITY OF CONTINUOUSLY DISTRIBUTED MASSES

For the system of continuously distributed masses firstly is introduced the concept of *medium volumetric density*, as a ratio $\Delta m/\Delta V$ where ΔV is the volume and Δm is the mass in the volume. Then, it can be introduced the concept of *density of a given body at a given point M* as

$$\sigma = \lim_{\Delta V \to 0} \frac{\Delta m}{\Delta V} = \frac{\mathrm{d}m}{\mathrm{d}V},$$

where dm is the mass differential and dV is the differential of the corresponding volume. In general case, the density σ depends on the position of the point M in the given body. It is expressed by the following equation $\sigma = f(M) = f(\mu)$, where μ is the radius-vector of point M with respect to a origin, i.e. of permanent position O to the body, that is $\mu = \overrightarrow{OM}$. If the vector μ is determined using the Cartesian coordinates (x, y, z) of the point M, then the density is scalar function $\sigma = f(x, y, z)$. Finally, if the density is given for all points of volume V, the mass of the body m is determined by the integral (Bilimović, 1961; Dorogovtsev, 1987)(in english):

$$m = \iiint_V \sigma \mathrm{d}V = \iiint_V \sigma(x, y, z)\mathrm{d}x\mathrm{d}y\mathrm{d}z$$

extended to the entire volume V of the body.

Regardless of each mass having have to occupy a volume, it can also be discussed on the surface and the linear distribution of the masses. The examples of surface mass distribution can be material plates, covers, shells, sheet metal, etc. and the examples for linear distribution of masses can be rods, wires, cords etc. Related to such distributions we can talk about *medium surface density* $\Delta m/\Delta A$, where Δm is the mass and ΔA is a part of the surface of the mass. Limit value

$$\sigma_1 = \lim_{\Delta A \to 0} \frac{\Delta m}{\Delta A} = \frac{\mathrm{d}m}{\mathrm{d}A},$$

is surface density in the given point M. Similarly,

$$\sigma_2 = \lim_{\Delta \ell \to 0} \frac{\Delta m}{\Delta \ell} = \frac{\mathrm{d}m}{\mathrm{d}\ell},$$

is *the linear density* (of a given wire at a given point M).

Note that the above densities have different dimensions, i.e. it is valid

$$[\sigma] = ML^{-3}, \qquad [\sigma_1] = ML^{-2}, \qquad [\sigma_2] = ML^{-1}$$

where M is the mass, as measured by, say, grams, and L indicates the length in centimeters. Determination of body mass of density is calculated as the double integral

$$m = \iint_A \sigma_1(u, v)\sqrt{EG - F^2}\mathrm{d}u\mathrm{d}v = \iint_A \sigma_1(x, y)\mathrm{d}x\mathrm{d}y,$$

where A is the surface of the body. In the case of linear mass distribution we have the following integral

$$m = \int_L \sigma_2(\ell)\mathrm{d}\ell,$$

⋆ Corresponding author: gordana.jelic@pr.ac.rs

where $\mathrm{d}\ell$ is the element of length extended to the entire length of the curve. For a real wire it is

$$m = \iint_L \sigma_2(x)\mathrm{d}x.$$

If $\sigma, \sigma_1, \sigma_2$ are constant values, the matter of the body is *homogeneous* and to calculate body mass it is sufficient to know the volume i.e. the surface or the length of the body, because in these cases

$$m = \sigma V = \sigma_1 A = \sigma_2 L.$$

In the cases of *non-homogeneous (heterogeneous) matter*, body mass is not proportional to the density.

CENTER OF MASSES OR CENTER OF INERTIA

If related to the point M is the mass m and $\overrightarrow{AM}$ is the vector of position of the point M in respect to point A, the result $m\overrightarrow{AM}$ is called *the position vector burdened by mass m* (of the point M in respect to point A)(Bessonov & Song, 2001). Suppose that we have a set of n points of $M_1, M_2, ..., M_n$ with masses $m_1, m_2, ..., m_n$ and one particular point of space A. The position vector for each point of this set may be constructed burdened by mass relative to point A and we can make a summation of all constructed vectors $m_1\overrightarrow{AM_1} + \cdots + m_n\overrightarrow{AM_n}$. The result of this sum is a vector starting at point A. If this vector is divided by the entire mass $m = \sum_{j=1}^{n} m_j$, we will get a new vector, whose the end we will mark with C. In this manner, the vector equation

$$m\overrightarrow{AC} = \sum_{j=1}^{n} m_j\overrightarrow{AM_j} \tag{1}$$

determines the point C. Thus defined point C is called *the center (of inertia of the masses)*.

In following, we shall examine some typical properties of the center of inertia. In this sense, we shall prove two simple propositions that justify the meaning that this point was called the center.

Theorem 1. *The position of point C of a given material system do not depends on the choice of point A, i.e. the beginning of the position vector of all constructed points.*

Proof. Let us take as the starting point, besides A, some other an arbitrary point $A_1 \neq A$. If we denote with C_1 the appropriate center of inertia of the point A_1, we obtain the new vector equation

$$m\overrightarrow{AC_1} = \sum_{j=1}^{n} m_j\overrightarrow{A_1M_j}. \tag{2}$$

Notice that $\overrightarrow{AC_1} = \overrightarrow{A_1A} + \overrightarrow{AC} + \overrightarrow{CC_1}$ and $\overrightarrow{A_1M_j} = \overrightarrow{A_1A} + \overrightarrow{AM_j}$, $j = 1, \ldots, n$ (see Fig. 1). Now, if we put those vectors in the Eq.(2), and taking into account the Eq.(1), we get

$$m\overrightarrow{A_1A} + m\overrightarrow{AC} + m\overrightarrow{CC_1} = \sum_{j=1}^{n} m_j\overrightarrow{A_1A} + \sum_{j=1}^{n} m_j\overrightarrow{AM_j}$$

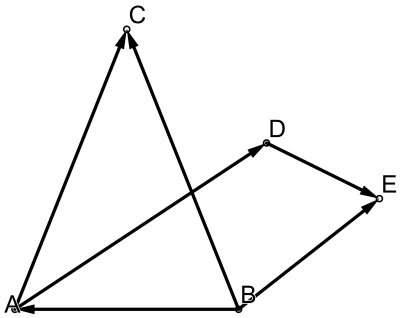

Figure 1. Determining the center (of inertia of the masses).

which implies $\overrightarrow{CC_1} = \overrightarrow{0}$. Thus, the center C_1 coincides with the original one.

Remark 2. According to Theorem 1, it follows that the position of the center depends only on the size of the masses and the distribution of these masses in the area. Therefore, the center of masses is an important natural point of any material system.

Theorem 3. *The sum of the position vectors of points M_j, in relation to the center C and weighted by the masses m_j is equal to zero, i.e.*

$$\sum_{j=1}^{n} m_j\overrightarrow{CM_j} = \overrightarrow{0}. \tag{3}$$

Proof. Let us consider again the Eq.(1). In order to determine the point C, into this equation let we put $\overrightarrow{AM_j} = \overrightarrow{AC} + \overrightarrow{CM_j}$, $j = 1, \ldots, n$. Thus, we have:

$$m\overrightarrow{AC} = \sum_{j=1}^{n} m_j\left(\overrightarrow{AC} + \overrightarrow{CM_j}\right),$$

or, equivalently:

$$\sum_{j=1}^{n} m_j\overrightarrow{CM_j} = \overrightarrow{0},$$

which was supposed to be proven.

Remark 4. From the basic vector Eq.(1) for the center C it follows that:

$$\overrightarrow{AC} = \sum_{j=1}^{n} \lambda_j\overrightarrow{AM_j} \tag{4}$$

where $\lambda_j = m_j/m$, $j = 1, \ldots, n$ and $\sum_{j=1}^{n} \lambda_j = 1$. Thus, vector $\overrightarrow{AC}$ is the convex combination of vectors $\overrightarrow{AM_1}, \ldots, \overrightarrow{AM_n}$. In the Cartesian coordinates, Eq.(4) can be written as:

$$\overrightarrow{\mu_c} = \sum_{j=1}^{n} \lambda_j\overrightarrow{\mu_j}, \tag{5}$$

where $\overrightarrow{\mu}_c = \overrightarrow{AC} = (x_c, y_c, z_c)$ and $\overrightarrow{\mu}_j = \overrightarrow{AM_j} = (x_j, y_j, z_j)$. In this way, to the vector Eqs.(4)-(5) correspond the following three scalar equations

$$x_c = \sum_{j=1}^{n} \lambda_j x_j, \quad y_c = \sum_{j=1}^{n} \lambda_j y_j, \quad z_c = \sum_{j=1}^{n} \lambda_j z_j.$$

These are the basic scalar equations for determining the position of the center of masses.

Remark 5. If the masses of a material system are distributed in a certain area continuously, the sums extended to all material points of the system pass into defined integrals extended to the areas of continuous matter. Then we have the vector equations:

$$\overrightarrow{AC} \iiint\limits_V \mathrm{d}m = \iiint\limits_V \overrightarrow{\mu}\,\mathrm{d}m$$

or

$$\overrightarrow{AC} \iiint\limits_V \sigma \mathrm{d}V = \iiint\limits_V \sigma\overrightarrow{\mu}\,\mathrm{d}m.$$

The scalar form of O_x is:

$$x_c = \iiint\limits_V \sigma x \mathrm{d}V : \iiint\limits_V \sigma \mathrm{d}V$$

The analog integrals apply in the case of masses continuously distributed over the surface and along the lines.

Remark 6. If the matter of body is homogeneous, the multiplier of density σ entering the numerator and denominator can be shortened, and thus for the homogeneous bodies we have patterns in which the mass is not included. These patterns can be considered as forms for the determination of the center of inertia of a volume i.e. of a surface or line. Thus, we have:

$$x_c = \iiint\limits_V x\mathrm{d}V : \iiint\limits_V \mathrm{d}V,\ x_c' = \iint\limits_A x\mathrm{d}A : \iint\limits_A \mathrm{d}A,\ x_c'' = \int\limits_L x\mathrm{d}l : \int\limits_L \mathrm{d}l$$

Remark 7. If the arrangement is symmetrical with respect to a plane, or a line or point, the center of masses must lie in that plane, on the line or at that point.

PAPPOS-GULDIN'S THEOREMS

Regarding the concept of the center of masses we list two so-called Pappos-Guldin's theorems.

Theorem 8. *The area which is obtained by rotating the arc of a curve in the plane about an axis in the plane, which does not cut the curve, is equal to the product of the arc length and circumference of a circle described by the mass center of this arc.*

Proof.

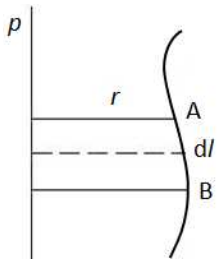

Figure 2. Arc of a curve in the plane.

Let a part of the flat curve, from point A to point B, rotate about an axis p on the curve plane and does not cut the curve, but only points A and B can belong to the axis. Let Δl be the distance between two very close points of the curve (see Fig. 2). Area formed by Δl in reversing (i.e. the side surface of the cylinder, coupe, truncated cone or a circular ring) is equal to $2\pi r_s \Delta l$, where r_s is the distance of the middle of the line Δl from the axis of rotation. Since in the border case the area is expressed by $2\pi r\mathrm{d}l$, where $\mathrm{d}l$ is the differential of the curve arc and r is the distance of an arbitrary point of the arc from the rotation axis, accordingly the surface S, described by the arc AB is equal to:

$$S = 2\pi \int\limits_L r\mathrm{d}l, \quad \text{where L is the arc of AB.}$$

If we use r_c to mark the distance of the center of mass C of the arc L from the straight line p, then we have the equation:

$$Lr_c = \int\limits_L r\mathrm{d}l.$$

If this value of integral is put into the previous equation it gives:

$$S = 2\pi r_c L.$$

Theorem 9. *The volume which is obtained by rotating the flat surface around the axis in the plane, which does not cut the surface, equals to the product of the surface value and the circumference of a circle described by the center of masses of the surface.*

Proof. Suppose that the flat surface P rotates around the axis p,

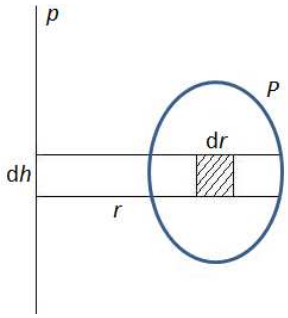

Figure 3. Flat surface in a plane.

which does not cut the contour of the surface (see Fig. 3). Volume V, which is obtained by reversing the surface, can be calculated using the double integral:

$$V = 2\pi \iint\limits_P r\mathrm{d}r\mathrm{d}h$$

where r is the distance of the point of elementary rectangle of dimensions dr and dh from the axis of rotation. If we write down the equation for determining the center of mass C of the area P with respect to line p, the following is obtained

$$Pr_c = \iint\limits_P r\mathrm{d}r\mathrm{d}h$$

where r_c is the distance of the center of mass of the surface P from the line p. When this integral value is put into the previous equation, we get:

$$V = 2\pi r_c P$$

which is supposed to be obtained.

AXIAL SQUARE MOMENT OF INERTIA

Let there be given the line p and the material point of the mass m at the distance d from the line. The product md^2 is called *the axial square moment* of the given material point relative to the given line. If there are more material points with masses $m_1, m_2, \ldots, m_n$ at distances $d_1, d_2, \ldots, d_n$ of the given line p, for the moment of inertia of the system we have the equation and the mark:

$$I_p = \sum_{i=1}^{n} m_i \mathrm{d}_i^2$$

If the coordinates of mass m_i are marked by x_i, y_i, z_i in relation to the Cartesian coordinate system, then three moments of inertia can be introduced:

$$I_x = \sum m_i \left(y_i^2 + z_i^2\right),\ I_y = \sum m_i \left(z_i^2 + x_i^2\right),\ I_z = \sum m_i \left(x_i^2 + y_i^2\right).$$

For continuously distributed masses the sums are replaced by integrals. For the moment of inertia about the x-axis we have:

$$I_x = \iiint_V \sigma(x, y, z)\left(y^2 + z^2\right)\mathrm{d}x\mathrm{d}y\mathrm{d}z.$$

It is similar for the other axis.

The term axial moment of inertia can be applied both to masses spread across the surface and the curve, both in the case when the curve and axis lie in the same plane, and in the case when the curve, which can also be spatial, occupies an arbitrary position in relation to the axis of moment of inertia.

To better explain the afore mentioned mechanical phenomena, the concept of kinetic energy i.e. energy of movement can further be introduced. This highlights the importance of multiple integrals in mechanics. For a material point of mass m, moving at speed of intensity v, the kinetic energy is calculated by the form $\frac{1}{2}mv^2$.

When a solid body is moving translational its points have the same speed. Then taken for the representative of the body is the center of masses point C, and as the speed of all points $\overrightarrow{v_c}$ velocity is determined with intensity v_c. If T marks the kinetic energy of a solid in the case of translational movement, then it follows:

$$T = \frac{1}{2}\sum_{i=1}^{n} m_i v_c^2 = \frac{1}{2} m v_c^2$$

where m is the overall mass of the body. Accordingly, in the translational motion, the kinetic energy of the body is expressed in the same way as the kinetic energy of a single material point.

Now we look at a rotary motion of a solid body, i.e. rotation about a fixed axis. The velocity intensity v_i of some point M_i of the body which is at the distance d_i from the axis can be calculated using the formula:

$$v_i \lim_{\Delta t \to 0} \frac{\Delta S_i}{\Delta t} = \lim_{\Delta t \to 0} \frac{\mathrm{d}_i \Delta\alpha}{\Delta t} = \mathrm{d}_i \lim_{\Delta t \to 0} \frac{\Delta\alpha}{\Delta t} = \mathrm{d}_i \overline{\omega}$$

where ΔS_i is the element of the roundabout of point M_i, $\Delta\alpha$ infinitely small rotation angle and:

$$\overline{\omega} = \lim_{\Delta t \to 0} \frac{\Delta\alpha}{\Delta t}$$

the intensity of angular velocity of the body. Thus, for the kinetic energy of each point of a solid body it can be put as follows:

$$\frac{1}{2} m_i \mathrm{d}_i^2 \overline{\omega}^2 = \frac{1}{2}\overline{\omega}^2 \left(m_i \mathrm{d}_i^2\right),$$

and for the whole body we will get:

$$T = \frac{1}{2} I \overline{\omega}^2 \ \text{ where } \ I = \lim_{n \to \infty} \sum_{i=1}^{n} m_i \mathrm{d}_i^2,$$

i.e. moment of inertia of the body about the axis of rotation.

If we compare the expressions:

$$T = \frac{1}{2} m v_c^2 \ \text{ and } \ T = \frac{1}{2} I \overline{\omega}^2$$

we see that in the first expression the kinetic energy depends on the square of the linear velocity, and in the other on the square of the angular velocity. In the first expression we have a coefficient m, and in the second I and both are called *inertial coefficients*-the first for the translational movement and the second for rotational movement.

REFERENCES

Awrejcewicz, J. 2012. In: Classical Mechanics, Springer, pp. 131-185.

Bessonov, N. M. & Song, D. J. 2001. Application of vector calculus to numerical simulation of continuum mechanics problems. Journal of Computational Physics, 167(1), pp. 22-38.

Bilimović, A. 1961. Integralni račun sa primenama.

Dorogovtsev, A. Y. 1987. Mathematical analysis: Collection of problems. Vishcha school.

Mirtich, B. 1996. Fast and accurate computation of polyhedral mass properties. Journal of graphics tools, 1(2), pp. 31-50.

Whitaker, S. 1992. The species mass jump condition at a singular surface. Chemical Engineering Science, 47(7), pp. 1677-1685.

Bulletin of Natural Sciences Research
Vol. 10, No. 2, 2020, pp. 38-42.

DOI: https://doi.org/10.5937/bnsr10-29584
Original Scientific Paper

MATHEMATICS TEACHER'S PERCEPTIONS ABOUT INFLUENCE OF DIFFERENT ICT USAGE STRATEGIES ON THEIR COMPETENCIES

EUGEN LJAJKO[1*]

[1]Faculty of Sciences, University in Priština – Kosovska Mitrovica, Kosovska Mitrovica, Serbia

ABSTRACT

Teacher competencies are among the key factors of a successful mathematics instruction. The main goal of the study was to compare teachers' beliefs and attitudes affected by different strategies in organizing the instruction process. The study gives a comparison of teachers' competencies in three groups of teachers – one teaching mathematics without ICT, the second using ready-made GeoGebra applets and the third one developing their own GeoGebra applets in cooperation with their students. The survey includes 65 mathematics teachers working in 21 primary and secondary schools in southern regions of Serbia. We observed, assessed and compared affective-motivational characteristics of teachers – their beliefs and professional motivation. Results indicate that the teachers' affective-motivational characteristics depend on the way they employ technology in representing the content they teach. If the technology is used in an inappropriate manner it can impede the students' creativity, but it also obstructs teachers in deploying their full abilities in the process. The results also bring to the fore issues concerning ways to maintain positive effects achieved through ICT empowered instruction organized in the way the third group of teachers did.

Keywords: GeoGebra, Dynamic worksheets, Teachers' competencies, Learning environments.

INTRODUCTION

One of the goals of the 21st century education is to fulfill needs of modern society for experts ready to cope with various problems that will be current in the future. Mathematics instruction is no exception. There are many aspects of the instruction that can contribute in fulfilling these tasks and others that can lead students and teachers develop habits not in line with the modern society needs.

Modern day instruction undoubtedly relies on Informatics-Communication Technologies (ICT) usage. A number of studies dealt with influence that ICT usage in Mathematics instruction can have on students' creativity, knowledge building, quality of knowledge and their academic achievements. Some of them suggest that ICT usage in the Mathematics instruction can boost students' parameters (Arbain & Shukor, 2015; Brown, 2010; Hopper, 2009; Rajagopal et al., 2015), but there are more studies (Bennett & Maton, 2010; Bullen et al., 2011; Oblinger & Oblinger, 2005; White & Le Cornu, 2011) showing that the context is the key factor in understanding quality and efficiency of ICT impact on students' parameters.

One of the most important aspects of the ICT usage in the instruction process is that it requires teachers be able to meaningfully incorporate a new technology into the process. Several studies (Tatar, 2013; Zakaria & Lee, 2012; Senk et al., 2012) indicate that using ICT in instruction process helps teachers improve and diversify their teaching techniques. Others (Jimoyiannis, 2010; Kelly, 2002) point at an urgent need to coordinate students' interests and teachers' competencies in ICT learning environment. This study explores whether the way ICT are used in the Mathematics instruction can have impact on teachers' competencies.

Teachers' competencies. A successful teacher can be recognized through developed teachers' competencies. Though there are different approaches to describing the competencies, we based our study on the framework given in Döhrmann et al. (2012). There (ibid., p.327), the teachers' competencies are classified into two facets: cognitive abilities and affective-motivational characteristics, Figure 1.

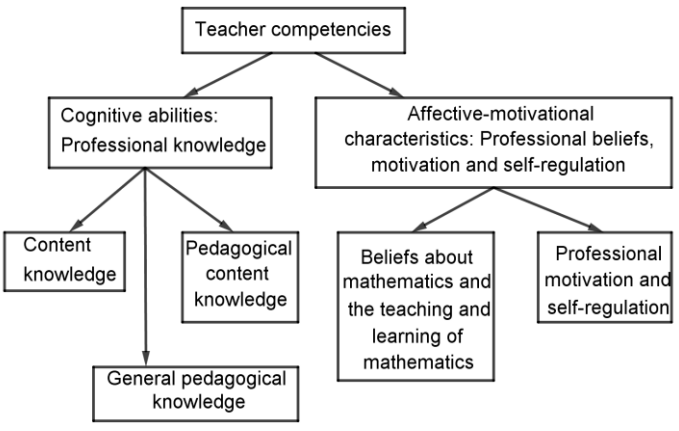

Figure 1. Teachers' professional competencies, according to Döhrmann et al. (2012).

* Corresponding author: eugen.ljajko@pr.ac.rs

Both, teachers and students show changes in their classroom interactions when the instruction is ICT-empowered. The interactions tend to move towards more informal group work (Farrell, 1996). Fuglestat et al. (2010) came to a conclusion that "by involving teacher in all stages of the design process, the full extent of the repercussions involved in using digital tools in the classroom – their impact on not only students' learning and teachers' didactic approaches but also on classroom management, on teaching time, and on mathematical knowledge itself – becomes more apparent. (p.309)" Teachers develop their cognitive abilities mostly in their pre-service period, but their affective-motivational characteristics can be susceptible during their lifetime. Goos et al. (2010) state that "teacher characteristics (their mathematical and pedagogical knowledge, beliefs and attitudes) … influence the integration of digital technologies into mathematics teaching." (ibid. p. 327). On the other hand, the influence that ICT usage can have on teachers' characteristics is poorly investigated. Therefore, we paid attention at teachers' affective-motivational characteristics and assessed the impact that the quantity and quality of ICT usage in the Mathematics instruction can have on this set of competencies.

About GeoGebra. In order to explore and assess impact that ICT usage can have on teachers' beliefs and attitudes, we introduced GeoGebra software into the instruction process – i.e. some of the teachers included in the survey organized their lessons using it. GeoGebra was chosen due to its ease of use and popularity among Serbian students and teachers. It is an open source dynamic mathematics software. Its interaction window has many different perspectives – algebra and graphics windows, spreadsheet, CAS, 3D graphics, etc. Work with GeoGebra is mostly organized through building worksheets – GeoGebra applets.

There are studies showing that teachers express very positive attitudes toward using GeoGebra in mathematics instruction (Hohenwarter et al., 2008, Preiner, 2008, Zakaria & Lee, 2012), but they do not compare and assess different approaches to introduce technology into the instruction process. Teachers included in our research used two types of GeoGebra applets – ready-made or the ones developed by themselves in cooperation with their students. The ready-made applets were developed earlier, and the teachers were offered to incorporate them into the instruction process. Another group of teachers was consisted of the ones that had previous experience with GeoGebra, and they were required to develop their own applets. In that process they used to include their students, mostly through homework.

METHOD

Sampling. The sample was comprised of 65 mathematics teachers from 21 primary and secondary schools in southern regions of Serbia. According to the way they organized instruction process and level of ICT usage, the teachers were divided into three groups: those teaching mathematics without ICT – 41 teachers, the ones teaching mathematics using ready-made GeoGebra applets – 13 teachers, and the ones that used to develop GeoGebra applets together with their students – 11 teachers.

Objectives. The main objective of this research is to examine and assess influence of ICT usage on affective-motivational characteristics of teachers. Having in mind various possibilities to employ technology in the classroom, we decided to find out if there are differences in the influence levels that different approaches to technology usage in the classroom affect the teachers' characteristics. In other words, our task is to answer the following question: To what extent the way ICT is used in the instruction shapes the teachers' beliefs and attitudes?

Instruments and survey. The participants to the survey filled in a questionnaire consisted of two parts. The first part covered general information about participants – their age, education and work experience. In the second part there were five items – statements expressing teacher's beliefs about the instruction process. For every statement teachers could pick one of five assessments representing their attitude about the statement –"I strongly disagree", "I disagree", "I am neutral", "I agree" and "I strongly agree". In order to compare teachers' attitudes and estimate their beliefs, we assigned numerical values to the assessments – 1 for "I strongly disagree" to 5 for "I strongly agree". The statements of the second part of the questionnaire were:

1. *I find it easy to prepare teaching materials.*
2. *Using ICT in Mathematics instruction helps students understand the subject material.*
3. *Mathematics is easy for students to learn.*
4. *Relations between my students and me in the classroom are relaxed.*
5. *I can easily make my students interested in subject material.*

Data collection and analysis. All the teachers covered with the survey had similar background – they were all from southern regions of Serbia, mostly with rural background. Their age and work experience varied very slightly between the groups.

We used methods of descriptive statistics (average values; standard deviations) to process general data collected through the survey. In order to statistically estimate differences in attitudes between the groups of teachers, we conducted *t*-tests for every statement.

NUMERICAL RESULTS

In Tables 1-5 we present data concerning the second part of the questionnaire. Besides, we conduct *t*-tests to compare statistical differences between the groups concerning all five statements. Having in mind *t* and *p* values we obtained for all five criteria, we draw conclusions about statistical significance of

the differences between the groups. We observed statistical differences at 0.05 level.

Table 1. Average values and standard deviations for the first statement.

Group	Count	Average	SD
1.	41	2.51	1.25
2.	13	3.46	1.21
3.	11	3.18	1.27

For this statement we obtained following results:

1.1. For the first and the second groups, we have $t = -2.35$, $df = 52$, $p = 0.02$.

1.2. For the first and the third groups, we have $t = -1.54$, $df = 50$, $p = 0.13$.

1.3. For the second and the third groups, we have $t = 0.53$, $df = 22$, $p = 0.60$.

The first criterion was about difficulties teachers encounter while preparing teaching materials. The only statistically significant difference was between the first and the second groups, in favor of the second one. It could be expected, considering that the second group of teachers worked with ready-made materials. On the other hand, the difference between the second and the third groups was not statistically significant, though the third group teachers had to develop their own applets.

Table 2. Average values and standard deviations for the second statement.

Group	Count	Average	SD
1.	41	2.56	1.13
2.	13	2.69	1.20
3.	11	3.82	1.27

For the second statement we obtained following results:

2.1. For the first and the second groups, we have $t = -0.35$, $df = 52$, $p = 0.73$.

2.2. For the first and the third groups, we have $t = -3.14$, $df = 50$, $p = 0.0029$.

2.3. For the second and the third groups, we have $t = -2.14$, $df = 22$, $p = 0.044$.

The second criterion expressed teachers' opinion on influence of ICT usage in the instruction process to students' understanding of materials taught. The differences appeared to be significant between the first and the third, and the second and the third groups, in both cases in favor of the third group. Though the difference between the first and the third groups could be expected, it could be useful to understand why the difference between the second and the third groups was statistically significant, and was not in case 1 – 2. The answer lies in the way the second group of teachers used technology in the instruction. Generally, usage of ready-made applets impedes students' creativity which is in direct connection to understanding the subject materials.

Table 3. Average values and standard deviations for the third statement.

Group	Count	Average	SD
1.	41	2.85	1.12
2.	13	2.92	1.27
3.	11	3.27	1.35

For the third statement we obtained following results:

3.1. For the first and the second groups, we have $t = -0.19$, $df = 52$, $p = 0.85$.

3.2. For the first and the third groups, we have $t = -1.03$, $df = 50$, $p = 0.31$.

3.3. For the second and the third groups, we have $t = -0.62$, $df = 22$, $p = 0.54$.

The third criterion is teachers' perception on difficulties students meet while learning Mathematics. All three groups of teachers had very similar scores – from 2.85 to 3.27, and there was no statistically significant difference between any of the groups. This means that teachers expect students can learn Mathematics easily, regardless of the technology used in the instruction process.

Table 4. Average values and standard deviations for the fourth statement.

Group	Count	Average	SD
1.	41	2.41	1.06
2.	13	3	1.24
3.	11	3.91	1.16

For the fourth statement we obtained following results:

4.1. For the first and the second groups, we have $t = -1.63$, $df = 52$, $p = 0.11$.

4.2. For the first and the third groups, we have $t = -3.99$, $df = 50$, $p = 0.0037$.

4.3. For the second and the third groups, we have $t = -1.76$, $df = 22$, $p = 0.092$.

The fourth criterion was the nature of the teacher-students relations in the classroom. The difference was statistically significant only between the first and the third groups. Although the second group also used ICT in the classroom, it came out that it did not ease the relations as it did with the third group of the teachers. On the other hand, the difference between the second

and the third groups, tough very high ($t = -1.76$, $df = 22$, $p = 0.092$), was not statistically significant.

Table 5. Average values and standard deviations for the fifth statement.

Group	Count	Average	SD
1.	41	2.56	1.08
2.	13	2.85	1.23
3.	11	4	1.13

For the fifth statement we obtained following results:

5.1. For the first and the second groups, we have $t = -0.78$, $df = 52$, $p = 0.44$.

5.2. For the first and the third groups, we have $t = -4.12$, $df = 50$, $p = 0.033$.

5.3. For the second and the third groups, we have $t = -2.28$, $df = 22$, $p = 0.0001$.

Finally, the fifth criterion was teachers' opinion about their ability to make students understand teaching materials. The difference was statistically significant in cases 1 – 3 and 2 – 3, and in case 1 – 2 the difference was not statistically significant. These suggest that teachers are more successful in helping students understand subject materials when they develop GeoGebra applets with students, than in cases when they use ready-made applets or do not use them at all.

A more comprehensive picture can be obtained if all these conclusions are taken together, Table 6, wherefrom one can see that, comparing to the first two groups of teachers, the third one expresses significantly more positive attitude and beliefs about efficiency of the instruction and their relation to students.

Table 6. Statistical significance of differences between the groups at 0.05 level.

Pair of groups	1 – 2	1 – 3	2 – 3
1.	Yes	No	No
2.	No	Yes	Yes
3.	No	No	No
4.	No	Yes	No
5.	No	Yes	Yes

CONCLUSIONS AND DISCUSSION

Introducing GeoGebra applets into the instruction process can alleviate teachers' efforts in preparing mathematics instruction. But the alleviation depends on the type of the applets. Teachers find developing applets more difficult than using ready-made ones.

Teachers that used to develop GeoGebra applets together with their students (the third group) consider their type of instruction helpful for students to understand subject material. On the other hand, those using ready-made applets (the second group) found their students less able to understand the subject material. The difference could be understood taking in consideration cognitive efforts the second group students need to incorporate the mathematics and the technology.

Concerning the teacher-students relations in the classroom, the most relaxed ones were with the third group of the teachers. Though this conclusion sounds similar to what Farrell stated in (1996), it clearly points that a mere introduction of ICT into the instruction process does not necessarily lead to a better interrelationship in the instruction. The reason was obviously the way technology was introduced in the classroom. Time and energy spent in developing the applets and the communication during the process contributes to a friendlier atmosphere in the classroom.

Increasing students' interest for, and their understanding of the subject material is not an easy task for a teacher. Modern day students are very keen of ICT, but different ways we use them in the classroom induce different students' reactions. For that reason, students that took part in developing GeoGebra applets representing mathematical ideas, concepts or procedures showed better understanding of the subject material. Another possibility is that the teachers cooperating with students had better insight into their students' ideas about the subject material.

The research points out that introduction of ICT into mathematics instruction, though a necessity today, has to be carefully organized. The way we use ICT in the instruction impacts many aspects of the teaching/learning process (teachers' preparations of teaching materials, students' interest and understanding, interrelations in the classroom). Introducing ICT in the instruction in a way that requires more student activities and student-teacher cooperation brings more positive results. On the other hand, using ready-made applets can result in lessening teachers' efforts and declining students' commitment to learn, which can be reflected through their achievements and teachers' perceptions.

Finally, the research and its results lead to some questions that need to be addressed in future research. Some of the most important issues following this research are:

- Does the level of difficulty/ease of preparing teaching materials in an ICT environment impact readiness of teachers to cooperate with students and thus initiate fuller engagement of their capacities? If it does, in what manner?
- Can better relations between students and teachers in the classroom, achieved in this way, lead to better academic achievements of students?
- Can the students' interest for the subject material achieved an ICT classroom, organized in a manner the third group of teachers did, be maintained?

REFERENCES

Arbain, N., & Shukor, N. 2015. The effects of GeoGebra on students' achievements, Procedia Social and Behavioral Sciences, 172, pp. 208-214.

Bennett, S., & Maton, K. 2010. Beyond the 'digital natives' debate: Towards a more nuanced understanding of students' technology experiences. Journal of Computer Assisted Learning, 26, pp. 321-331.

Brown, R. 2010. Does the introduction of the graphics calculator into system-wide examinations lead to change in the types of mathematical skills tested? Educational Studies in Mathematics, 73(2), pp. 181-203.

Bullen, M., Morgan, T., & Qayyum, A. 2011. Digital Learners in Higher Education: Generation is Not the Issue. Canadian Journal of Learning Technology, 37(1), pp. 1-24.

Döhrmann, M., Kaiser, G., & Blömeke, S. 2012. The conceptualisation of mathematics competencies in the international teacher education study TEDS-M, ZDM, 44(3), pp. 325-340.

Farrell, A. 1996. Roles and behaviors in technology-integrated precalculus classrooms. Journal of Mathematical behavior, 15, pp. 35-53.

Fuglestad, A. B., Healy, L., Kynigos, C. & Monaghan, J. 2010. Working with teachers: Context and Culture. In C. Hoyles, and J.-B. Lagrange (Eds.), Mathematics education and technology—rethinking the terrain. The 17th ICMI study, pp. 293-310. Heidelberg: Springer.

Goos, M. & Lavergne, S., with Assude, T., Brown, J., Kong, C., M., Glover, D., Grugeon, B., Laborde, C., Lavicza, Z., Miller, D., & Sinclair, M. 2010. Teachers and teaching: Theoretical perspectives and issues concerning Classroom implementation. In C. Hoyles, and J.-B. Lagrange (Eds.), Mathematics education and technology—rethinking the terrain. The 17th ICMI study, pp. 311-328. Heidelberg: Springer.

Hohenwarter, J., Hohenwarter, M., & Lavicza, Z. 2009. Introducing Dynamic Mathematics Software to Secondary School Teachers: the Case of GeoGebra. Journal of Computers in Mathematics and Science Teaching, 28(2), pp. 135-146. Waynesville, NC USA: Association for the Advancement of Computing in Education (AACE). Retrieved March 17, 2018 from https://www.learntechlib.org/p/30304/.

Hopper, S. 2009. The effect of technology use on Student interest and understanding in Geometry, Studies in Teaching, Research Digest, pp. 37-42.

Jimoyiannis, A. 2010. Designing and implementing an integrated technological pedagogical science knowledge framework for science teachers' professional development. Computers & Education, 55(3), pp. 1259-1269. doi: 10.1016/ j.compedu.2010.05.022

Oblinger, D., & Oblinger, J. 2005. Is it Age or IT: First steps towards understanding the net generation? In: D. Oblinger and J. Oblinger Eds., Educating the Net Generation. (2.1-2.20). Boulder, CO: EDUCAUSE.

Preiner, J. 2008. Introducing dynamic mathematics software to mathematics teachers: The case of GeoGebra. PhD Thesis, University of Salzburg Austria.

Rajagopal, S., Ismail, Z., Ali, M., & Sulaiman, N. 2015. Attitude of secondary students towards the use of GeoGebra in learning loci in two dimensions, International Educational Studies, 8(13), pp. 27-32.

Senk, S.L., Tatto, M.T., Reckase, M., Rowley, G., Peck, R., & Bankov, K. 2012. Knowledge of future primary teachers for teaching mathematics: An international comparative perspective. ZDM - The International Journal on Mathematics Education, 44(3), pp. 307-324.

Tabach, M., Hershkowitz, R., & Dreyfus, T. 2013. Learning beginning algebra in a computer-intensive environment, The International Journal on Mathematics Education, 45, pp. 377-391.

Tatar, E. 2013. The effect of dynamic software on prospective mathematics teachers' perceptions regarding information and communication technology, Australian Journal of Teacher Education, 38(12), pp. 1-16.

White, D.S., & Le Cornu, A. (2011). Visitors and Residents: A new typology for online engagement. First Monday, 16, pp. 9-15.

Zakaria, E., & Lee. L. S. 2012. Teachers' perceptions towards the use of GeoGebra in the teaching and learning Mathematics, Journal of Mathematics and Statistics, 8(2), pp. 253-257.

Bulletin of Natural Sciences Research
Vol. 10, No. 2, 2020, pp. 43-50.

DOI: https://doi.org/10.5937/bnsr10-29239
Original Scientific Paper

COVID-19 RISK ASSESSMENT IN PUBLIC TRANSPORT USING AMBIENT SENSOR DATA AND WIRELESS COMMUNICATIONS

İZZET FATIH ŞENTÜRK[1], NURETTIN GÖKHAN ADAR[1], STEFAN PANIĆ[2*], ČASLAV STEFANOVIĆ[2], METE YAĞANOĞLU[3], BOJAN PRILINČEVIĆ[4]

[1]Faculty of Engineering and Natural Sciences, Bursa Technical University, Bursa, Turkey
[2]Faculty of Sciences, University in Priština - Kosovska Mitrovica, Kosovska Mitrovica, Serbia
[3]Faculty of Engineering, Ataturk University, Erzurum, Turkey
[4]Higher Technical School of Professional Studies, Zvečan, Serbia

ABSTRACT

Covid-19 causes one of the most alarming global health and economic crises in modern times. Countries around the world establish different preventing measures to stop or control Covid-19 spread. The goal of this paper is to present methods for the evaluation of indoor air quality in public transport to assess the risk of contracting Covid-19. The first part of the paper involves investigating the relationship between Covid-19 and various factors affecting indoor air quality. The focus of this paper relies on exploring existing methods to estimate the number of occupants in public transport. It is known that increased occupancy rate increases the possibility of contamination as well as indoor carbon dioxide concentration. Wireless data collection schemes will be defined that can collect data from public transportation. Collected data are envisioned to be stored in the cloud for data analytics. We will present novel methods to analyze the collected data by considering the historical data and estimate the virus contagion risk level for each public transportation vehicle in service. The methodology is expected to be applicable for other airborne diseases as well. Real-time risk levels of public transportation vehicles will be available through a mobile application so that people can choose their mode of transportation accordingly.

Keywords: Airborne diseases, Covid-19, Sensor data, Transportation systems, Wireless communications.

INTRODUCTION

Covid-19, also known as coronavirus disease 2019, is a contagious respiratory illness caused by the transmission of severe acute respiratory syndrome coronavirus 2 (SARS-CoV-2) among human beings (Gorbalenya et al., 2020). The first identified case of coronavirus infection has been noticed in December 2019. In a period of less than a year, more than 45 million cases and 1.2 million deaths caused by Covid-19 worldwide have been identified.

Coronavirus spreads mainly through droplets and aerosols after an infected person is coughing, sneezing, singing, talking, or breathing. The spreading happens when those droplets come into the contact with mouth, nose, or eyes of other humans who are in close proximity with the coronavirus-infected human-being. Moreover, the droplets can evaporate into aerosols, which can sustain in the air for many hours, enabling airborne way of transmission usually in crowded and poorly ventilated indoor environments, such as bars, restaurants, nightclubs, transportation stations, busses, etc. Strategies imposed by authorities for prevention against Covid-19 spread are social distancing, using protective masks, hands hygiene, avoiding contacting the mouth, eyes, and nose with hands, and ventilation and air filtration in public spaces in order to expel the undesirable aerosols.

There are important research evidences that suggest the transmission of Covid-19 through aerosol in indoor spaces. Important publications are related to i.) measurement of Covid-19 in the air, including the distance beyond recommended for the droplet transmission (Van Doremalen et al., 2020; Santarpia et al., 2020; Fears et al., 2020), ii.) some physically established models of emissions of Covid-19 aerosols and dynamics of those aerosols (Qian et al., 2018; Liu et al., 2017; Riediker & Tsai; 2020), iii.) evidence of airborne transmission for the SARS and MERS infections (Yu et al., 2004; Xiao et al. 2018), iv.) Epidemiological evidences of possible airborne transmission, though other routes cannot be excluded (Shen et al., 2020). The available research evidences support the use of protective measures against transmission of Covid-19 in indoor environments as an addition to other protective strategies already used in practice (for example protective masks, hands hygiene and etc.) (Morawska et al., 2020).

Economic and social effects of the Covid-19 outbreak impact all economic sectors, cause financial crises, social inequality, and insecurity stops transportation systems or impacts adversely. Covid-19 presents a great challenge for transportation systems all over the world in order to sustain regular services to customers. There are several factors that can be applied in practice in order to reduce the probability of Covid-19 infection risk in public transportation (for example control of the number of occupants in buses or trains, number of occupants at stations, trip length time, the use of face masks and the application of

* Corresponding author: stefan.panic@pr.ac.rs

recommended hygiene standards and the ventilation of busses and trains) (Tirachini et al., 2020; Wielechowski et al., 2020).

Moreover, considering the decreased proximity to other passengers in the public transportation, the ability to evaluate the indoor air quality in the public transit in a timely manner becomes extremely important to assess the risk of Covid-19 contagion (Fattorini & Regol, 2020). Air quality can be defined by using several different measures including volatile organic compounds (VOCs), carbon monoxide (CO), particle matter (PM), other pollutants (carbon dioxide, methane, etc.), temperature, and humidity levels.

On the other hand, wireless sensors networks and wireless communications are already playing an important role in the era of Covid-19 (Saaed et al., 2020; Kamal et al., 2020; Ndiaye et al., 2020). The wireless communication technologies can be used to enable monitoring of the virus spreading, to enable healthcare automation, and to allow virtual education and conferencing. The wireless communication systems are envisioned to help the sustainability of the global economy by assisting in different industry sectors. Moreover, in (Howerton et al., 2020) the LoRaWAN-based system of air quality sensors in the city has been proposed. The generated data are used for a comparative spatial model used for the determination of air quality before and during the COVID-19 outbreak.

In the second part of this work, we will investigate measures to estimate the number of occupants in the public transport based on the device and device-free wireless-based methods. In the third part, a low-energy sensor node will be recommended. In the final part, the general architecture of the system will be provided. Wireless data collection schemes will be defined to collect data from public transportation and to be stored in a data cloud for further processing.

To the best of the author's knowledge, no paper addresses the ambient sensor data and wireless communications for evaluation of air-quality in transportation systems for Covid-19 risk assessment.

THEORETICAL PART

The occupancy rate in public transport is an essential parameter that must be considered while assessing indoor Covid-19 spread risk. Despite the availability of modern ticketing systems that support ticket validation during boarding, typically, stops that passengers exit are not recorded (Kostakos et al., 2010). Therefore, actual occupancy rates are usually not available. To address the problem of occupancy estimating, various solutions are available in the literature. In this study, we focus on solutions for indoor occupancy estimation. Such solutions can be classified into two broad groups based on whether user involvement is required or not. Some solutions require carrying a particular device (e.g., RFID tags, smart devices) or installing a certain mobile application. Such solutions are regarded as device-based solutions. Some solutions require deploying sensors or cameras to monitor either passenger directly or their impact on the environment. Such solutions do not require passengers to carry any device and are classified as device-free solutions.

Also, it would be of interest to observe one high profile measure from telecommunication theory, level crossing rate (LCR). If RF signal level at the transmission is adequately set, which can be accomplished after series of measurements and tests, then LCR values obtained at the reception could identify number of passengers traveling within the bus during the time between two signal receptions. Namely, LCR defines the rate at which random process R crosses predetermined level r, which can be expressed mathematically as:

$$N_R(r) = \int_0^\infty \dot{r} p_{\dot{r}|r}\left(\dot{r}|r\right) p_R(r) d\dot{r} = p_R(r) \frac{\sigma_{\dot{r}|r}}{\sqrt{2\pi}} \tag{1}$$

where $p_R(r)$ denotes probability density function (PDF) of random process R, while variance of PDF of random process $\dot{r}$, time derivative of R conditioned over R, is defined with $\sigma_{\dot{r}|r}^2$.

DEVICE-BASED SOLUTIONS

Ahorrar (Jain & Madamopoulos, 2016) is an indoor localization and occupancy counting framework designated to improve energy efficiency in office buildings through controlling the heating/cooling, ventilation (HVAC), and lighting. Ahorrar exploits participatory sensing to obtain the real-time distribution of occupants. Given the fact that some occupants carry multiple smart devices, Ahorrar employs a probabilistic and information-theoretical approach to classify ownership of devices. The classification procedure of devices considers device locations using wireless signal strengths, mobility states of the devices, and data traffic patterns. Data is collected with existing wireless access points. For offline occupants without smartphones, it is recommended to provide wearable hardware platforms at building entrances. Data processing is performed at central locations to avoid the burden on occupants' devices. The goal of the proposed solution is to achieve an accuracy of 95% in terms of occupancy numbers. Despite some novelties such as ownership classification for occupants with multiple smart devices, we expect smart devices ownership at lower levels in our case. Also, public transportation has a different mobility pattern of occupants compared to office buildings. For instance, Ahorrar assumes that when the person walks away with a subset of her devices, the rest of her devices will remain stationary (probably on her desk) until she returns. This is not a device mobility case that we expect in public transport. Also, assumptions such as distributing smart wearables at the entrance is not a viable option in our case.

An occupancy counting system is proposed by iAbacus (Nitti et al., 2020) specifically for public bus transportation. The

main idea of the system is based on the identification of individual devices using the MAC address of the Wi-Fi network interface. Recent versions of popular mobile operating systems employ software-based randomization techniques to generate MAC addresses to improve user privacy and use the periodically changed random MAC addresses in successive messages. iAbacus system requires the installation of a Wi-Fi packet sniffer to collect probe request frames broadcasted by nearby mobile devices. iAbacus checks the first 6 octets of the obtained MAC addresses and evaluates whether the obtained address is a valid Organizationally Unique Identifier (OUI) assigned by IEEE. If the MAC address is not listed as an OUI, it is considered as a random MAC address and the proposed de-randomization algorithm is applied before the counting process. The counting algorithm is executed on the cloud and assesses whether a device is on the bus or nearby out of the bus. The data is transferred to the bus using a cellular connection during mobility or through Wi-Fi connections at bus stops. Experiments are conducted regarding static and dynamic conditions. For the case of the static condition, experiments are executed in a university room for 15 minutes. To test dynamic conditions, mobility of the bus is simulated by switching on/off devices according to an existing bus route and its stops. The experiments involve 8 devices where 3 of them employ random MAC addresses. The system achieves 100% accuracy with static conditions and 94% accuracy for dynamic cases. iAbacus assumes computed device count reflects the actual number of occupants which is not true considering offline passengers without a smartphone or when the Wi-Fi is disabled. Also, occupants with multiple smart devices can be counted multiple times. Despite contributions such as de-randomization and the counting algorithm, the proposed system is evaluated in a small-scale simulation and obtained results can be misleading for a real deployment.

Another solution that employs Wi-Fi probe requests is presented in (Tang et al., 2018). The goal of this approach is to estimate indoor crowd density. The solution consists of a positioning algorithm based on RSSI (received signal strength indicator) based fingerprints. The fingerprinting mechanism is claimed to be dynamic to minimize the inaccuracy of RSSI measurements. Considering the fact that a person may have multiple smart devices, a multiple linear regression model is applied to compute the likelihood of a person generating the Wi-Fi signal. The system is composed of a sniffer connected to a cloud server. Besides the MAC address, RSSI measurements are also collected in probe request messages. Since RSSI typically fluctuates even for the same device, 3 highest probability RSSI values are used to signify a device. Cloud server is responsible for fingerprints management positioning algorithm, crowd density estimation, and signal probability analysis to identify a person with multiple smart devices. One of the major drawbacks of the proposed solution is the requirement of equipping smart devices located at fixed positions. In the experiments, 1 fixed smartphone is employed per 10 square meters. Furthermore, when multiple fixed smart devices are used, they are required to be evenly distributed across the test area, “most of the fixed devices” are supposed to be non-blocked by objects and each fixed device is expected ted to be deployed to a certain location. MAC randomization is not considered in this work.

Another wireless connectivity-based occupancy estimation solution is presented by (Kostakos et al., 2010). The main goal of the proposed solution is to identify trip durations per passenger. The proposed approach exploits Bluetooth discovery requests to obtain unique Bluetooth identifiers of the onboard passengers. This approach requires the availability of Bluetooth adapters. Despite the prevalence of Bluetooth enabled smart devices, the proposed solution requires Bluetooth adapters set on for device detection. The system is implemented and tested on actual routes with busses equipped with GPS. Obtained Bluetooth data is correlated with the localization data considering the bus stop locations on the route. Device discovery time is used to identify the bus stop where the passenger boards. Likewise, the time when the devices disappear implies the bus stop where the passenger exits. The duration of the trip is also used to identify false device detections such as other passengers waiting at the bus stops. This approach assumes that Bluetooth is not switched off/on during the trip. Another drawback of this approach is the over counting of passengers with multiple Bluetooth devices.

Accuracy in counting people is crucial for the evacuation of building occupants in case of an emergency. SmartEvacTrak (Ahmed et al., 2015) is such a solution that provides occupancy counting and localization. The proposed system is composed of a mobile application for data collection and a server for data analysis. SmartEvacTrak assumes not only smartphones but also the availability of certain sensors onboard along with the mobile applications installed on the phones. The proposed approach also requires the deployment of permanent magnets at gates to detect entries and exits using magnetometers and inertial sensors on occupants’ phones. Localization is enabled using RSSI measurements obtained from occupants’ WiFi adapters. SmartEvacTrak reaches 98% counting accuracy and 97% localization accuracy. Certain parameters such as floor plans, access point locations, the thickness of the obstacles, etc. must be present in the configuration repository. Strict hardware and software requirements on the occupants’ side, certain deployment requirements on the building infrastructure, and the requirement of the configuration repository complicate the applicability of the proposed solution.

(Li et al., 2016) proposes an indoor crowd monitoring system based on RSSI measurements. The main idea of the proposed system is deploying a wireless sensor network and collecting WiFi RSSI through sensor nodes. Collective data provided by the nodes indicate the location of the devices where the probe requests are issued. The presented approach considers maximum RSSI when two or more nodes receive probe requests

from the same device. (Li et al., 2016) considers mobility of the occupants and handles cases when an occupant leaves and returns to the coverage of a node. The system is tested at a lab and classrooms in a university. The time interval between probe requests is varied in the experiments to assess the impact on the performance of the system.

Wi-Counter (Li et al., 2015) is an indoor occupancy counting system employing RSS of the WiFi signals. The system consists of a mobile application to crowdsource RSS data from different locations and a server to train the collected data. The training phase is offline and performed after the crowdsourcing phase. The training phase filters noise and then applies a neural network solution to model the relationship between RSS and the occupancy count. The system is tested in classrooms at a university. 7 access points are used in a classroom of size 96-meter square. During the online counting phase, the mean and standard deviation of the obtained RSS is provided to the neural network model to estimate the people count in the classroom. The system reaches up to 93% accuracy even with random mobility.

DEVICE-FREE SOLUTIONS

Camera-based Solutions

Several different methods exist in the literature for counting people in indoor and outdoor applications. In recent years, camera systems are used for detection and counting people with the development of image processing techniques.

The use of cameras for people counting systems has some disadvantages. The application of this method indoors or outdoors determines the quality of the counting process. It is possible to get more successful results than the outdoor environment due to the possibility of controlling the light intensity in the indoor environment. However, the outdoor environment makes counting difficult due to uncontrolled environments such as background, natural light changes, and climate factors.

Another problem is the perception of people with the camera is the number of individuals at the scene. As the number of individuals increases, it makes the counting process difficult due to collective action and individuals closing the camera view (Reis, 2014). Also, the image processing technique for counting people requires expensive hardware for camera and processing and hardware cannot provide its energy from the rechargeable battery.

According to (Aziz et al., 2011) and (Chan et al., 2008), people detection and counting using image processing techniques can be divided into 3 main groups: Trajectory clustering approach, Feature-based regression approach, Individual pedestrian detection.

An algorithm has been developed with a maximum 10% average error for detection and classification of moving objects in different outdoor environments with image processing (Sacchi et al., 2001). RBG camera and depth sensor can be used together in counting people which cross a virtual line (Del Pizzo et al., 2016). Vision-based method for counting people can be divided into two groups, namely neural-based crowd estimation and blob detection and blob tracking (Schlögl et al., 2001). The first method uses a trained neural network. The accuracy of this system depends on the data set used to train the neural network. There are some research papers that use Neural-Based Crowd Estimation (Regazzoni & Tesei, 1996, Cho et al., 1999, Chow et al., 1999). Blob detection and tracing are based on separating an object from the background (Kettnaker & Zabih, 1999, Haritaoglu et al., 2000). blob detection has poor accuracy when there are crowded people on the stage.

Sensor-based Solutions

(Jin et al., 2015) presents an indoor occupancy detection solution based on the ambient CO_2 level. The proposed system assumes humans as the main source of CO_2 production in the environment. Depending on the application area, this assumption can be misleading. Another factor that needs to be considered is the time needed for CO_2 accumulation in the area indicating the actual concentration level. The configuration of the room where the system will be used should also be studied. Depending on the air ventilation, the rate of the fresh incoming air can vary. Sensor locations and the locations of air supply and exit vents are also critical on the obtained results. The approach proposed by (Jin, 2015) follows sensing by proxy methodology using partial differential equations.

Another device-free occupancy detection solution is presented in (Pan et al., 2016). The main goal of (Pan et al., 2016) is to detect occupancy estimation even for multiple monitored people using vibration sensors. The system can detect the traffic of up to 4 people. The proposed system monitors ambient structural vibration. However, the applicability of the proposed system can be low for mobile systems such as vehicles due to various levels of vibration during mobility. Although the system is proposed for indoor environments, the maximum number of people that can be detected by (Pan et al., 2016) can be limiting for most of the indoor applications.

(Shih & Rowe, 2015) employs ultrasonic chirps for indoor occupancy estimation. The main idea of the proposed solution is to transmit an ultrasonic chirp and analyzing how the signal dissipates over time. The human body absorbs sound and increased occupancy is expected to reduce the amplitude of signal reflections. This approach requires a training phase to understand the characteristics of the room with a known number of occupants. For training, machine learning methods are employed. To adapt to slight changes in the room, the model must be retrained. The signal is transmitted in the ultrasonic frequency range for silent sensing. The proposed system is motivated by applications such as concert halls and the maximum number of people that can be detected is reported as

50. Despite its advantages, the system is not designated for mobile environments. Therefore, its performance in public transportation can be lower due to the varying mobility of the platform.

Doorjamb (Hnat et al., 2012) is an indoor room-level tracking system to detect passing people. The proposed system employs ultrasonic range sensors located above the doors to identify crossing people. This solution can identify the walking direction and by following the sequence of the crossed doors, room-level tracking becomes possible. To identify individuals, the system checks the heights of the people and their movement sequences between adjacent rooms. To detect boarding and exiting people in public transport, a similar solution can be adopted. Adjacent rooms may or may not be possible in the public transport depending on the vehicle type and model.

RF-based Solutions

Device-free radio frequency (RF) based occupancy counting methods are useful since they do not impose passengers to use their devices. Device-free RF methods can be classified into different groups depending on the type and utilization of the RF signal they use for the measurements and evaluation of the number of occupants: i.) RSSI, ii.) channel state information (CSI) and iii.) ultra-wideband (UWB) signals (Kouyoumdjieva et al., 2019).

RSSI-based solutions evaluate the signal power strength level at the receiver that originates from a radio transmitter (for example such as an access point (AP) from WiFi infrastructure). In ideal propagation conditions when the line-of-sight (LOS) transmission is achieved and multipath fading and shadowing effects are negligible, RSSI is expected to be constant with time. Otherwise, the signal strength varies over time. One of the causes is the presence of people that can block or effect RF transmission between receiver and transmitter. Accordingly, the number of people in an environment can be determined based on measured RSSI values at the receiver node. In ideal circumstances, the RSSI value would result only from the signal strength received through LOS transmission. Although, in an indoor environment, multipath propagation is expected to impact the RSSI value highly. Thus, the measurements usually have to be reevaluated in order to remove other factors. In (Nakatsuka et al., 2008), the RSSI-based method for determination of the number of occupants is first introduced in 2008. It has been shown that the RSSI level decreases with an increasing number of occupants. The proposed model is capable to register up to 30 occupants. In (Xu et al., 2012), the fingerprinting-based method applies a probabilistic model for the occupant's localization. In the first phase, the RSSI level is measured with no occupants and then one occupant enters the room. This one person enters a different location in turn, stands in the middle of a different location, and then moves randomly.

The data are collected and sent to a centralized unit for further processing. The variation of RSSI values between these two phases, also known as RSSI footprint, is stored for a different location and channel links, and a classifier is developed based on RSSI values. This method is capable of mitigating errors caused by multipath in indoor environments but also helps to improve localization precision.

CSI-based people counting methods are similar to RSSI-based methods. Moreover, CSI provides additional information on channel properties of wireless links derived from the physical layer of the system. It describes signal transmission between transmitter and receiver and addresses the impact of multipath, shadowing, and power decay with distance. Furthermore, the CSI is capable to account for the environmental variances caused by moving objects more accurately than RSSI-based methods. Similar to RSSI, CSI-based methods also rely on WLAN infrastructure that is usually available in indoor environments. CSI-based people counting methods are more applicable in environments with high mobility. It is important to notice that counting immobile occupants in the environment can be more difficult if they move since fewer variations in CSI values are expected. However, available results from literature show that CSI may be a more appropriate choice than RSSI for application in people counting systems in indoor environments (Kouyoumdjieva et al., 2019).

In the ultra-wide band (UWB) based technique, the UWB signal is transmitted, the signal is then reflected by targets, and received to detect occupants within the radar range (Niu-Varshney, 2006). It is known that the received UWB signals can be reflected by every object in a particular environment. Thus, undesirable signals are needed to be detected and removed. The number of occupants can be determined by detecting the signal's waveform of each individual occupant or determining the number of occupants based on the pattern of the waveform of the received signals (Choi et al., 2017).

Infection Risk in Public Transportation

The constant use of mass land transport increases the risk of transmission of the virus, as countless people are placed close together. The causes of transmission of the virus are based on high passenger density, overcrowding in a confined space, insufficient ventilation, recirculation of polluted air, and increased exposure time to infected individuals (Tatem et al., 2006, Nasir et al., 2016).

(Pestre et al., 2012) showed that, flu can spread rapidly in a closed area where there is not enough air renewal. In their study, (Baker et al., 2010) showed that, flu transmission can occur during modern commercial air travel. As a result of the study, the risk is concentrated among people sitting between two rows of infected passengers with symptoms that are consistent with transmission of other respiratory infections during the flight.

SYSTEM ARCHITECTURE

We regard the proposed solution as Covid-19 Risk Assessment System with Occupancy Estimation (CORAS-OE). CORAS-OE system architecture is composed of three main components, namely CORAS-OE-node, CORAS-OE -cloud, and CORAS-OE-mobile. CORAS-OE-node is the sensor node unit deployed onboard the public transport system to be monitored. CORAS-OE-node is equipped with an integrated sensor combining multiple sensors to track events and monitor environmental conditions. Some of the sensors employed on x-node are CO_2, Volatile Organic Compounds (VOCs), temperature, humidity, and light sensors. We are concerned with the mobility of the vehicle to detect stops. CORAS-OE-node exploits WiFi probe requests to detect passengers with smart devices. Unless their WiFi network adapter is disabled, passengers on board the vehicle can be detected. The system is desired to distinguish people outside the bus and avoid over counting people with multiple smart devices. CORAS-OE-node is also equipped with a microcontroller for local computing and an SD card for local storage of the collected data.

CORAS-OE-node preprocesses the local data and sends it to x-cloud periodically. To minimize the amount of data that needs to be sent to the cloud, CORAS-OE-node applies various techniques including filtering and data compression. CORAS-OE-node can evaluate assess the risk level of Covid-19 spread locally based on the normalized values obtained from x-cloud daily. However, certain data is sent to CORAS-OE-cloud for analysis and also to update the current risk level. Data transfer frequency is dynamically set. In the worst case, it is updated at every stop. However, there will be no update unless the risk level changes above the given threshold which is also set dynamically at the beginning of the daily service by CORAS-OE-cloud.

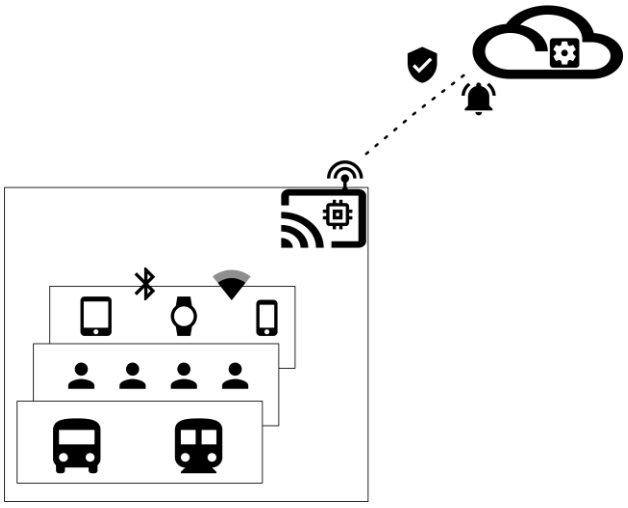

Figure 1. Proposed system architecture.

CORAS-OE-cloud is the cloud component of the system. X-cloud collects data from x-nodes across the city. Data is stored as a time series. Historical data plays an important role in determining the normalized values that can vary based on seasonal changes. Other than the batch analysis, the main task of CORAS-OE-cloud is to feed CORAS-OE-mobile. CORAS-OE-mobile is the mobile application that people can use to monitor risk levels on different routes and vehicles. CORAS-OE-mobile is not a crowd-sourcing application to collect data but only the front end of the system to share the results with passengers. The sample illustration of the proposed architecture can be found in Figure 1.

CONCLUSION

The paper proposes an efficient method for assessment of air quality in the public transport system to examine the risk of contracting Covid-19. The introduction of the paper provides data examining the relationship between Covid-19 and various factors affecting indoor air quality. The theoretical part of this work introduces techniques to estimate the number of occupants in the public transport based on the camera, device, and device-free wireless-based methods. The system's overall architecture consisting of sensor node units, wireless data collection schemes, and cloud storage systems is proposed for the evaluation of air-quality in transportation systems for Covid-19 risk assessment.

ACKNOWLEGMENTS

The authors would like to acknowledge the Erasmus+ KA107 project 2020-1-TR01-KA107-091598 and COST actions CA16220 (EUIMWP) and CA16222 (WISE-ACT).

REFERENCES

Ahmed, N., Ghose, A., Agrawal, A.K., Bhaumik, C., Chandel, V. & Kumar, A. 2015. Smartevactrak: A people counting and coarse-level localization solution for efficient evacuation of large buildings. In 2015 IEEE International Conference on Pervasive Computing and Communication Workshops (PerCom Workshops), pp. 372-377. IEEE.

Aziz, K. E., Merad, D., Fertil, B., & Thome, N. 2011. Pedestrian head detection and tracking using skeleton graph for people counting in crowded environments. Proceedings of the 12th IAPR Conference on Machine Vision Applications, MVA 2011, pp. 516-519.

Baker, M. G., Thornley, C. N., Mills, C., Roberts, S., Perera, S., Peters, J., ... & Wilson, N. 2010. Transmission of pandemic A/H1N1 2009 influenza on passenger aircraft: retrospective cohort study. Bmj, 340, c2424.

Chan, A. B., Liang, Z. S. J., & Vasconcelos, N. 2008. Privacy preserving crowd monitoring: Counting people without people models or tracking. 26th IEEE Conference on Computer Vision and Pattern Recognition, CVPR.

Cho, S. Y., Chow, T. W. S., & Leung, C. T. 1999. A neural-based crowd estimation by hybrid global learning algorithm. IEEE Transactions on Systems, Man, and Cybernetics, Part B: Cybernetics, 29(4), pp. 535-541.

Choi, J. W., Yim, D. H. & Cho, S. H. 2017. People counting based on an IR-UWB radar sensor. IEEE Sensors Journal, 17(17), pp. 5717-5727.

Chow, T. W. S., Yam, J. Y. F., & Cho, S. Y. 1999. Fast training algorithm for feedforward neural networks: Application to crowd estimation at underground stations. Artificial Intelligence in Engineering, 13(3), pp. 301-307.

Del Pizzo, L., Foggia, P., Greco, A., Percannella, G., & Vento, M. 2016. Counting people by RGB or depth overhead cameras. Pattern Recognition Letters, 81, pp. 41-50.

Fattorini, D., & Regoli, F. 2020. Role of the chronic air pollution levels in the Covid-19 outbreak risk in Italy. Environmental Pollution, p. 114732.

Fears, A. C., Klimstra, W. B., Duprex, P., Hartman, A., Weaver, S. C., Plante, K. S., Mirchandani, D., Plante, J. A., Aguilar, P. V., Fernández, D., & Nalca, A. 2020. Persistence of severe acute respiratory syndrome coronavirus 2 in aerosol suspensions. Emerging infectious diseases, 26(9), p. 2168.

Gorbalenya, A. E., Baker, S. C., Baric, R. S., de Groot, R. J., Drosten, C., Gulyaeva, A. A., Haagmans, B. L., Lauber, C., Leontovich, A. M., Neuman, B. W., & Penzar, D. 2020. The species severe acute respiratory syndrome related coronavirus: classifying 2019-nCoV and naming it SARS-CoV-2. Nat Microbiol 5: pp. 536-544.

Haritaoglu, I., Harwood, D., & Davis, L. S. 2000. W4: Real-time surveillance of people and their activities. IEEE Transactions on Pattern Analysis and Machine Intelligence, 22(8), pp. 809-830.

Handte, M., Iqbal, M. U., Wagner, S., Apolinarski, W., Marrón, P. J., Navarro, E. M. M., Martinez, S., Barthelemy, S. I., & Fernández, M. G. 2014. Crowd Density Estimation for Public Transport Vehicles. In EDBT/ICDT Workshops, pp. 315-322.

Hnat, T. W., Griffiths, E., Dawson, R., & Whitehouse, K. 2012. Doorjamb: unobtrusive room-level tracking of people in homes using doorway sensors. In Proceedings of the 10th ACM Conference on Embedded Network Sensor Systems, pp. 309-322.

Howerton, J. M., & Schenck, B.L. 2020. The Deployment of a LoRaWAN-Based IoT Air Quality Sensor Network for Public Good. In 2020 Systems and Information Engineering Design Symposium (SIEDS), pp. 1-6. IEEE.

Jain, S., & Madamopoulos, N. 2016. Ahorrar: Indoor occupancy counting to enable smart energy efficient office buildings. In 2016 IEEE International Conferences on Big Data and Cloud Computing (BDCloud), Social Computing and Networking (SocialCom), Sustainable Computing and Communications (SustainCom)(BDCloud-SocialCom-SustainCom), pp. 469-476. IEEE.

Jin, M., Bekiaris-Liberis, N., Weekly, K., Spanos, C., & Bayen, A. 2015. Sensing by proxy: Occupancy detection based on indoor CO2 concentration. UBICOMM 2015, 14.

Kamal, M., Aljohani, A., & Alanazi, E. 2020. IoT meets COVID-19: Status, Challenges, and Opportunities. arXiv preprint arXiv:2007.12268.

Kettnaker, V., & Zabih, R. 1999. Counting people from multiple cameras. International Conference on Multimedia Computing and Systems -Proceedings, 2, pp. 267-271.

Kouyoumdjieva, S. T., Danielis, P., & Karlsson, G. 2019. Survey of non-image based approaches for counting people. IEEE Communications Surveys & Tutorials.

Kostakos, V., Camacho, T., & Mantero, C. 2010. Wireless detection of end-to-end passenger trips on public transport buses. In 13th International IEEE Conference on Intelligent Transportation Systems, pp. 1795-1800. IEEE.

Li, H., Chan, E. C., Guo, X., Xiao, J., Wu, K., & Ni, L. M. 2015. Wi-counter: smartphone-based people counter using crowdsourced wi-fi signal data. IEEE Transactions on Human-Machine Systems, 45(4), pp. 442-452.

Li, H., Lu, H., Chen, X., Chen, G., Chen, K., & Shou, L. 2016. Vita: A versatile toolkit for generating indoor mobility data for real-world buildings. Proceedings of the VLDB Endowment, 9(13), pp.1453-1456.

Li, Y., Qian, H., Hang, J., Chen, X., Hong, L., Liang, P., Li, J., Xiao, S., Wei, J., Liu, L., & Kang, M., 2020. Evidence for probable aerosol transmission of SARS-CoV-2 in a poorly ventilated restaurant. medRxiv.

Liu, L., Li, Y., Nielsen, P.V., Wei, J., & Jensen, R. L. 2017. Short- range airborne transmission of expiratory droplets between two people. Indoor Air, 27(2), pp. 452-462.

Morawska, L., Tang, J. W., Bahnfleth, W., Bluyssen, P. M., Boerstra, A., Buonanno, G., Cao, J., Dancer, S., Floto, A., Franchimon, F., & Haworth, C. 2020. How can airborne transmission of COVID-19 indoors be minimised?. Environment international, 142, p. 105832.

Nakatsuka, M., Iwatani, H., & Katto, J. 2008. A study on passive crowd density estimation using wireless sensors. In The 4th Intl. Conf. on Mobile Computing and Ubiquitous Networking (ICMU 2008).

Nasir, Z. A., Campos, L. C., Christie, N. & Colbeck, I. 2016. Airborne biological hazards and urban transport infrastructure: current challenges and future directions. Environmental Science and Pollution Research, 23(15), pp. 15757-15766.

Ndiaye, M., Oyewobi, S. S., Abu-Mahfouz, A. M., Hancke, G. P., Kurien, A. M., & Djouani, K. 2020. IoT in the Wake of COVID-19: A Survey on Contributions, Challenges and Evolution. IEEE Access, 8, pp. 186821-186839.

Nitti, M., Pinna, F., Pintor, L., Pilloni, V., & Barabino, B. 2020. iABACUS: A Wi-Fi-Based Automatic Bus Passenger Counting System. Energies, 13(6), p.1446.

Niu, R., & Varshney, P. K. 2006. Target location estimation in sensor networks with quantized data. IEEE Transactions on Signal Processing, 54(12), pp. 4519-4528.

Pan, S., Mirshekari, M., Zhang, P., & Noh, H. Y., 2016. Occupant traffic estimation through structural vibration sensing. In Sensors and Smart Structures Technologies for Civil, Mechanical, and Aerospace Systems 2016., 9803, p. 980306. International Society for Optics and Photonics.

Pestre, V., Morel, B., Encrenaz, N., Brunon, A., Lucht, F., Pozzetto, B., & Berthelot, P. 2012. Transmission by super-spreading event of pandemic A/H1N1 2009 influenza during road and train travel. Scandinavian journal of infectious diseases, 44(3), pp. 225-227.

Qian, H., & Zheng, X. 2018. Ventilation control for airborne transmission of human exhaled bio-aerosols in buildings. Journal of thoracic disease, 10(Suppl 19), p. S2295.

Riediker, M., & Tsai, D. H. 2020. Estimation of SARS-CoV-2 emissions from non-symptomatic cases. medRxiv.

Regazzoni, C. S., & Tesei, A. 1996. Distributed data fusion for real-time crowding estimation. Signal Processing, 53(1), pp. 47-63.

Sacchi, C., Gera, G., Marcenaro, L., & Regazzoni, C. S. 2001. Advanced image-processing tools for counting people in tourist site-monitoring applications. Signal Processing, 81(5), pp. 1017-1040.

Saeed, N., Bader, A., Al-Naffouri, T. Y., & Alouini, M. S. 2020. When Wireless Communication Faces COVID-19: Combating the Pandemic and Saving the Economy. arXiv preprint arXiv:2005.06637.

Santarpia, J. L., Rivera, D. N., Herrera, V., Morwitzer, M. J., Creager, H., Santarpia, G. W., Crown, K. K., Brett-Major, D., Schnaubelt, E., Broadhurst, M. J., & Lawler, J. V. 2020. Transmission potential of SARS-CoV-2 in viral shedding observed at the University of Nebraska Medical Center. MedRxIV.

Schlögl, T., Wachmann, B., Kropatsch, W., & Bischof, H. 1832. Evaluation of People Counting Systems. Image Processing, August.

Shen, Y., Li, C., Dong, H., Wang, Z., Martinez, L., Sun, Z., Handel, A., Chen, Z., Chen, E., Ebell, M., & Wang, F. 2020. Airborne transmission of COVID-19: epidemiologic evidence from two outbreak investigations.

Shih, O., & Rowe, A. 2015. Occupancy estimation using ultrasonic chirps. In Proceedings of the ACM/IEEE Sixth International Conference on Cyber-Physical Systems, pp. 149-158.

Tang, X., Xiao, B., & Li, K. 2018. Indoor crowd density estimation through mobile smartphone wi-fi probes. IEEE transactions on systems, man, and cybernetics: systems.

Tatem, A. J., Rogers, D. J., & Hay, S. I. 2006. Global transport networks and infectious disease spread. Advances in parasitology, 62, pp. 293-343.

Tirachini, A., & Cats, O. 2020. COVID-19 and public transportation: Current assessment, prospects, and research needs. Journal of Public Transportation, 22(1), p.1.

Vasco Dantas dos Reis, J. 2014. Image Descriptors for Counting People with Uncalibrated Cameras.

Van Doremalen, N., Bushmaker, T., Morris, D. H., Holbrook, M. G., Gamble, A., Williamson, B. N., Tamin, A., Harcourt, J. L., Thornburg, N. J., Gerber, S. I., & Lloyd-Smith, J. O. 2020. Aerosol and surface stability of SARS-CoV-2 as compared with SARS-CoV-1. New England Journal of Medicine, 382(16), pp.1564-1567.

Wielechowski, M., Czech, K., & Grzęda, Ł. 2020. Decline in Mobility: Public Transport in Poland in the time of the COVID-19 Pandemic. Economies, 8(4), p.78.

Xiao, S., Li, Y., Sung, M., Wei, J., & Yang, Z. 2018. A study of the probable transmission routes of MERS- CoV during the first hospital outbreak in the Republic of Korea. Indoor Air, 28(1), pp. 51-63.

Xu, C., Firner, B., Moore, R. S., Zhang, Y., Trappe, W., Howard, R., Zhang, F., & An, N. 2013. SCPL: Indoor device-free multi-subject counting and localization using radio signal strength. In Proceedings of the 12th international conference on Information processing in sensor networks, pp. 79-90.

Yu, I. T., Li, Y., Wong, T. W., Tam, W., Chan, A. T., Lee, J. H., Leung, D. Y., & Ho, T. 2004. Evidence of airborne transmission of the severe acute respiratory syndrome virus. New England Journal of Medicine, 350(17), pp. 1731-1739.

Bulletin of Natural Sciences Research
Vol. 10, No. 2, 2020, pp. 51-58.

DOI: https://doi.org/10.5937/bnsr10-27731
Short Report

SPATIAL CHARACTERIZATION OF TELECOMMUNICATION SATELLITES VISIBLE ABOVE THE REPUBLIC OF SERBIA

SLAVIŠA ĐUKANOVIĆ[1], VLADIMIR MLADENOVIĆ[2*], MILAN GLIGORIJEVIĆ[1], DANIJELA MILOŠEVIĆ[2], IVONA RADOJEVIĆ ALEKSIĆ[2]

[1]University of Criminal Investigation and Police Studies, Belgrade, Serbia
[2]Faculty of Technical Sciences in Cacak, University of Kragujevac, Cacak, Serbia

ABSTRACT

This paper deals with the general technical, spatial, and temporal characteristics of satellite telecommunications systems. Particular attention was paid to the peculiarities of the territory of the Republic of Serbia in terms of implementation and use of modern satellite telecommunication infrastructure. The overview shows how and on which way to use various satellite telecommunication systems to configure and exploit next-generation networks, especially modern communications such as 5G technology and IoT. Their work cannot be imagined without the high speeds and high frequencies that allow us to transmit a wealth of information - from short messages/news to HD video on a mobile phone. We need either a base station network or in the case of the high seas or areas where the base station system is difficult to imagine, we need satellite communication. The paper presents data that give a numerical and graphical overview of geostationary satellites visible from the territory of the city of Belgrade, depending on the orbital position and the associated angle of azimuth and elevation, which would also be valid for the leading territory of Serbia.

Keywords: Satellite's orbites, 5G technologies, IoT, Azimuth, Elevation.

INTRODUCTION

Satellite telecommunication systems represent a significant part of the global telecommunication market. Alongside the evolution of technology, these systems, whether global or local, provide users with a wide range of services. The constant application of commercial satellite systems in military, diplomatic, and industrial purposes arises the question of how to protect signals thus transmitted. The reconnaissance of telecommunications is a complex activity that implies a wide range of actions: the examination of radio-frequency spectrum, signal reception, goniometric assessment, technical analysis of signals, and data processing. The complexity of the telecommunication reconnaissance process is directly associated with compound communication transmission techniques applied. Thus, new possibilities in the implementation of various detection and signal and parameter estimation methods emerge aimed at quality reconnaissance of telecommunication via specified systems.

The main function of the reconnaissance system is to detect the object significant for observation and to continuously monitor it regardless of the time variability of its characteristics, the presence of the distraction signals, and the influence of present whirs. The application of the time-varying system parameters estimation increases the effectiveness and robustness of the reconnaissance systems.

In general, the reconnaissance of satellite systems represents one of the crucial components of the electronic reconnaissance as a whole. The reconnaissance of satellite systems provides technical data (technical characteristics of satellite systems in general, satellite telecommunication systems and signals used in satellite telecommunications) and operative-technical data (levels of operational and technical application, the type and purpose of the satellite, satellite radio-transmission intensity data, etc.).

The possibility of detecting and monitoring a satellite, in general, is considered through the implementation of radar reconnaissance techniques, radio-reconnaissance, IC reconnaissance, and using laser systems. The term reconnaissance implies the analyzed possibility to discern the observed object as a satellite and determine that the examined signal originates from the satellite, not any other source in the same spacial sector.

The methodology of the satellite telecommunication reconnaissance is divided into several phases:

- The detection, observation and monitoring phase with the application of the estimation techniques,
- The identification phase and the analysis phase.

The detection, observation, and monitoring phase implies space exploration, tracking mobile satellites via antenna systems of radio-reconnaissance station. These are followed by the application of characteristic parameters estimation methods and techniques, radio spectrum examination, representation, detection, and primary analysis of the signals. The identification phase comprises the elements of the spatial and frequency satellite categorization, primary function identification, and a

* Corresponding author: vladimir.mladenovic@ftn.kg.ac.rs

confirmation that a single satellite originates from a satellite system. The analysis procedure includes following activities: analyzing the satellite orbit parameters, satellite frequency agility analysis, determination of type and transmission parameters (modulation), determination of the correspondents with which the connection is maintained, issuing command and synchronization impulses, extraction of the signals carrying a useful message and analytic processing of received messages.

The main goal of this paper is the representation of the territorial peculiarities of the Republic of Serbia in terms of implementation and use of modern satellite telecommunication infrastructure. The paper points out the way to use various satellite telecommunication systems to configure and exploit next-generation networks, especially modern communications such as 5G technology and IoT.

CLASSIFICATION OF SATELLITES BASED ON TYPE OF ORBIT

Communications satellites can be classified by the service they perform. However, these satellites are classified into those for radio-diffusion, mobile, and fixed satellite services. Communications satellites that provide mobile satellite services are used for Mobile Satellite Communications – MSC in applications, both rural and urban radio systems. Satellites can be classified by the orbital height of a satellite. Thus, CCIR distinguishes four main types of satellites:

- Low-Earth Orbit Satellites circling at altitudes from 100 to 5000 km above the Earth with orbital periods from 2 to 4 hours.
- Medium-Earth Orbit Satellites circling at altitudes from 5000 to 20000 km above the Earth with orbital periods from 4 to 20 hours.
- High-Earth Orbit Satellites circling at altitudes about 36000 km above the Earth with orbital periods of 24 hours.
- Orbits at great altitudes, about 36000 km above the Earth (Gligorijević et al., 2011).

The following satellites can be distinguished depending on the orbit and the satellite's relative circling above the Earth. Synchronous satellites have an average period of stellar rotation around the body equal to the average rotational period of the body on its axis, thus they can be referred to as - geosynchronous.

If these satellites orbit on the equatorial plane, they are referred to as - geostationary satellites. Their subsatellite point occupies an unvaried position, so to ground observers it appears motionless, i.e. stationary. Since these periods last about 23h and 56 minutes, these satellites circle the Earth in a sidereal day. Their orbit plane may have null or any other inclination towards the Earth's equatorial plane, such as polar or satellites with other inclination.

Subsynchronous satellites have the average rotational period of the body orbited on its axis equal to the entire multiple of the average rotational period of the satellite around the body. It means that they orbit over the same spot on Earth twice, or they circle it twice, i.e. their orbit lasts 12 hours. Elliptical orbit satellites and other satellites with circular orbit inclination belong to this category.

Non-synchronous satellites circle the earth more than twice in 24 hours, i.e. their orbit period is longer than 12 hours.

Satellites may be classified by the type of activity regarding the territory of the Republic of Serbia (Andrews & Phillips, 1998):

1) Satellites that do not broadcast signals in the direction of the Republic of Serbia (spare, malfunctioning or remnants of the satellites, satellites out of work, observatory satellites which emit the results of their observation only above certain spots outside the territory of the Republic of Serbia, satellites that are activated only in emergencies – crises and wars)
2) Satellites that probably broadcast signals in the direction of the territory of the Republic of Serbia. It is difficult to detect what these satellites transmit (telecommunication relay satellites with strongly directed spot beam radio transmissions, satellites that broadcast radio signals through widened spectrum and satellites which broadcast for a short period);
3) Satellites that publicly broadcast in the direction of the territory of the Republic of Serbia (satellites with civil purposes: telecommunication satellites, radio-diffusion, meteorological, navigation, satellites for transmitting the precise time signal; military satellites and other satellites of classificatory purposes: navigation, meteorological, observation, research, diplomatic, etc.)

When identifying satellites and their activity regarding the territory of the Republic of Serbia, movement parameters and types of satellite orbits are especially important. These are:

- Orbit shape with data on perigee, apogee, and inclination (circular and elliptic),
- Height and type of orbit, and
- Speed, that is a period of circulating the Earth.

Orbit's height and shape, satellite's speed and direction, and effective reflection area of the satellite are significant parameters during radar characterization (Panić et al., 2013).

Classification of the satellites regarding parameters significant for radio-characterization is possible to determine considering frequency spectrum and working frequencies, types of transmission, modulation types, and shapes of radiation diagram (spot beam, global beam, and multi-beam).

Types of satellite orbits

Taking into consideration the fact that astronomical objects freely move and mutually attract in the interplanetary space following the well-known laws, it is impossible to construct a satellite that would be fixed because it would be domed.

Having this in mind, artificial satellites can orbit in the circular and elliptical orbit planes of the geocentric coordinate system. Apart from ESO (Elliptical Satellite Orbit), there are three other circular orbits: GSO (Geostationary Satellite Orbit), PSO (Polar satellite Orbit), and inclined circular geosynchronous orbit, figure 1.

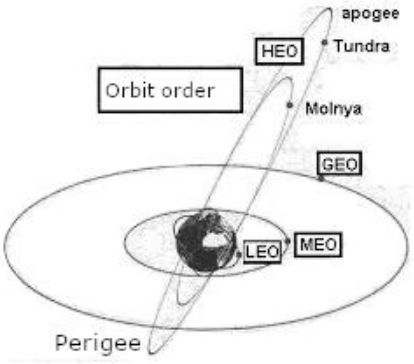

Figure 1. Overview of satellite orbit types.

Satellites circulation in the Earth's orbit can be depicted using Newton's Law of Gravitation while the concept of the elliptical or circular orbit is based on three Kepler's Laws. After launching, a satellite remains in the orbit due to balance established between the first force or the Earth's gravitational centripetal attraction and the second force, i.e. satellite's centrifugal acceleration in the circular orbit. Other forces have a negligible impact on the satellite's orbit.

Elliptical orbit

An elliptical orbit is an ellipse with the inclination angle of about 63° and an orbit period of 12 hours. It belongs to a group of subsynchronous orbits. Satellites in elliptical orbits cover polar zones and wider zones of the globe with the transition time from 8 to 10 hours out of 12 hours. The satellite's velocity varies. It is approximately about 10150 m/s at perigee and about 1610 m/s at apogee, while the velocity of the point on the equator is about 465 m/s. Marking the traces of the elliptical path is a far more complicated process due to inconsistencies that appeared as a result of the complex interrelation between satellite's speed and the Earth's rotation.

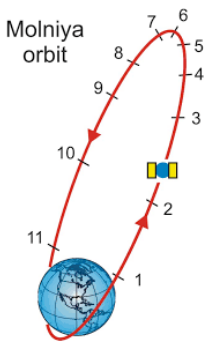

Figure 2. Elliptic satellite orbit.

Russian EOS MOLNIA-1 is a prototype of satellites in this orbit, Figure 2 (David 2020).

General data of the Molnya satellite are given in Table 1.

Table 1. Basic information about the MOLNIA satellite.

EOS Parameters	Technical characteristics
Apogee height	39957 km (above north hemisphere)
Perigee height	548 km (above south hemisphere)
Inclination	63.4°
Eccentricity	0.74°
Argument of perigee	270°
Approximate period	12 hours

Disadvantages of the EOS are due to a relative satellite orbiting in relation to the Earth and the fact that ZSS must be equipped with a highly complicated antenna system for reconnaissance of the satellites, though this could be achieved by automatic search. With EOS, the period of satellite obscuration should be taken into consideration to avoid energy loss.

The fact that less energy is needed to launch the EOS and that no additional motors for orbit correction are necessary are the advantages of the EOS. Thus energetic possibilities that EOS electronic devices possess are significantly greater than ones GSS has. Besides, another advantage of EOS satellites is the fact that ZSS in geographic positions at high latitudes there are greater elevation angles that enable loss reduction during propagation and decrease in satellite line blocking.

Circular satellite orbit

There are three different types of circular satellite orbits depending on the angle of inclination formed between the satellite's orbital plane and the equatorial plane. These are: polar when $i=90°$ (orbit 1), inclined with the proportion $0°<i<90°$ i $90°<i<180°$ (orbit 2), and equatorial GSS when $i=0°$ (orbit 3).

Geostationary (circum equatorial) orbit

If an artificial satellite is orbiting in the equatorial plane from west to east following the direction of Earth's rotation, its angular velocity will match the angular velocity of the Earth's rotation on its axis, thus to a ground observer, the satellite appears motionless. We are referring to synchronous GSS which presents a constellation of the INMARSAT system, (Đukanović 2006a). The GSS subsatellite points occupy various positions on the equator depend on their number and arrangement, while the length of equatorial arc from where an artificial satellite can be seen is 162° 36′ 30″ or 18102 km. An equatorial arc length, which is not covered by two GSS, is 34° 47′ (3872 km), while the total length of the equatorial arc from where it is possible to see two or three artificial satellites is 14232 km (26.21%), table 2.

Table 2. Parameters of GSO.

GSS parameters	Technical characteristics
Height above the equator	35784 km
Periods of rotation relative to the Sun.	24 hours
BY. in relation to the sidereal day	23 h 56 min i 4.091 sec
Circulation speed	3076 m/sec
Orbital inclination	0°
Earth's surface coverage	42.5% (0° elevacije)
Global coverage	3 GSS with shift of 120°
Theoretical coverage of the area	<81° N&S

The advantages of GSO are simple retrieval, there are no problems with the transmission, because the losses during signal propagation are quite limited, except during weather variations, almost constant connection range. Only one GSS is sufficient for regional uninterrupted coverage, high antenna signal amplification.

The disadvantages of GSO are the delay due to propagation, loss of free space, uncovered polar regions, and very important for MSC, there is no possibility of direct connections of MSS in one, with ZSS in another ocean area.

Circuminclination orbit

The circumclination orbit is obtained when the plane of the satellite's orbit is inclined at a certain angle to the equatorial plane, which is called the inclination angle. It can be defined as the angle that coincides between the equator and the sub-satellite point when the satellite enters the northern hemisphere and can have values from 0° to 90° and from 90° to 180°. In the case of a synchronous orbit, the satellite will not be visible from the Earth in a constantly determining direction but will be visible from the same point of the Earth's ball at different times and at different heights above the horizon. Thus, in this way, a trace of the path of subsatellite points in the shape of an elongated figure eight can be projected, the shape of which depends on the size of the inclination angle.

There are two circumminclination orbits that can be used for all forms of mobile applications.

CIRCULAR INCLINATION ORBIT

This orbit is used for the existing global navigation system, whose configuration consists of 24 satellites in three equilateral orbits. At a minimum, three satellites in each of the three orbits are equipped with polar communication equipment, to ensure continuous coverage of the polar zones (Đukanović 2006b).

Circumpolar orbit

When the inclination of the plane of the satellite's path towards the equator is 90°, a circumpolar orbit is obtained, which is in the plane of the Earth's axis. If the satellite orbit time is synchronous, a synchronous circular path is obtained. The relative position of such a satellite changes constantly, and every 24 hours it appears at the zenith of the same point on Earth, whose trace has the shape of a broad figure eight. However, for the case of a 12-hour orbit, the trajectory has the shape of two cross eights, and for the case of a 6-hour orbit, the trail is in the shape of four elongated eights. This type of satellite enables better coverage of regions at the highest latitudes and polar regions above 70° N and S, which are poorly or not at all covered by the existing GSS constellation.

Geometric relations of satellite orbit

During the design and operation of MSK, it is necessary to know the launch of satellites and orbital elements, all parameters, and laws of satellite shortening, as well as geographical and horizontal coordinates of satellites and their mutual relations. Kepler's laws describe the behavior of natural satellites if the mass of the central body is so far away that it is considered concentrated in its center and when their orbits are not under the influence of some other systems.

However, these conditions are not fully met when it comes to the Earth and its artificial satellites, since their mutual distances are not great, because the Earth is flattened and the masses in its interior are not properly distributed. Therefore, the satellites move unevenly, ie faster or slower on certain sections of the orbit, and this represents a certain deviation from the essence of Kepler's laws (Đukanović 2004).

The characteristics of an elliptical orbit are determined from the elements of the ellipse and its position relative to the Earth, Figure 3. Ellipse parameters, such as eccentricity e, major semiaxis a, minor semiaxis b, the axis between the center of the Earth and ellipse c, and focal parameter p, are obtained from the following expressions. The equation of the ellipse (Kepler trajectory) from the polar coordinates has the form:

$$r = \frac{p}{1 + e\cos\theta} \tag{1}$$

where the radius of the orbit is $r=R+H$, while e is a right anomaly, and θ is the angle between the directions from the center of the Earth to the perigee and the satellite, and E is an eccentric anomaly, whose expressions are:

$$\cos E = \frac{\cos\theta + e}{1 + e\cos\theta} \tag{2}$$

The speed of the satellite at point S, distant from the center of the Earth by r, is obtained from the expression:

$$v = \sqrt{\mu\left(\frac{2}{r} - \frac{1}{a}\right)} \tag{3}$$

where μ is the gravitational constant ($\times 10^5$ km^3/s^2), or Kepler's constant, the major semiaxis α.

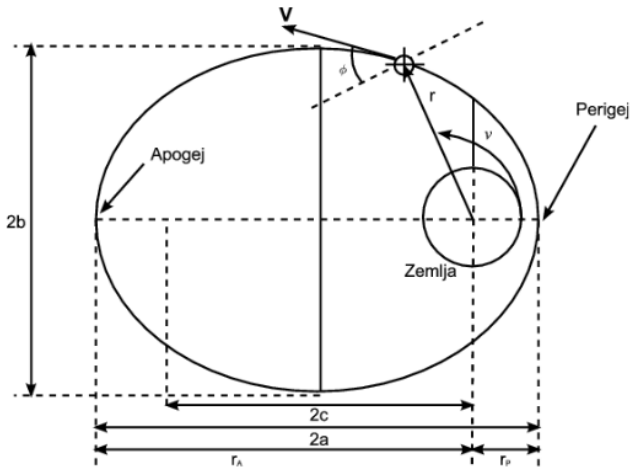

Figure 3. Elliptical satellite orbit parameters.

The behavior of artificial Earth satellites from the moment they enter orbit, similar to natural satellites, is determined by the laws of celestial mechanics. Thus, according to Kepler's third law, the sidereal or stellar time of a satellite orbit around the Earth in an elliptical orbit is:

$$t = 2\pi\sqrt{\frac{a^3}{\mu}} \tag{4}$$

where R is the mean radius of the Earth, while h is the height of the orbit.

A circular orbit is a special case of an elliptical orbit that arises from the following relations: $a=b=r$ and $e=0$. The speed of the satellite in a circular orbit can be determined from the following expression:

$$v = \sqrt{\frac{\mu}{r}} = 631.65\sqrt{R+h} \tag{5}$$

The duration of one full rotation of the Earth in relation to the standing stars is T=23h 56min 4.09s. If the satellite rotates around the Earth in the direction of rotation, the apparent rotation time t' will be:

$$t' = \frac{T \cdot t}{T - t} \tag{6}$$

The satellite is geostationary if $t=T$. Synodic time is obtained between successive passages of satellites above the meridian, whose expression reads:

$$T = \frac{t}{\left[1 - \Omega t / 2\pi\right]} \tag{7}$$

The synodic day is the time interval between two consecutive passages of the solar center through the meridian of the same name.

The Table 3 shows that a geostationary orbit can be established at an altitude of about 36000 km. The height of the satellite's orbit can be calculated based on the expression:

$$H = (r - 6378)$$
$$H = \sqrt[3]{\frac{\mu t^2}{4\pi^2}} - R \tag{8}$$

Table 3. Overview of dependence, time of orbiting the earth on the height of the orbiting satellite.

Orbital height in km	t(h)	T(h)
1700	2	2.18
10400	6	8
14000	8	12
20200	12	24
36000	24	-

It can be seen from expression (6) and Table 4 that the speed of a satellite does not depend on its mass but decreases with increasing altitude.

Table 4. Overview of satellite orbit parameters for satellites visible above the Republic of Serbia.

Parameters of orbite	Orbit parameter values					
Orbit time (h)	≈3	≈4	≈6	≈8	≈12	≈24
Altitude (km)	4163	6391	10354	13982	20184	35784
Radius (km)	10541	12770	16733	20720	26562	42162
Speed (km/s)	6149	5584	4881	4434	3874	3100

VISIBILITY ZONE AND DISTANCE OF SATELLITES

The zone of visibility of the GSS, ie the area it covers on the Earth, depends on the parameters of the orbit, its position in relation to the ZSS and geographical coordinates, Figure 4. These relations are quite simple if the subsatellite point P is the center of the surface to be covered, while otherwise, they are somewhat more complex. The first similarity of GSS visibility from the Earth's surface can be considered from the geometric relations in Figure 5. When determining the position of GSS towards a ZSS, ie towards MSS or ZSS, the following geometric values are relevant: actual height h (R+H), Earth radius R, elevation angle ε, azimuth angle A, direct distance d, and central angle ψ or subsatellite angle, which corresponds to the angle used to determine the aperture of the satellite dish δ, otherwise known as half the radius of the line of sight.

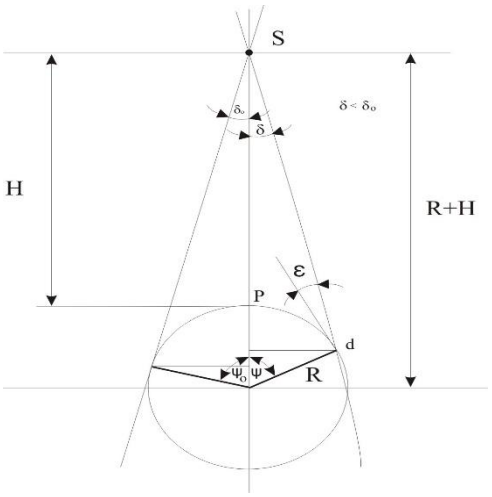

Figure 4. Overview of the visibility zone of a geostationary satellite.

The zone of visibility of the satellite is shown in Figure 4, within a boundary that at all times has the following regular interrelationships:

$$\delta + \varepsilon + \Psi = 90^0 \tag{9}$$

Since the height of the orbit *H* represents the distance of the satellite from the subsatellite point *P*, the expression for the height of the dome is:

$$H' = R(1 - \cos\Psi) \tag{10}$$

The limit of possible coverage with GSS on smooth surfaces of the Earth is reached when the elevation angle is ε=0, ie. when the satellite is on the horizon. This limitation can be expressed by a central angle or angular parameter of the visibility zone, the relation of which is:

$$\Psi = \frac{\pi}{2} - \arcsin k = \arccos\frac{R}{R+H} = \arccos\frac{6378{,}16}{42164{,}20} = \\ = \arccos(0.15126956) = 81^0\,17'\,58.18'' \tag{11}$$

Therefore, all ZSSs that are located at latitude and longitude above ψ=81° will not be covered, because GSS cannot be seen. However, zero elevation angles should be avoided even when maximum coverage is desired because then the noise temperature of the receiving antenna increases. For practical applications, the elevation angle of the receiving antenna must be greater than 5° (UHF / SVF band) or greater than 20° (EVF band). Difficult reception also occurs for cases of medium hilly terrain when the satellite can be shaded.

The angle at which a satellite can see the MSS is called the subsatellite angle. The furthest ZSS from the subsatellite point in the corresponding satellite region, ie if the position of the ZSS at the northern and southern latitudes is greater than Δλ=70° or at longitude φ=70° away east or west of the subsatellite point, the satellite can theoretically see at the minimum elevation angle ε=0°. Namely, such a relation can be calculated from simple trigonometric relations (Đukanović 2006b).

An angle Ψ is connected to the angle δ, which can determine the aperture of the radiation beam of the satellite dish. The GSS antenna for global coverage of the Earth is built so that it has a beam of radiation of width 2δ′=17.3°. According to Figure 5, the following relationship:

$$\tan\delta = \frac{0.15126956\cdot\sin\Psi}{(1+0.15126956\cdot\cos\Psi)} \tag{12}$$

that is, a 2δ′ wide beam aperture provides the maximum coverage possible for a satellite in a synchronous circular orbit.

Determining the position and number of satellites in the visibility zone

The position of the satellite in the zone of visibility of the satellite from the point of signal reception depends on the minimum elevation angle of the receiving antenna, the parameters of the satellite orbit, and the geographical coordinates of the ZSS map. Visibility is also affected by the shape of the orbit (circular or elliptical), (Đukanović 2013).

In order to determine the position of the satellite in relation to the observer from the Earth, Figure 5, ie in relation to the ZSS, specific quantities are used, which are called horizontal coordinates, such as:

1. The elevation angle of the satellite or the angle of the observation point - "ε", is formed between the horizon line and the vertical satellite direction seen from the point of view, ie. from the respective position of ZSS.
2. The angle of azimuth - "*A*" coincides starting from the line of the north-south towards the satellite direction on the horizon seen from the point of view, ie. from the respective position of ZSS.

Otherwise, from point d in Figure 4 or point A in Figure 5, a satellite can be seen at an elevation angle of:

$$\tan\varepsilon = \frac{\cos\Psi - k}{\sin\Psi} \tag{13}$$

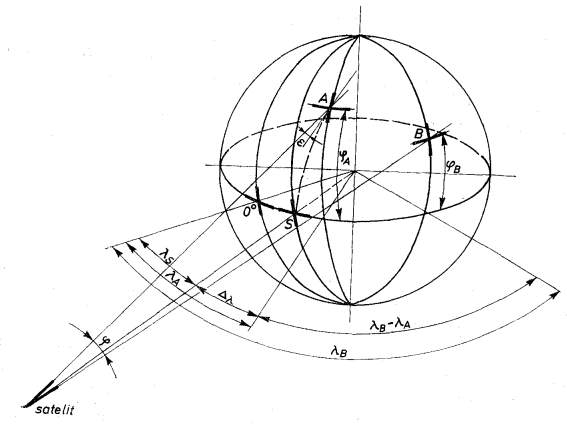

Figure 5. Overview of spatial geometry ZSS-GSS.

Figure 6 shows a Mercator map with a projection of elevation angles and with one example of that angle for a particular ZSS position. It can be concluded that the ZSS at the respective position (ε=25° for IOR and 16° for AOR) has the possibility to alternatively use both GSS to establish a radio connection with any ZSS located within the overlapping area of these two satellites. Satellite azimuth and subsatellite point from the ZSS position, i.e. point A on the earth's surface is obtained from the relation:

$$\tan A' = \frac{tg\Delta\lambda_A}{\sin\varphi_A} \tag{14}$$

However, if the MSS, ie point *A*, is not in the subsatellite point, then the azimuth is obtained from the following relation:

$$\tan A' = \frac{\sin\Delta\lambda_A}{\tan\varphi_A} \tag{15}$$

In this case, the magnitude *A′* meridian is the angle between the meridian plane of point *A* and the plane of the great circle through that and the subsatellite point, while *A* is the angle between that great circle and the meridian through the subsatellite point. Also in this case the MSS can establish a satellite connection with any ZSS from overlapping satellite areas. Various plans, graphs and tables are used for practical calculation of azimuth angle and GSS elevation for the needs of ZSS, Table 5.

For example, tables for ZSS positions (φ′ and λ′) are used to obtain longitudinal differences between ZSS and satellites for four possible ZSS positions: N and W, SIW, N and E and S and E from satellites, as in Figures 6 a, b, cid respectively.

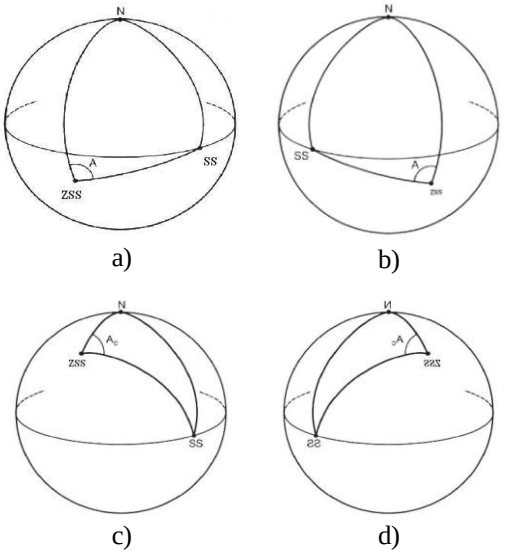

Figure 6. Overview of azimuth angle calculation for all possible ZSS positions.

Table 5. Calculation of the azimuth angle ZSS in relation to the orbital position GSS.

The direction of the GSS in relation to the ZSS	Azimuth angle calculation
to S and W, Fig. 6. a).	A=A′
to S and W, Fig. 6. c).	A=180°-A′
to S and W, Fig. 6. d).	A=180°+A′
to S and W, Fig. 6. b).	A=360°-A′

If the ZSS is at a higher altitude then the elevation angle is compensated by the following magnitude:

$$x = \arccos\left(1 - \frac{N}{R}\right) \tag{16}$$

where N is the altitude of the observer. For example, if the ZSS is located at an altitude of 1000 m, it is x≈1°.

Based on the previous analysis, the following can be concluded: If an antenna with a minimum elevation angle (5°) is used at the receiving station, then those GSS whose longitudinal position in orbit is in the range of 50°W W (west) can be seen from the territory of Serbia. to 90°E (east),

CONCLUSION

In this paper, we deal with the general technical, spatial, and temporal characteristics of satellite telecommunications systems. Particular attention was paid to the peculiarities of the territory of the Republic of Serbia in terms of implementation and use of modern satellite telecommunication infrastructure. The use of various satellite telecommunication systems lead to configure and exploit next-generation networks, especially modern communications such as 5G technology and IoT. Their work cannot be imagined without the high speeds and high frequencies that allow us to transmit a wealth of information - from short messages/news to HD video on a mobile phone. The paper presents data that give a numerical and graphical overview of geostationary satellites visible from the territory of the city of Belgrade, depending on the orbital position and the associated angle of azimuth and elevation, which would also be valid for the leading territory of Serbia.

ACKNOWLEGMENTS

This paper was supported by the Ministry of Education, Science and Technological Development of the Republic of Serbia, and these results are parts of the Grant No. 451-03-68/2020-14/200132 with University of Kragujevac - Faculty of Technical Sciences Čačak.

REFERENCES

Andrews, L. C., & Phillips, R. L. 1998. Laser Beam Propagation Through Random Media, SPIE.

David Darling 2020. https://daviddarling.info/encyclopedia/M/Molniya-type_orbit.html

Đukanović, S. 2004. Izviđanje satelitskih komunikacija u funkciji savremenih operacija 1,Vojnotehnički glasnik. 52(3-4), pp. 390-399.

Đukanović, S. 2006a. Elektronsko izviđanje komercijalnih satelitskih komunikacija, Bezbednost, Beograd – Info, 48(1), pp. 100-117.

Đukanović, S. 2006b. Neke specifičnosti izviđanja satelitskih veza u L opsegu, TELFOR.

Đukanović, S. Papić, V., & Đurović, Ž. 2013, Procena učestanosti kanala u satelitskim komunikacijama korišćenjem tehnika robusnog filtriranja I skrivenih Markovljevih modela, ETRAN.

Gligorijević, M., & Đukanović, S. 2011, GPS – Global positioning system and its applications in policing, Archibald Reiss Days.

Panić, S., Stefanović, M., Anastasov, J., & Spalević, P. 2013. Fading and Interference Mitigation in Wireless Communications, CRC Press.

Wolfram, http://functions.wolfram.com/

Bulletin of Natural Sciences Research
Vol. 10, No. 2, 2020, pp. 59-64.
DOI: https://doi.org/10.5937/bnsr10-27949
Original Scientific Paper

ELEMENTAL CONCENTRATIONS AND SOIL-TO-MOSS TRANSFER FACTORS OF RADIONUCLIDES IN THE ENVIRONMENT OF NORTH KOSOVO AND METOHIJA

LJILJANA GULAN[1*], TATJANA JAKŠIĆ[1], BILJANA MILENKOVIĆ[2], JELENA STAJIĆ[2]

[1]Faculty of Sciences, University in Priština - Kosovska Mitrovica, Kosovska Mitrovica, Serbia
[2]University of Kragujevac, Institute for Information Technologies, Kragujevac, Department of Science, Kragujevac, Serbia

ABSTRACT

This paper deals with investigations of elemental concentrations and soil-to-moss transfer factors of radionuclides in area of municipalities Kosovska Mitrovica and Zubin Potok. Twelve samples of soil and moss *Hypnum cupressiforme Hedw.* were collected during May 2018. Transfer factors of radionuclides: ^{226}Ra, ^{232}Th, ^{40}Kand ^{137}Cs were calculated with regard to elemental concentrations of radionuclides in soil and moss samples. Analysis was done in order to indicate the different ways of adopting radionuclides by mosses. According to calculated transfer factors and analysis, authors concluded that the soil is dominant source of natural radionuclides and their concentration in moss occurred due to resuspension of soil particles, while artificial ^{137}Cs is present in soil and moss samples as a consequence of atmospheric dry and wet deposition.

Keywords: Elemental concentration, Transfer factor, Radionuclide, Moss, Soil.

INTRODUCTION

Primordial radionuclides ^{226}Ra, ^{232}Th and ^{40}K are present in all soils and rocks. They are permanent source of irradiation of all biological species in nature, since they have long half-lives. Different chemical forms of these naturally occurring radionuclides emit gamma radiation which is known as terrestrial background. Therewith natural background radiation includes cosmic radiation and radon inhalation.

Besides natural radioactivity, the environment is uneven contaminated with artificial radionuclides, among them the radiologically most important is ^{137}Cs (half-life 30.07 y). It occurred in significant amounts particularly after the Chernobyl accident, as well as a consequence of nuclear tests and accidents after II World War. Therefore, exposure to any type of radiation poses some risk (UNSCEAR, 2008).

Radionuclides are incorporated in biological systems through the food chain, because plants rather absorb nutrients from soil than foliar (from particles suspended in air, transported by wind and precipitated by rainfall). On the other hand, the biological species that have ability to accumulate trace elements could serve as bio-indicators of radioecological status of an area.

Mosses are suitable for monitoring the ambient changes in the environment, since they have widespread geographical distribution and "evergreen phase" during the year. They also have high surface in comparison to volume and slowly grow with little morphological changes during the lifespan (Aceto et al., 2003; Ivanić et al., 2019; Fernandez & Carballeira, 2000).

Mosses are sensitive to climatic variations, which affect their growing, physiological activity, uptake and retention of elements (Zechmeister et al., 2008; Dolegowska & Migaszewski, 2019). Bioaccumulation of trace elements in moss tissue depends on: the atmospheric concentrations and uptake of contaminants, precipitation, elevation, vegetation cover and topography of the sampling site.

Recently, radionuclides in soils and mosses have been investigated in regions of Serbia by many authors (Mitrović et al., 2009; Dragović & Mihailović, 2009; Grdović et al., 2010; Dragović et al., 2010; Čučulović et al., 2012; Mitrović et al., 2016; Krmar et al., 2018).

This is the first environmental study which used mosses as indicators of radiological contamination in area of Kosovska Mitrovica and Zubin Potok municipalities, North Kosovo and Metohija. The aims of this work were to determine elemental concentrations of radionuclides (^{226}Ra, ^{232}Th and ^{40}K) and concentrations of radioactive ^{137}Cs from atmospheric fallout in soil and moss samples, as well to calculated transfer factors in order to discuss various adopting ways of radionuclides.

MATERIALS AND METHODS

Study area

This study deals with the investigation of elemental concentration of radionuclides in soil and moss samples in the area of municipalities Kosovska Mitrovica and Zubin Potok (Figure 1). Twelve sampling sites of hilly terrain, in the slopes of surrounding mountains (Mokra Gora, Rogozna and Kopaonik) were marked (S1-S12) on the Figure 1.

The relief is characterized by a diverse geological structure with rocks of different origin and age (granite, serpentinite, shale, marble, andesite, limestone).

*Coresponding author: ljiljana.gulan@pr.ac.rs

The mainly sedimentary, but magmatic and metamorphic rocks consist of shales, gabbro amphibolite, andesites and quartz latites. The part of relief was undergone the karst process in the carbonate rocks with the tectonic movements, which caused numerous fissures and cracks (Dimitrijević, 1997).

The study area belongs to moderately continental climate with cold winter and moderately warm summers. The edges of mountains and valleys between 1000 and 1500 meters of height have sub-mountainous climate (Ivanović et al., 2016). An average amount of precipitation is more than 700 mm and increased with altitude. The measured precipitation in the nearest town Kosovska Mitrovica (510 m a.s l.) was 657.6 mm and 535.7 mm during 2017 and 2018, respectively (Hydrometeorological Yearbook of Kosovo, 2017-2018).

Figure1. Map of the study area.

Sample collection and preparation

Moss samples of *Hypnum cupressiforme* Hedw. and soil samples were collected from 12 locations (Figure 1). Sampling was performed in open areas away from trees, and far from towns, single houses and motorways during May 2018. Four samples of moss and soil from area of Kosovska Mitrovica, and eight ones from Zubin Potok were collected.

Hypnum cupressiforme Hedw. (Hypnaceae) is a group of mosses species with a wide variety of habitats in different climatic zones. It has irregularly branched shoots (older parts are brown color, and younger are green) covered with strongly curved leaves; the stem leaves are concave and sickle-shaped. Capsules with spores are located on the top of the stems. They are rootless, and usually grow 3-5 years on tree trunks, rocks, ground and other surfaces (Frahm, 2009).

The collected moss samples were of carpet-forming growth types. A compound sample was made from five to ten sub-samples collected and mixed in within the same site. Samples were stored in paper bags. After transporting to the laboratory, they have been cleaned from litter and dead leaves. Only green and greenish-brown parts of the moss were used for gamma spectrometric analysis. These moss parts represent 3-5 years of plant growth. Underlying soil samples (0-10 cm) were also collected, cleaned from stones and roots, dried to constant weight, pulverized and sieved. All samples were packed in Marinelli beakers (450 mL), sealed, and left aside for a month to ensure equilibrium between ^{226}Ra and its progeny.

Gamma spectrometry

Gamma spectrometric measurements of soil and moss samples were performed with coaxial HPGe detector (GEM30-70 ORTEC) of 30% relative efficiency and 1.65 keV FWHM at 1.33 MeV (^{60}Co) and 717 eV at 122 keV (^{57}Co). Detector was shielded with 10 cm of lead to reduce the background.

Specific activities of ^{226}Ra, ^{232}Th, ^{40}K and ^{137}Cs in soil and moss samples were measured for 21600 s and 172800 s, respectively. System calibration was done with standard mixture MBSS 2 of gamma-emitting isotopes (^{241}Am, ^{109}Cd, ^{139}Ce, ^{57}Co, ^{60}Co, ^{137}Cs, ^{113}Sn, ^{85}Sr, ^{88}Y, ^{203}Hg, ^{152}Eu) provided by the Czech Metrology Institute. Maestro 32 was used for peak readings. The intensities and gamma lines of considering radionuclides are presented in Table 1.

Table 1. Intensities and gamma lines of radionuclides.

Radionuclide	Progeny	Gamma energy (keV)	Intensity (%)
^{226}Ra	^{214}Pb	351.9	37.1
	^{214}Bi	609.3	46.1
	^{214}Bi	1764.5	15.9
^{232}Th	^{228}Ac	338.3	12
	^{228}Ac	911.1	29
	^{228}Ac	968.9	17.5
	^{208}Tl	583.0	86
	^{208}Tl	860.6	12
^{40}K		1460.7	10.7
^{137}Cs		661.6	84.6

The total uncertainty of the activity measurements which includes the uncertainty of calibration source activity, efficiency of calibration and counting statistical errors were in the range of 3-10%.

Elemental concentrations of radionuclides

Elemental concentrations of ^{226}Ra, ^{232}Th and ^{40}K were obtained by converting their specific activities according the following equation (Tzortzis & Tsertos, 2004; Dragović et al., 2006):

$$F_E = \frac{M_E C}{\lambda_{E,i} N_A f_{E,i}} A_E \quad (1)$$

where F_E is the fraction of element E in the sample, $M_E, \lambda_{E,i}, f_{E,i}$ and $A_{E,i}$ are the atomic mass (kg/mol), the decay constant of the measured isotope *i* of the element E (1/s), the fractional atomic abundance in nature and measured specific activity of the element E (Bq/kg), respectively, N_A is the Avogadro's number ($6.023 \cdot 10^{23}$ 1/mol), and C is a constant with a value of 10^6 for radium/thorium, and 10^2 for potassium. Hence, elemental concentrations F_E are reported in units of ppm (equivalent to mg/kg) for ^{226}Ra and ^{232}Th, and as a percentage (%) for ^{40}K. Thus, if it is assumed that in uranium series radioactive equilibrium exists, then the concentrations of ^{226}Ra, ^{232}Th and ^{40}K can be calculated using the conversion factors:

1 Bq/kg of ^{226}Ra = 0.08097 ppm of U;
1 Bq/kg of ^{232}Th = 0.246305 ppm of Th;
1 Bq/kg of ^{40}K = 0.003195 % of K.

Transfer factor and discrimination factor

The ability of plants to uptake elements, expressed as the transfer factor, is similar for trees, grasses, and mosses (Zolotareva et al., 1983; Kabata-Pendias & Pendias, 2001). The parameters needed for quantification of radionuclide transfer to biota are continually updated and are used for reconsideration of transfer factors recommended by the International Atomic Energy Agency (IAEA, 1994). Transfer factors (*TF*) from soil to moss were calculated as follows:

$$TF = \frac{A_{moss}}{A_{soil}} \quad (2)$$

Where A_{moss} and A_{soil} are concentrations of radionuclides in moss and soil, respectively.

It has been accepted that caesium enters the plant mainly via potassium transport system. ^{40}K is a part of natural potassium which is the most abundant essential element in soil and plants. Since caesium and potassium belong to the same group of the periodic table and have similar chemical properties, mosses can discriminate between ^{40}K and ^{137}Cs in the process of uptake of these radionuclides. Discrimination factor (*DF*) is defined as:

$$DF = \frac{TF_{Cs}}{TF_K} \quad (3)$$

where TF_{Cs} and TF_K are transfer factors of ^{137}Cs and ^{40}K, respectively. DF value less than unity means that ^{40}K is more efficiently absorbed by the plant than ^{137}Cs (Zhu & Smolders, 2000).

RESULTS AND DISCUSSION

Elemental concentrations of ^{226}Ra, ^{232}Th and ^{40}K in soil and moss samples were calculated and presented in Table 2. Mean values of elemental concentrations are in good agreement with results reported for surface soils in Serbia (Dragović et al., 2014). The values of elemental concentration in moss are lower than in soil, which is expected, since the main source of primordial radionuclides is soil. The mean values of ^{232}Th elemental concentration for all the soil and moss samples were higher than for ^{226}Ra. ^{226}Ra easily enters plants from soil and due to chemical activity it behaves similarly to calcium in an organism (Čučulović, 2016). ^{226}Ra elemental concentrations in mosses is related to direct deposition of ^{222}Rn progenies attached to the dust particles, which are accumulated by mosses from soil resuspension, through dry and/or wet atmospheric deposition of aerosols (Kiliç et al., 2019). Due to originally present potassium in the moss tissue, and ongoing physicochemical processes uptake pathways of ^{40}K might be complex. Only sample S5 has higher percentage of ^{40}K in moss than in soil.

Table 2. Elemental concentrations of radionuclides in soil and moss and descriptive statistics.

Sample	^{226}Ra (ppm)		^{232}Th (ppm)		^{40}K (%)	
	soil	moss	soil	moss	soil	moss
S1	9.59	1.06	35.32	6.67	3.95	0.54
S2	1.17	0.15	3.65	0.84	0.51	0.38
S3	3.00	0.53	16.03	2.49	3.61	0.75
S4	2.28	0.15	12.22	1.11	1.44	0.36
S5	0.15	<MDA*	0.39	<MDA*	0.07	0.25
S6	1.40	0.08	5.49	0.20	0.51	0.38
S7	1.45	0.40	4.68	1.55	0.68	0.66
S8	2.74	0.23	11.58	1.08	1.89	0.51
S9	2.53	0.22	9.68	0.39	1.16	0.38
S10	1.68	0.09	7.86	0.71	0.77	0.34
S11	3.29	0.15	16.21	0.57	3.30	0.43
S12	2.84	0.29	13.50	1.50	2.43	0.48
Min	0.15	<MDA*	0.39	<MDA*	0.07	0.25
Max	9.59	1.06	35.32	6.67	3.95	0.66
Mean	2.68	0.30	11.38	1.56	1.69	0.45
Median	2.04	0.22	10.63	1.08	1.30	0.40
SD	2.36	0.28	9.04	1.81	1.33	0.14
Skewness	2.54	2.17	1.71	2.63	0.62	0.91

MDA*- 0.05 for ^{226}Ra; 0.17 for ^{232}Th

Figure 2 presents concentration of ^{137}Cs in soil and moss samples; the highest concentration in soil was noted in duff/mull soil (S5). Values of ^{137}Cs concentration in soil were higher than concentration in moss in six samples. Since ^{137}Cs is present more

than thirty years in environment mainly from atmospheric Chernobyl's fallout, this is expectable. At the other side, the reasons of higher ^{137}Cs concentrations in moss than in soil samples could be related with altitude and pine forest. It could be considered in terms of features of localities: this occurred in coniferous forests (mosses in pine and spruce forests more readily uptake radionuclides than oak forests), and it could be related with acidic conifer needles, its retaining the soil moisture and making different substrate. Džoljić et al. (2017) reported very low TF_{Cs} for spruce needles (range from not detected to 0.02), which could confirm washing out effect and deposition in substrate by precipitation.

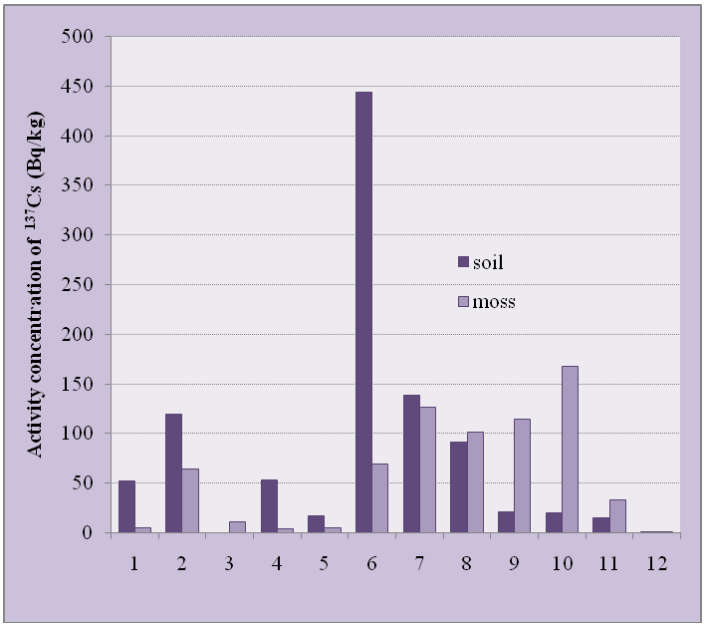

Figure2. Concentrations of ^{137}Cs in soil and moss samples.

The most important way of ^{137}Cs deposition in moss tissue is possibility that ^{137}Cs remains on the surface, which influences soil resuspension and transport to mosses (Ioannidou & Papastefanou, 2006, Krmar et al., 2018); also, ^{137}Cs can be transported during growing period from older sections to newer sections of moss tissue (Krmar et al., 2018). Furthermore, physiological and morphological features of the same moss species may vary among localities; it includes different growing ages of moss tissue, different dynamic processes of biosorption by different sections of mosses) and hence, the accumulation of atmospheric fallout may differ (Kiliç et al., 2019). In addition, variability of radionuclide activities might be attributed to local climatic conditions (amount of rainfall, humidity and wind direction). The results indicate that these moss species absorb water and nutrients as well as other trace elements primarily through wet and dry deposition rather than from soil.

Transfer factors of ^{226}Ra, ^{232}Th, ^{40}K and ^{137}Cs were calculated and presented in Table 3. TF for available data was in the range of 0.04-0.28 for ^{226}Ra, 0.03-0.33 for ^{232}Th and 0.13-3.63 for ^{40}K. A similar range for TF_{Ra} (0.05-0.57) and TF_{Th} (0.06-0.48) was obtained by Dragović et al. (2010) in the region of Zlatibor Mt. Moss capacity for absorption and retention of ^{226}Ra is much higher than in vascular plants (Tsikritzis et al., 2003). The TF_K is found to be more than unity for samples S5. With this exception, the values of TF_K mainly fall into the range of results obtained from the Zlatibor mountain area, 0.15-0.96 (Dragović, 2010) and non-urban area in Southern Serbia, 0.19-0.90 (Popović, 2008). A range of soil-to-moss transfer factors of natural radionuclides ^{226}Ra and ^{232}Th can be explained by similar geochemical behavior which influences radionuclide distribution based on the topography and environmental processes such as weathering. Some researchers confirmed the existence of a synergistic and antagonistic relationship between individual elements (Kabata-Pendias & Pendias, 2001).

Table 3. Transfer factors and discrimination factors.

Sample	TF_{Ra}	TF_{Th}	TF_K	TF_{Cs}	DF
S1	0.11	0.19	0.14	0.10	0.73
S2	0.13	0.23	0.74	0.53	0.72
S3	0.18	0.16	0.21	-	-
S4	0.07	0.09	0.25	0.09	0.34
S5	-	-	3.63	0.30	0.08
S6	0.06	0.04	0.74	0.16	0.21
S7	0.28	0.33	0.96	0.91	0.95
S8	0.09	0.09	0.27	1.11	4.14
S9	0.09	0.04	0.32	5.58	17.22
S10	0.05	0.09	0.44	8.50	19.39
S11	0.04	0.03	0.13	2.28	17.72
S12	0.10	0.11	0.20	1.22	6.21

On the other hand transfer factors are spanning from 0.02-8.50 for ^{137}Cs (for available data). The values of TF_{Cs} are lower than those reported by Dragović et al. (2010) for Zlatibor Mt. (1.01-13.1). The TF_{Cs} are found to be more than unity for five of eight locations in Zubin Potok which could be attributed to mainly hilly terrain and higher precipitation rate. Some authors reported that the average transfer factor for ^{137}Cs in *Hypnum cupressiforme* was up to two-fold higher than for other moss species (Dragović et al., 2010).

The DF ranges from 0.08 to 19.39 for sampling locations (Table 3). For certain location (mosses in coniferous and mixed forests), DF is found to be more than unity which indicated that ^{137}Cs uptake by moss tissue is more readily than ^{40}K. Also, some authors report that certain synergistic effects have been observed for antagonist pairs of elements, which largely depend on the corresponding reaction of the plant species (Kabata-Pendias & Pendias, 2001).

CONCLUSION

The mean values of ^{226}Ra, ^{232}Th and ^{40}K elemental concentration and 137Cs activity concentrations measured in soil

samples were comparable to the worldwide averages. Elemental concentrations in soil samples were in the range of 0.15-9.59 ppm for ^{226}Ra, 0.39-35.32 ppm for ^{232}Th, and 0.07-3.95% for ^{40}K. Mean elemental concentration of ^{232}Th in soil and moss samples was higher than ^{226}Ra. Wide ranges of values were observed; the values of natural radionuclides in moss are lower than in soil, since the main source of primordial radionuclides is soil. However, concentration of artificial ^{137}Cs does not show such a trend; it was higher in half of soil samples. ^{137}Cs activity concentrations in soil samples are spanning from 0.39-443.4 Bq/kg, while activity of this isotope in moss samples ranged from 1-168.1 Bq/kg. The variability of radionuclide activities might be attributed to local climatic conditions (amount of rainfall, humidity and wind direction). The results indicate that these moss species absorb water and nutrients as well as other trace elements primarily through wet and dry deposition rather than from soil. It was concluded that this occurred mainly in broad leaved, deciduous forest, while concentration of Cs in another six samples (coniferous and mixed forests) is higher in moss samples than in soil. Transfer factors of ^{226}Ra, ^{232}Th, and ^{40}K were in the range of 0.04-0.28, 0.03-0.33 and 0.13-3.63, respectively. A range of soil-to-moss transfer factors of natural radionuclides ^{226}Ra and ^{232}Th can be explained by similar geochemical behavior which influences radionuclide distribution based on the topography and environmental processes such as weathering. The TF_{Cs} are found to be more than unity for five of eight locations in Zubin Potok which could be attributed to mainly hilly terrain and higher precipitation rate. DF is found to be more than unity which indicated that ^{137}Cs uptake by moss tissue is more readily than ^{40}K.

Based on results and discussion it can be pointed out that significant radiological contamination in terms of natural and artificial radionuclides in area of Kosovska Mitrovica and Zubin Potok municipalities does not exist.

ACKNOWLEGMENTS

The present work was supported by Serbian Ministry of Education, Science and Technological Development (Agreement No. 451-03-68/2020-14/200378) and supported by the Faculty of Natural Sciences and Mathematics, University of Priština, Kosovska Mitrovica within the project No. IJ01-17.

REFERENCES

Aceto, M., Abollino, O., Conca, R., Malandrino, M., Mentasti, E., & Sarzanini, C. 2003. The use of mosses as environmental metal pollution indicators. Chemosphere 50, pp. 333–342. DOI;10.1016/S0045-6535(02)00533-7

Hydrometeorological Yearbook of Kosovo, 2017-2018. https://www.ammk-rks.net/?page=2,25

Čučulović A., Čučulović R., Sabovljević M., Radenković M.B., & Veselinović D. 2016. Natural radionuclide uptake by mosses in eastern Serbia in 2008-2013. Arhiv za Higijenu Rada i Toksikologiju 67, pp. 31–37. DOI: 10.1515/aiht-2016-67-2695

Čučulović, A., Popović, D., Čučulović, R., & Ajtić, J. 2012. Natural radionuclides and ^{137}Cs in moss and lichen in Eastern Serbia. Nuclear Technology and Radiation Protection 27, pp. 44–51. DOI: 10.2298/NTRP1201044Č

Dimitrijević, M. D. 1997. Geology of Yugoslavia. Geol. Inst. GEMINI, Belgrade.

Dolegowska, S. & Migaszewski Z.M. 2019. Biomonitoring with mosses: Uncertainties related to sampling period, intra-site variability, and cleaning treatments. Ecological Indicators 101, pp. 296–302. DOI: 10.1016/j.ecolind.2019.01.033

Dragović, S., Janković Lj., Onjia A., & Bačić G. 2006. Distribution of primordial radionuclides in surface soils from Serbia and Montenegro. Radiation Measurements 41, pp. 611 – 616. DOI:10.1016/j.radmeas.2006.03.007

Dragović, S., Janković-Mandić, Lj., Dragović, R., Đorđević, M., Đokić, M., & Kovačević, J. 2014. Lithogenic radionuclides in surface soils of Serbia: Spatial distribution and relation to geological formations. Journal of Geochemical Exploration 142, pp. 4–10. DOI: 10.1016/j.gexplo.2013.07.015

Dragović, S., & Mihailović, N. 2009. Analysis of mosses and topsoils for detecting sources of heavy metal pollution: multivariate and enrichment factor analysis. Environmental Monitoring and Assessment. 157, pp. 383–390. DOI: 10.1007/s10661-008-0543-8

Dragović, S., Mihailović N., & Gajić B. 2010. Quantification of transfer of ^{238}U, ^{226}Ra, ^{232}Th, ^{40}K and ^{137}Cs in mosses of a semi-natural ecosystem. Journal of Environmental Radioactivity 101, pp. 159–164. DOI: 10.1016/j.jenvrad.2009.09.011

Džoljić, A. J., Stević, M. S., Todorović, J. D., Polavder, M. S., Rajačić, M. M., & Krneta Nikolić, N. J. 2017. Natural and artificial radioactivity in some protected areas of south east Europe. Nuclear Technology and Radiation Protection, 32, pp. 334-341. DOI: 10.2298/NTRP1704334D

Fernandez, J. A., & Carballeira, A. 2000. Evaluation of contamination by different elements in terrestrial mosses. Archives of Environmental Contamination and Toxicology 40, pp. 461–468. DOI:10.1007/s002440010198

Frahm, J. P. 2009. A preliminary study of the infraspecific taxa of Hypnum cupressiforme in Europe. Archive for Biology 40, pp. 1–10. ISSN 0945-3466.

Grdović, S., Vitorović, G., Mitrović, B., Andrić, V., Petrujkić, B., & Obradović, M. 2010. Natural and anthropogenic radioactivity of feedstuffs, mosses and soil in the Belgrade environment, Serbia. Archives of Biological Sciences 62 (2), pp. 301-307. DOI:10.2298/ABS1002301G

IAEA, 1994. Handbook of Parameter Values for the Prediction of Radionuclide Transfer in Temperate Environments. Technical Report Series No. 364. IAEA, Vienna.

Ioannidou, A., & Papastefanou, C. 2006. Precipitation scavenging of 7Be and 137Cs radionuclides in air. Journal of Environmental Radioactivity 85, pp.121–136. DOI: 10.1016/j.jenvrad.2005.06.005

Ivanić M., Fiket Ž., Medunić G., Furdek Turk M., Marović G., Senčar J., & Kniewald G. 2019. Multi-element composition of soil, mosses and mushrooms and assessment of natural and artificial radioactivity of a pristine temperate rainforest system (Slavonia, Croatia). Chemosphere 215, pp. 668-677.

Ivanović, R., Valjarević, A., Vukoičić, D., & Radovanović, D. 2016. Climatic regions of Kosovo and Metohija. University Thought Publication in Natural Sciences, 6(1), pp. 49-54.

Kabata-Pendias, A., & Pendias, H. 2001. Trace elements in soils and plants (3rd ed.). New York, London, Taylor and Francis Group Boca Ration: CRC Press

Kiliç, Ö., Belivermiş, M., Sıkdokur, E., Sezer, N., Erentürk, S.A., Haciyakupoglu, S., Madadzada, A., & Frontasyeva, M. 2019. Assessment of ^{210}Po and ^{210}Pb by moss biomonitoring technique in Thrace region of Turkey. Journal of Radioanalytical and Nuclear Chemistry 322**,** pp. 699–706. DOI: 10.1007/s10967-019-06721-4

Krmar, M., Radnović, D., Hansman, J., Mesaroš, M., Betsou, C., Jakšić, T., & Vasić, P. 2018. Spatial distribution of ^{7}Be and ^{137}Cs measured with the use of biomonitors. Journal of Radioanalytical and Nuclear Chemistry 318, pp. 1845–1854. DOI: 10.1007/s10967-018-6121-9

Mitrović, B., Ajtić, J., Lazić, M., Andrić, V., Krstić, N., Vranješ, B., & Vićentijević, M. 2016. Natural and anthropogenic radioactivity in the environment of Kopaonik mountain, Serbia. Environmental Pollution 215, pp. 273-279. DOI:10.1016/j.envpol.2016.05.031

Mitrović B., Vitorović G., Vitorović D., Pantelić G., Adamović I. 2009. Natural and anthropogenic radioactivity in the environment of mountain region of Serbia, Journal of Environmental Monitoring 11, pp. 383–388. DOI: 10.1039/b813102c

Popović, D., Todorović, D., Frontasyeva, M., Ajtić, J., Tasić, M., & Rajšić, S. 2008. Radionuclides and heavy metals in Borovac, Southern Serbia. Environmental Science & Pollution Research 15, pp. 509–520. DOI 10.1007/s11356-008-0003-6

Tsikritzis, L. I., Ganatsios, S. S., Duliu, O. G., & Sawidis, T. D. 2003. Natural and artificial radionuclides distribution in some lichens, mosses, and trees in the vicinity of lignite power plants from West Macedonia, Greece. Journal of trace and microprobe techniques 21, pp. 543–554. DOI:10.1081/TMA-120023070

Tzortzis, M., & Tsertos, H. 2004. Determination of thorium, uranium and potassium elemental concentrations in surface soils in Cyprus. Journal of Environmental Radioactivity 77, pp. 325–338. DOI: 10.1016/j.jenvrad.2004.03.014

UNSCEAR, 2008. Report to the General Assembly, Annex B: Exposure of the public and workers from various sources of radiation. United Nations, New York.

Zechmeister, H. G. 1995. Growth rates of five pleurocarpous moss species under various climatic conditions. Journal of Bryology 18, pp. 455-468. DOI:10.1179/jbr.1995.18.3.455

Zhu, Y-G., & Smolders E. 2000. Plant uptake of radiocaesium: a review of mechanisms, regulation and application. Journal of Experimental Botany 51, pp.1635-1645. DOI:10.1093/jexbot/51.351.1635

Zolotareva, B. N., Skripnichenko, I. I., Ableev, M. Kh., Ostroumov, V. E., Geletyuk, N. I., Shitova (Koroleva), E. G., & Zablotskaya, L. V. 1983. Heavy metals in biogeocenoses of the Prioksko-Terrasny Biosphere Reserve, in Ecological Monitoring of the Prioksko-Terrasny Biosphere Reserve 56 (in Russian).

Bulletin of Natural Sciences Research
Vol.10, No.2, 2020, pp. 65-70.

DOI: https://doi.org/10.5937/bnsr10-27823
Original Scientific Paper

ON THE STARK BROADENING OF Os II SPECTRAL LINES

MILAN S. DIMITRIJEVIĆ[1,2,⋆]

[1]Astronomical Observatory, Volgina 7, 11060 Belgrade, Serbia
[2]Sorbonne Université, Observatoire de Paris, Université PSL, CNRS, LERMA, F-92190, Meudon, France

ABSTRACT

Stark broadening parameters, full widths at half maximum (FWHM) and shifts for 13 Os II lines have been calculated. The plasma parameters are: electron density of 10^{17} cm^{-3} and temperatures from 5 000 K to 80 000 K. Calculations have been performed with the simplified modified semiempirical (SMSE) approach. The results are also used for the consideration of Strak width and shift regularities within the Os II 6s^{6}D-6p^{6}D^o multiplet.

Keywords: Stark broadening, Spectral lines, Line profiles, Os II.

INTRODUCTION

Spectral line profiles in spectra emited from various plasmas are very useful and precious source of informations about plasma conditions, like electron density, temperature and chemical composition. Among different line broadening mechanisms, Stark broadening due to interaction of emitter/absorber with surrounding charged particles has many useful applications in astrophysics (see e.g. (Tankosić et al., 2003; Milovanović et al., 2004; Simić et al., 2006)), as well as for laboratory plasmas investigation and especially diagnostics (Konjević, 1999). Stark broadening data are also usefull for different investigations and modelling of fusion plasma (Griem, 1992), laser produced plasma diagnostic (Sorge et al., 2000) and analysis, as well as for its different applications in industry and technology as for example for welding, melting and piercing of metals by laser produced plasmas (see for example Hoffman et al. (2006)). Such data are also needed for design and development of light sources using different plasmas (Dimitrijević & Sahal-Bréchot, 2014), as well as for development of laser devices (Csillag & Dimitrijević, 2004).

Osmium is a metal in the platinum group of chemical elements. Its alloys with platinum, iridium, and other platinum-group metals are used for fountain pen nib tipping, for electrical contacts, and in other different applications where extreme durability and hardness are needed, since it is the densest naturally occurring element. In stellar interiors, osmium is created by rapid neutron capture (r-process) and Os I and Os II lines are present in Solar and stellar spectra (Quinet et al., 2006). For example the abundance of osmium has been determined from an Os II line in chemically peculiar Ap star HR 465 (Cowley et al., 1973; Hartoog et al., 1973), in HgMn star HD 175640 of late B type (B9 V) (Castelli & Hubrig, 2004), Os II lines have been observed in peculiar A type stars HD 25354 and HD 5797 (Kuchowicz, 1973), in Ap stars HD2453, HD25354, HD42616, HD71866 and HD 137909 (Brandi & Jaschek, 1970), where and Os I spectral lines have been identified, and in the UV spectrum of the HgMn star κ Canc, where Bord & Davidson (1982) found that osmium is overabundant by a factor 10^4. The presence of Os I and Os II lines in the spectrum of α^2 CVn has been discussed by Cowley (1987) and Cowley et al. (2006) concluded that presence of Os II spectral lines in the spectrum of chemically peculiar star HD65949 is highy probable. Wahlgren et al. (1998) found several Os II lines in the spectrum of χ Lupi, and they stated that lines λ 2282.278 and 2067.229 Å are particularly suitable for osmium abundance determination. Ivarsson et al. (2004) experimentally determined oscillator strengths for 27 Os II lines and used them to establish osmium abundance for χ Lupi. Osmium has been found and in the spectrum of Vela supernova remnants (Wallerstein et al., 1995), and its spectral lines have been used for the investigation of ejecta of neutron star mergers (Tanaka et al., 2020), as well as for synthezis of the spectrum of ι Herculis, a B3 IV star (Castelli & Bonifacio, 1990).

For determination of abundances, radiative transfer calculations, stellar opacity calculations, modelling of stellar atmospheres and stellar spectra analysis and synthezis, Stark broadening data are needed for white dwarfs, where Stark broadening is the principal pressure broadening mechanism (Beauchamp et al., 1997; Tankosić et al., 2003; Milovanović et al., 2004; Simić et al., 2006). Stark broadening is often non negligible and in the case of A type stars and late B type (see for example Simić et al. (2005a,b, 2009)).

As we can see, Stark broadening data for Os II spectral lines are needed for various problems in astrophysics, but atomic data for osmium are scarce and there is neither experimental nor theoretical data for Stark broadening of its spectral lines. Consequently, in order to provide such data, we calculated here, Stark full widths at half maximum (FWHM - W) and shifts d for 13 Os II spectral lines by using the simplified modified semiempirical method (Dimitrijević & Konjević, 1987). The obtained results are used for investigation of regularity of behaviour of Stark broadening parameters within Os II 6s^{6}D-6p^{6}D^o multiplet.

The Stark broadening parameters for Os II spectral lines will be implemented in the STARK-B (Sahal-Bréchot et al., 2015, 2020) database.

⋆ Corresponding author: mdimitrijevic@aob.rs

SIMPLIFIED MSE FORMULA

The simplified modified semiempirical method (Dimitrijević & Konjević, 1987), formulated for Stark broadening of isolated spectral lines of singly and multiply charged ions in plasma is convenient for Os II lines, since a set of atomic data, needed for more accurate semiclassical perturbation calculations (Sahal-Bréchot, 1969a,b; Sahal-Bréchot et al., 2014) does not exist. For the case of considered Os II lines we checked the validity condition

$$x_{jj'} = E/|E_{j'} - E_j| \leq 2 \tag{1}$$

and it is satisfied for electron temperatures less than 80000 K. Here, j=i,f, where i is for initial atomic energy level of the considered spectral line and f for final, $E_{j'}$ (j'=i' or f') is the nearest atomic energy level with possibility to have an allowed dipole transition from or to the energy level i or f. According to (Dimitrijević & Konjević, 1987), full width at half intensity maximum is:

$$W(\text{Å}) = 2.2151 \times 10^{-8} \frac{\lambda^2(\text{cm}) N(\text{cm}^{-3})}{T^{1/2}(\text{K})} (0.9 - \frac{1.1}{Z}) \times$$

$$\times \sum_{j=i,f} (\frac{3n_j^*}{2Z})^2 (n_j^{*2} - \ell_j^2 - \ell_j - 1). \tag{2}$$

where N is the electron density, T temperature, $E = 3kT/2$ the energy of perturbing electron, $Z-1$ the ionic charge (charge seen by optical electron), n^{*2} the effective principal quantum number, ℓ_j (j=i,f) orbital angular momentum quantum number and λ the wavelength.

Similarly, in the case of the shift

$$d(\text{Å}) = 1.1076 \times 10^{-8} \frac{\lambda^2(\text{cm}) N(\text{cm}^{-3})}{T^{1/2}(\text{K})} (0.9 - \frac{1.1}{Z}) \frac{9}{4Z^2} \times$$

$$\times \sum_{j=i,f} \frac{n_j^{*2} \varepsilon_j}{2\ell_j + 1} \{(\ell_j + 1)[n_j^{*2} - (\ell_j + 1)^2] - \ell_j (n_j^{*2} - \ell_j^2)\}. \tag{3}$$

In the case when all levels $\ell_{i,f} \pm 1$ exist, an additional summation may be performed in Eq. (3) and we obtain:

$$d(\text{Å}) = 1.1076 \times 10^{-8} \frac{\lambda^2(\text{cm}) N(\text{cm}^{-3})}{T^{1/2}(\text{K})} (0.9 - \frac{1.1}{Z}) \frac{9}{4Z^2} \times$$

$$\times \sum_{j=i,f} \frac{n_j^{*2} \varepsilon_j}{2\ell_j + 1} (n_j^{*2} - 3\ell_j^2 - 3\ell_j - 1), \tag{4}$$

where $\varepsilon = +1$ for j = i and -1 for j = f.

RESULTS AND DISCUSSION

Atomic energy levels needed for calculation using the simplified modified semiempirical (SMSE) method (Dimitrijević & Konjević, 1987) have been taken from Kramida et al. (2020) and Moore (1971). Data on atomic energy levels for Os II are scarse so that the more accurate semiclassical perturbation method (Sahal-Bréchot, 1969a,b; Sahal-Bréchot et al., 2014) is not applicable in an adequate way. The best data are for the multiplet $6s^6D$-$6p^6D^o$ and SMSE is the most advanced method that could be successfully used for the corresponding calculations. The condition to apply so called "one electron approximation" (Griem, 1974), i.e. to average energies for energy levels within this multiplet and calculate Stark broadening parameters for the multiplet as a whole, is that the distance of energy levels in particular terms making this multiplet is much lower than the closest distance between two terms. In our case, largest separation of atomic energy levels in $6s^6D$ term is 6636.57 cm^{-1} and in $6p^6D^o$ term it is 4325.72 cm^{-1}. The smaller distance between two terms is 37165.79 cm^{-1} and the condition that this distance is much larger than the separation of levels within a term is not well satisfied. We calculate one value for the whole multiplet when this quantity is at least ten times larger, so here the accuracy will be better if we calculate Stark broadening parameters for each spectral line within the considered multiplet, separately.

For the considered transitions of Os II one additional simplification is possible. Namely, if we look at the perturbing levels for each particular line within multiplet the one electron approximation is always satisfied. For example, in the case of the line $6s^6D_{7/2}$-$6p^6D^o_{5/2}$, perturbing levels for $6s^6D_{7/2}$ level are $6p^6D^o_{9/2}$, $6p^6D^o_{7/2}$ and $6p^6D^o_{5/2}$ and the distance between them is 2571.15 cm^{-1}. In the case of the upper level, perturbing levels are $6s^6D_{7/2}$, $6s^6D_{5/2}$ and $6s^6D_{3/2}$ and the distance is 1998.9 cm^{-1}. Since the smaller distance between two sets of perturbing levels, i. e. between $6s^6D_{3/2}$ and $6p^6D^o_{7/2}$ is 38210.31 cm^{-1} we can see that this value is more than ten times larger than the distances of perturbing levels for each of perturbed levels. Consequently, we can average not all levels in the multiplet but only perturbing levels of each perturbed level. An additional difficulty is that all atomic energy levels belonging to $6s^6L$-$6p^6L'^o$ supermultiplet are not known. So we take this averaged perturbing level as representative of other missing levels. Investigations of Wiese & Konjević (1982) demonstrated that Stark widths within a supermultiplet should be not different more than 30%. So, the error introduced by this approximation would be within these limits.

For calculation of averaged energies we used the expression:

$$E = \frac{\sum_J (2J+1) E_J}{\sum_J (2J+1)}, \tag{5}$$

where E is the averaged energy and E_J and J energy and total angular momentum of a particular energy level.

Table 1. This table gives electron-impact broadening (Stark broadening) Full Widths at Half Intensity Maximum (W) and shifts (d) for Os II spectral lines, for a perturber density of 10^{17} cm^{-3} and temperatures from 5 000 to 80 000 K.Also, the $3kT/2\Delta E$, quantity is given, where ΔE is the energy difference between closest perturbing level and the closer of initial and final levels. In order that the used method is valid, this quantity should be less or equal two.

Transition	T(K)	W[Å]	d[Å]	W[10^{12} s^{-1}]	d[10^{12} s^{-1}]	3kT/2ΔE
Os II $6s^6D_{9/2}$-$6p^6D^o_{7/2}$	5000.	0.486E-01	-0.171E-01	0.176	-0.619E-01	0.131
λ = 2282.279 Å	10000.	0.344E-01	-0.121E-01	0.124	-0.438E-01	0.262
	20000.	0.243E-01	-0.856E-02	0.878E-01	-0.310E-01	0.523
	40000.	0.172E-01	-0.606E-02	0.621E-01	-0.219E-01	1.05
	80000.	0.121E-01	-0.428E-02	0.439E-01	-0.155E-01	2.09
Os II $6s^6D_{9/2}$-$6p^6D^o_{9/2}$	5000.	0.480E-01	-0.167E-01	0.178	-0.618E-01	0.128
λ = 2256.6 Å	10000.	0.339E-01	-0.118E-01	0.126	-0.437E-01	0.256
	20000.	0.240E-01	-0.835E-02	0.888E-01	-0.309E-01	0.512
	40000.	0.170E-01	-0.590E-02	0.628E-01	-0.218E-01	1.02
	80000.	0.120E-01	-0.418E-02	0.444E-01	-0.154E-01	2.05
Os II $6s^6D_{7/2}$-$6p^6D^o_{7/2}$	5000.	0.595E-01	-0.212E-01	0.181	-0.647E-01	0.131
λ = 2486.247 Å	10000.	0.420E-01	-0.150E-01	0.128	-0.457E-01	0.262
	20000.	0.297E-01	-0.106E-01	0.906E-01	-0.323E-01	0.523
	40000.	0.210E-01	-0.751E-02	0.640E-01	-0.229E-01	1.05
	80000.	0.149E-01	-0.531E-02	0.453E-01	-0.162E-01	2.09
Os II $6s^6D_{7/2}$-$6p^6D^o_{9/2}$	5000.	0.586E-01	-0.207E-01	0.183	-0.645E-01	0.130
λ = 2455.7 Å	10000.	0.414E-01	-0.146E-01	0.129	-0.456E-01	0.259
	20000.	0.293E-01	-0.103E-01	0.915E-01	-0.323E-01	0.519
	40000.	0.207E-01	-0.730E-02	0.647E-01	-0.228E-01	1.04
	80000.	0.147E-01	-0.516E-02	0.458E-01	-0.161E-01	2.07
Os II $6s^6D_{7/2}$-$6p^6D^o_{5/2}$	5000.	0.555E-01	-0.186E-01	0.191	-0.640E-01	0.130
λ = 2336.807	10000.	0.392E-01	-0.131E-01	0.135	-0.453E-01	0.259
	20000.	0.277E-01	-0.928E-02	0.956E-01	-0.320E-01	0.519
	40000.	0.196E-01	-0.656E-02	0.676E-01	-0.226E-01	1.04
	80000.	0.139E-01	-0.464E-02	0.478E-01	-0.160E-01	2.07
Os II $6s^6D_{5/2}$-$6p^6D^o_{7/2}$	5000.	0.607E-01	-0.217E-01	0.182	-0.649E-01	0.131
λ = 2507.185 Å	10000.	0.429E-01	-0.153E-01	0.128	-0.459E-01	0.262
	20000.	0.303E-01	-0.108E-01	0.908E-01	-0.325E-01	0.523
	40000.	0.214E-01	-0.766E-02	0.642E-01	-0.230E-01	1.05
	80000.	0.152E-01	-0.542E-02	0.454E-01	-0.162E-01	2.09
Os II $6s^6D_{5/2}$-$6p^6D^o_{3/2}$	5000.	0.568E-01	-0.192E-01	0.191	-0.643E-01	0.132
λ = 2367.360 Å	10000.	0.402E-01	-0.135E-01	0.135	-0.455E-01	0.264
	20000.	0.284E-01	-0.958E-02	0.955E-01	-0.322E-01	0.528
	40000.	0.201E-01	-0.677E-02	0.675E-01	-0.227E-01	1.06
	80000.	0.142E-01	-0.479E-02	0.477E-01	-0.161E-01	2.11
Os II $6s^6D_{5/2}$-$6p^6D^o_{5/2}$	5000.	0.565E-01	-0.189E-01	0.192	-0.643E-01	0.131
λ = 2355.295 Å	10000.	0.400E-01	-0.134E-01	0.136	-0.454E-01	0.262
	20000.	0.283E-01	-0.947E-02	0.959E-01	-0.321E-01	0.523
	40000.	0.200E-01	-0.670E-02	0.678E-01	-0.227E-01	1.05
	80000.	0.141E-01	-0.473E-02	0.480E-01	-0.161E-01	2.09
Os II $6s^6D_{3/2}$-$6p^6D^o_{3/2}$	5000.	0.625E-01	-0.212E-01	0.194	-0.657E-01	0.132
λ = 2465.2 Å	10000.	0.442E-01	-0.150E-01	0.137	-0.465E-01	0.264
	20000.	0.312E-01	-0.106E-01	0.968E-01	-0.328E-01	0.528
	40000.	0.221E-01	-0.749E-02	0.685E-01	-0.232E-01	1.06
	80000.	0.156E-01	-0.530E-02	0.484E-01	-0.164E-01	2.11
Os II $6s^6D_{3/2}$-$6p^6D^o_{5/2}$	5000.	0.621E-01	-0.210E-01	0.195	-0.656E-01	0.131
λ = 2451.370 Å	10000.	0.439E-01	-0.148E-01	0.138	-0.464E-01	0.262

Table 1. Continued.

Os II $6s^6D_{3/2}$-$6p^6D^o_{5/2}$	20000.	0.311E-01	-0.105E-01	0.973E-01	-0.328E-01	0.525
	40000.	0.220E-01	-0.741E-02	0.688E-01	-0.232E-01	1.05
	80000.	0.155E-01	-0.524E-02	0.486E-01	-0.164E-01	2.10
Transition	T(K)	W[Å]	d[Å]	W[10^{12} s^{-1}]	d[10^{12} s^{-1}]	3kT/2ΔE
Os II $6s^6D_{3/2}$-$6p^6D^o_{1/2}$	5000.	0.593E-01	-0.191E-01	0.202	-0.651E-01	0.129
λ = 2350.240 Å	10000.	0.419E-01	-0.135E-01	0.143	-0.460E-01	0.257
	20000.	0.296E-01	-0.955E-02	0.101	-0.326E-01	0.514
	40000.	0.210E-01	-0.676E-02	0.714E-01	-0.230E-01	1.03
	80000.	0.148E-01	-0.478E-02	0.505E-01	-0.163E-01	2.06
Os II $6s^6D_{1/2}$-$6p^6D^o_{3/2}$	5000.	0.664E-01	-0.226E-01	0.195	-0.666E-01	0.132
λ = 2529.568 Å	10000.	0.470E-01	-0.160E-01	0.138	-0.471E-01	0.264
	20000.	0.332E-01	-0.113E-01	0.977E-01	-0.333E-01	0.528
	40000.	0.235E-01	-0.800E-02	0.691E-01	-0.235E-01	1.06
	80000.	0.166E-01	-0.566E-02	0.489E-01	-0.166E-01	2.11
Os II $6s^6D_{1/2}$-$6p^6D^o_{1/2}$	5000.	0.629E-01	-0.204E-01	0.204	-0.660E-01	0.132
λ = 2409.398 Å	10000.	0.445E-01	-0.144E-01	0.144	-0.467E-01	0.264
	20000.	0.314E-01	-0.102E-01	0.102	-0.330E-01	0.528
	40000.	0.222E-01	-0.720E-02	0.721E-01	-0.233E-01	1.06
	80000.	0.157E-01	-0.509E-02	0.510E-01	-0.165E-01	2.11

Using SMSE method and above explained approximations we calculated Full Stark widths at half intensity maximum (W) and shifts (d) for 13 spectral lines of singly charged osmium (Os II) broadened by impacts with electrons, for an electron density of 10^{17} cm^{-3} while temperatures are 5 000, 10 000, 20 000, 40 000 and 80 000 K.

The obtained Stark broadening paramerers, W and d, are shown in Table 1. One should take into account that the linear dependence of Stark broadening parameters in function of electron density, for high densities may be influenced by Debye screening. The wavelengths shown in Table 1 are the observed ones from Ivarsson et al. (2004). In the last column the validity condition $3kT/2\Delta E$ is given, representing the ratio of the average energy of free electrons, $E = 3kT/2$, and the smaller of energy differences between the initial or final and the closest perturbing level i.e.:

$$\mathrm{Max}[E/\Delta E_{i,i'}, E/\Delta E_{f,f'}] \tag{5}$$

Namely the SMSE method is valid if elastic collisions dominate. Since the threshold for the corresponding inelastic transition is $3kT/2\Delta E = 1$, we can see that for values lower than one and close to one elastic collisions dominate and the method is valid. We use that for values larger than two there are already a significant contribution of inelastic collisions and the method becomes unreliable. Stark broadening parameters for values slightly larger than two are useful for better interpolation.

Stark broadening parameters are presented in Table 1 in Å-, which is the usual presentation and in angular frequency units, which is convenient for discussion of regularities since the influence of wavelength is eliminated. Stark widths and shifts are transformed to angular frequency units, using the expression:

$$W(\mathring{A}) = \frac{\lambda^2}{2\pi c} W(s^{-1}), \tag{6}$$

where c is the speed of light.

The investigations of regularities is useful because if they exist, they can be used for estimates of missing values from the known ones. The Stark widths obtained here, belong to the Os II $6s^6D$-$6p^6D^o$ multiplet. Wiese & Konjević (1982) and Wiese & Konjević (1992) demonstrated that Stark line widths in angular frequency units, are very similar in a multiplet, while shifts are within ± 10%. If we look at values in angular frequency units in Table 1, we can see that for T = 5000 K, the maximal value for the width is 15.9% higher than the minimal one. In the case of the shift, this is 7.77%. At the temperature of 80000 K, these differences are 16.2%for the width and 7.79% for the shift. Consequently, difference within the considered Os II multiplet are higher than predicted by Wiese & Konjević (1982), while for shift are within the limits predicted by Wiese & Konjević (1992). Also, we can see that these differences practically do not change with temperature.

CONCLUSION

By using the SMSE theoretical approach we have calculated Stark full widths at half intensity maximum and shifts for 13 Os II spectral lines within the $6s^6D$-$6p^6D^o$ for electrons as perturbers. The considered temperature range has been from 5000 K up to 80000 K and electron density is 10^{17} cm^{-3} . We examined the similarities of Stark broadening parameters for spectral lines within this multiplet and found that the differences for the widths are within the limits of 16.2% and for the shifts within 7.79%. The obtainrd data will be implemented in the STARK-B database (Sahal-

Bréchot et al., 2015, 2020) which also can be accessed through the portal (http://portal.vamdc.eu) of the european Virtual Atomic and Molecular Data Center - VAMDC (Dubernet et al., 2010; Rixon et al., 2011; Dubernet et al., 2016). Other experimental or theoretical data for Stark broadening parameters of Os II lines are missing in the literature, so that the obtained data may be of interest for investigation of stellar spectral lines of ionized osmium and determination of abundances, in particular for white dwarfs and A type stars, as well as for laboratory plasma investigations and diagnostics.

REFERENCES

Beauchamp, A., Wesemael, F., Bergeron, P. 1997. Spectroscopic Studies of DB White Dwarfs: Improved Stark Profiles for Optical Transitions of Neutral Helium, Astrophysical Journal Supplement, 108(2), pp. 559-573.

Bord, D. J., Davidson, J. P. 1982. An application of the method of wavelength coincidence statistics to the ultraviolet spectrum of Kappa Cancri. Astrophysical Journal, 258, pp. 674-682.

Brandi, E., Jaschek, M. 1970. Heavy elements in Ap stars. Publications of Astronomical Society of Pacific, 82, pp. 847-850.

Castelli, F., Bonifacio, P. 1990. A computed spectrum for the normal star IOTA Herculis (B3 IV) in the region 122.8-195.0 nm. Astronomy and Astrophysics Supplement Series, 84, pp. 259-375.

Castelli, F., Hubrig, S. 2004. A spectroscopic atlas of the HgMn star HD 175640 (B9 V) $\lambda\lambda$ 3040-10 000 Å. Astronomy and Astrophysics, 425, pp. 263-270. doi.org/10.1051/0004-6361:20041011

Cowley, C. R. 1987. Platinum and bismuth in HR 465. Observatory, 107, pp. 188-194.

Cowley, C. R., Hartoog, M. R., Aller, M. F., Cowley, A. P. 1973. Abundances of trace elements in HR465: Evidence for the rprocess. Astrophysical Journal, 183, pp. 127-131.

Cowley, C. R., Hubrig, S., González, G. F., Nuñez, N. 2006. HD 65949: the highest known mercury excess of any CP star?. Astronomy and Astrophysics, 455, pp. L21-L24. doi.org/10.1051/0004-6361:20065799

Csillag, L. Dimitrijević, M. S. 2004, On the Stark broadening of the 537.8 nm and 441.6 nm Cd+ lines excited in a hollow cathode laser discharge, Applied Physics B: Lasers and Optics, 78 (2), pp. 221-223. doi.org/10.1007/s00340-003-1368-3

Dimitrijević, M. S., Konjević, N. 1987. Simple estimates for Stark broadening of ion lines in stellar plasma. Astronomy and Astrophysics, 172, pp. 345-349.

Dimitrijević, M. S. Sahal-Bréchot, S. 2014. On the Application of Stark Broadening Data Determined with a Semiclassical Perturbation Approach, Atoms, 2, pp. 357-377. doi.org/10.3390/atoms2030357

Dubernet, M. L., Ba, Y. A., Delahaye, F., Dimitrijević, M. S., Doronin, M., ... Gagarin, S. V. 2016. The virtual atomic and molecular data centre (VAMDC) consortium. Journal of Physics B, Atomic, Molecular and Optical Physics, 49(7), 18. doi:101088/0953-4075/49/7/074003

Dubernet, M. L., Boudon, V., Culhane, J. L., Dimitrijević, M.S., Fazliev, A.Z., Joblin, C., ... Zeippen, C.J. 2010. Virtual atomic and molecular data centre. Journal of Quantitative Spectroscopy Radiative Transfer, 111(15), pp. 2151-2159. doi.org/10.1016/j.jqsrt.2010.05.004

Griem, H. R. 1974, Spectral line broadening by plasmas (New York.: Academic Press, Inc.)

Griem, H. R. 1992, Plasma spectroscopy in inertial confinement fusion and soft X-ray laser research, Physics of Fluids, 4(7), pp. 2346-2361.

Hartoog, M. R., Cowley, C. R., & Cowley, A. P. 1973. The application of wavelength coincidence statistics to line identification: HR 465 and HR 7575, Astrophysical Journal, 182, pp. 847-858.

Hoffman, J., Szymanski, Z., Azharonok, V. 2006. Plasma Plume Induced During LaserWelding of Magnesium Alloys, AIP Conference Proceedings, 812, pp. 469-472. DOI: 10.1063/1.2168887

Ivarsson, S., Wahlgren, G. M., Dai, Z., Lundberg, H., Leckrone, D. S. 2004. Constraining the very heavy elemental abundance peak in the chemically peculiar star Chi Lupi, with new atomic data for Os II and Ir II, Astronomy and Astrophysics, 425(1), pp. 353-360. doi.org/10.1051/0004-6361:20040298

Konjević, N. 1999. Plasma broadening and shifting of nonhydrogenic spectral lines: present status and applications, Physics Reports, 316 (6), pp. 339-401.

Kramida, A., Ralchenko, Yu., Reader, J., -NIST ASD Team 2020. NIST Atomic Spectra Database. Gaithersburg, MD: National Institute of Standards and Technology. (ver. 5.5.1), Retrived from https://physics.nist.gov/asd, 2020, 1st of April.

Kuchowicz, B. 1973. The peculiar A Stars and the Origin of the Heaviest Chemical Elements. Quarterly Journal of the Royal Astronomical Society, 14, pp. 121-140.

Milovanović, N., Dimitrijević, M. S., Popović, L. Č. Simić, Z. 2004, Importance of collisions with charged particles for stellar UV line shapes: Cd III, Astronomy and Astrophysics, 417(1), pp. 375-380. doi.org/10.1051/0004-6361:20034162

Moore, C. E. 1971. Atomic Energy Levels as Derived from the Analysis of Optical Spectra – Molybdenum through Lanthanum and Hafnium through Actinium. Nat. Stand. Ref. Data Ser. 35, Vol. III. Washington: Nat. Bur. Stand. US, pp. 1-245.

Quinet, P., Palmeri, P., Biémont, É., Jorissen, A., Van Eck, S., Svanberg, S., Xu, H. L., Plez, B. 2006. Transition probabilities and lifetimes in neutral and singly ionized osmium and the Solar osmium abundance. Astronomy and Astrophysics, 448(3), pp. 1207-1216. doi.org/10.1051/0004-6361:20053852

Rixon, G., Dubernet, M. L., Piskunov, N., Walton, N., Mason, N., Le Sidaner, P., ... Zeippen, C. J. 2011. VAMDC—The Virtual Atomic and Molecular Data Centre—A New Way to Disseminate Atomic and Molecular Data—VAMDC Level 1 Release. AIP Conference Proceedings, 1344, pp. 107-115. doi.org/10.1063/1.3585810

Sahal-Bréchot, S. 1969a. Impact theory of the broadening and shift of spectral lines due to electrons and ions in a plasma, Astronomy and Astrophysics, 1, pp. 91-123.

Sahal-Bréchot, S. 1969b. Impact theory of the broadening and shift of spectral lines due to electrons and ions in a plasma (continued), Astronomy and Astrophysics, 2, pp. 322-354.

Sahal-Bréchot, S., Dimitrijević, M. S., Ben Nessib, N. 2014. Widths and Shifts of Isolated Lines of Neutral and Ionized Atoms Perturbed by Collisions With Electrons and Ions: An Outline of the Semiclassical Perturbation (SCP) Method and of the Approximations Used for the Calculations, Atoms, 2, pp. 225-252. DOI: 10.3390/atoms2020225

Sahal-Bréchot, S., Dimitrijević, M. S., Moreau, N. 2020. STARK-B database. Observatory of Paris / LERMA and Astronomical Observatory of Belgrade. Retrieved from http://starkb. obspm.fr, 2020 May 1st.

Sahal-Bréchot, S., Dimitrijević, M. S., Moreau, N., Ben Nessib, N. 2015. The STARK-B database VAMDC node: a repository for spectral line broadening and shifts due to collisions with charged particles. Physica Scripta, 90(5), doi.org/10.1088/0031-8949/90/5/054008

Simić, Z., Dimitrijević, M. S., Kovačević, A. 2009. Stark broadening of spectral lines in chemically peculiar stars: Te I lines and recent calculations for trace elements, New Astronomy Review, 53(7-10), pp. 246-251. doi.org/10.1016/j.newar.2009.08.005

Simić, Z., Dimitrijević, M. S., Milovanović, N., Sahal-Bréchot, S. 2005a. Stark broadening of Cd I spectral lines, Astronomy and Astrophysics, 441(1), pp. 391-393. doi.org/10.1051/0004-6361:20052701

Simić, Z., Dimitrijević, M. S., Popović, L. Č., Dačić, M. 2005b. Stark Broadening of F III Lines in Laboratory and Stellar Plasma, Journal of Applied Spectroscopy, 72(3), pp. 443-446. doi.org/10.1007/s10812-005-0095-4

Simić, Z., Dimitrijević, M. S., Popović, L. Č., Dačić, M. 2006. Stark broadening parameters for Cu III, Zn III and Se III lines in laboratory and stellar plasma, New Astronomy, 12(3), pp. 187-191. doi.org/10.1016/j.newast.2006.09.001

Sorge, S., Wierling, A., Röpke, G., Theobald W., Sauerbrey R. Wilhein, T. 2000. Diagnostics of a laser-induced dense plasma by hydrogen-like carbon spectra, Journal of Physics B: Atomic, Molecular and Optical Physics, 33(16), pp. 2983-3000. doi.org/10.1088/0953-4075/33/16/304

Tanaka, M., Kato, D., Gaigalas, G., Kawaguchi, K. 2020. Systematic Opacity Calculations for Kilonovae. Monthly Notices of the Royal Astronomical Society, 496, pp. 1369-1392. oi.org/10.1093/mnras/staa1576

Tankosić, D., Popović, L. Č., Dimitrijević, M. S. 2003. The electron-impact broadening parameters for Co III spectral lines, Astronomy and Astrophysics, 399(2), pp. 795-797. doi.org/10.1051/0004-6361:20021801

Wahlgren, G. M., Leckrone, D. S., Brage, T., Proffitt, C. R., Johansson, S. 1998. Very Heavy Elements in the HgMn Star Chi Lupi. ASP Conference Series, 143, pp. 330-333.

Wallerstein, G., Vanture, A. D., Jenkins, E. B., Fuller, G. M. 1995. A search for r-process elements in the Vela supernova remnant. Astrophysical Journal, 449, pp. 688-694.

Wiese, W. L., Konjević, N. 1982. Regularities and similarities in plasma broadened spectral line widths (Stark widths). Journal of Quantitative Spectroscopy and Radiative Transfer, 28, pp. 185-198.

Wiese, W. L., Konjević, N. 1992. Regularities in experimental Stark shifts. Journal of Quantitative Spectroscopy and Radiative Transfer, 28, pp. 185-200.

CIP - Каталогизација у публикацији
Народна библиотека Србије, Београд

5

BULLETIN of Natural Sciences Research / editor in chief Nebojša Živić. - [Štampano izd.]. - Vol. 10, no. 2 (2020)- . - Kosovska Mitrovica : Faculty of Sciences, University in Priština, 2020- (Kruševac : Sigraf). - 29 cm

Polugodišnje. - Je nastavak: The University thought. Publication in natural sciences = ISSN 1450-7226. - Drugo izdanje na drugom medijumu: Bulletin of Natural Sciences Research (Online) = ISSN 2738-1013
ISSN 2738-0971 = Bulletin of Natural Sciences Research (Štampano izd.)
COBISS.SR-ID 28586505

Available Online

This journal is available online. Please visit http://www.bulletinnsr.com to search and download published articles.